NEW FRONTIERS FOR SOLAR CELLS AND LIGHT EMITTING DEVICES: From Organic Solar Cells and Light Emitting Devices to Policy

JOSEPH ASARE

A

DISSERTATION

PRESENTED TO THE FACULTY OF

THE AFRICAN UNIVERSITY OF SCIENCE AND TECHNOLOGY (AUST)

IN CANDIDACY FOR THE DEGREE

OF

DOCTOR OF PHILOSOPHY

RECOMMENDED FOR ACCEPTANCE

BY THE DEPARTMENT OF

PHYSICS

Advisor: Prof. W. O. Soboyejo

FEBRUARY 17, 2017

RECOMMENDED:

.....

Supervisor, Prof. W.O. Soboyejo

.....

Dr. M. G. Zebaze Kana

.....

Dr. Jing Du

.....

Head, Department of Theoretical and Applied Physics

APPROVED:

.....

Vice President, Academics

Date: February 17, 2017

ABSTRACT

Solar energy, with its abundance and availability, would ultimately replace dwindling fossil fuel reserves in this new era of cleaner and more efficient energy as the world surges on to new technologies and horizons. This research investigates new frontiers for solar cells and light emitting devices: from organic solar cells and light emitting devices to policy.

The effects of bending on the electrical, optical, structural and mechanical properties of flexible organic photovoltaic (OPV) cells were explored first. Bulk heterojunction organic solar cells were fabricated on Polyethylene terephthalate (PET) substrates using Poly-3-hexylthiophene: [6, 6]-phenyl-C61-butyric acid methyl ester (P3HT: PCBM) as the active layer and Poly (3, 4-ethylenedioxythiophene) Polystyrenesulfonate (PEDOT: PSS) as the hole injection layer. All the organic layers were deposited by the method of spin coating while the Al cathode was vacuum thermally evaporated. Electrical, optical and deformation characteristics were measured as layers were deposited. The relationship between the optoelectronic performance of the various device layers and the applied mechanical strains were analyzed. The effects of stress and strain on the current-voltage characteristics of the device and its failure were modeled using finite element analysis.

With this knowledge that bending strains affect the optoelectronic and failure mechanisms in bendable/ flexible OPVs, a year-long survey assessment was conducted on a rural off-grid community in central Kenya to determine the different factors that affected the adoption of solar lanterns in the community. Impact on the people's socio-economic, health, and education levels were also assessed. The lanterns were shown to have a 96% adoption rate in the sample community and this resulted in a 14.7% drop in annual lighting-related expenditures.

DEDICATION

This Dissertation is

Dedicated

To

My Father, Jehovah Elohim,

My Best Friend, the Holy Spirit, and

My Loving family and friends

ACKNOWLEDGEMENT

My deepest and most profound appreciation goes to the Almighty God for making this thesis a possibility. Secondly, I sincerely appreciate my supervisor, Professor W. O. Soboyejo for not giving up on me. When all hope seemed lost, his encouragement and support held me in my most challenging times. His passion for excellence always drives me to be the best that I can be. I thank him for this support. I learnt the true meaning of long suffering during my years of research at Princeton, USA, Sheda Science and Technology Complex (SHESTCO), Nigeria, and the African University of Science and Technology (AUST), Nigeria.

It is very true that I would never have made it this far without the help of advisors and sensational professors like Dr Jing Du, Dr Tudor Popov, Dr Zebaze-Kana, Dr Akin-Ojo, Professor Jean Chabi, Professor K. Osseo-Asare, Professor S. Y. Mensah, Dr Joe Berry, Dela Vowotor, Augustine Arthur, Daniel Botchway, Professor Buah-Bassuah, Dr Karen Malatesta, Professor Tannie Liverpool, Professor Terry Alford and the like who groomed me academically from my undergraduate years through masters to the doctorate level.

I would like to show my sincere and heartfelt gratitude to my family for their unfailing support even though I had to stay far away from home to pursue this degree. I have the best family on earth: Mr and Mrs John Asare and family, Mr and Mrs Obline Asare and family, Mrs Josephine Asare Adu-Gyamfi and family, Mr and Mrs Baoteng and family and my loving mother, Stella Afari. I say to you all: “Medamuase Paa!” Words can never articulate how loving and caring you have all been to me.

I thank the board of trustees of AUST, African Development Bank (AfDB), Pan African Materials Institute (PAMI), World Bank, African Capacity Building Foundation (ACBF), World

Bank Step-B Program, Ngozo Okongo Ekwela, Princeton University, Worcester Polytechnic Institute (WPI) and the Nelson Mandela Institute (NMI) for their financial support. Their scholarships blessed me with the opportunity to complete my Masters and PhD program in this prestigious pan African graduate Institution. I also extend my appreciation to the Soboyejo Research Group, SHESTCO and PRISM for all their help during my research. I cherish all the help given me from Mrs Onugu, Mr Oladipupo, Mrs Deborah Oyewole, Eng. Gadu, Mrs Iwok, Dr Shola, and Mr Obgona during my experimental work sessions in SHESTCO.

Due to the constructive criticisms, ideas and research discussions with brilliant minds like; Dr. Jing Du, Dr Annan, Dr Agyei-Tuffour, Dr Tiffany Tong, Dr Oyewole, Dr Emmanuel Arthur, Chukwuemeka Ani Joseph, Dr A. A. Fashina, Dr Damilola Momodu, Emre Tukoz, S. A. Adeniji, Dr R. Egidius and Edward Ampaw, I was able to publish my findings in international journals as contributions to the Scientific Society.

To my cherished helpers and allies, you will always have a place in my heart forever. Mrs Soboyejo, Mr and Mrs Itegie, Mrs Blessing Nkwocha, Mr and Mrs Arasah, Mr and Mrs Omidiji, Folorunsho, Mr and Mrs Angel-Symon Odey, Nancy Savage, Dr Damilola Momodu, Adama Momodu, Dr Oyewole and family, Dr and Mrs Anye, Dr Fashina, Dr Danyuo Yiporo, Dr Azeko, Dr and Mrs Patrice Ndambomve and family, Arreytambe Tabot, Dr Arthur, Edward Ampaw, Dr Benjamin Nforneh, Dr Annan, Dr and Mrs Agyei-Tuffour, Mr and Mrs Banitsi, Mr and Mrs Attricki, Ato Jesse, Pricilla Yeboah, Mr and Mrs William Nganje, Simon Sunday, Mr and Mrs Stephen Jolaiya, Mr and Mrs Innocent Shaibu, Peace Omale, Tabe Arreytambe, Bolade Igbagbo, Venessa Obiageli, Francis Musibau, Sam Manthalu, Walusungu Godwe, Bar. Joke Abdullahi, Ibukun Abdullahi, Mr and Mrs Chuka Madumelo, Sandra Achu, Mr and Mrs Ikpo and family, Amb and Mrs Dogonyaro, Hassana Dogonaro, Pasi Dogonyaro, John Dogonyaro, Pastor Ikiddeh,

Arc and Mrs Bidemi Shitu, Pastor Sarah Omakwu, Mr and Mrs Asanga, Deacon Inyang, Mr and Mrs Ehindero, Mr Israel Awudu, Dr Mrs Ogunbiyi and all my AUST and Family Worship Center (FWC-Abuja) family and friends, you will always have a place in my heart. I love you for making my journey sweet with your smiles, encouragement, gifts and unquenchable care. I would like to show my deepest love for my mothers, Miss Stella Afari and the late Mrs Theresa Asare. These great women taught me some of the most precious virtues for life; humility and patience.

To conclude, I would like to thank all loved ones for their inspiration and sacrificial love. These helped to usher me in the right direction in graduate school when faced with challenging situations. I extend a heartfelt gratitude to them for being my rock and fortress especially during this doctorate degree program.

TABLE OF CONTENT

LIST OF TABLES

LIST OF FIGURES

CHAPTER ONE

INTRODUCTION

1.1 Background and Introduction

The global consumption of energy on the earth surface is estimated to be 15TW yearly. 32TW is the total geothermal energy available, 870TW is that of wind and direct solar offers up to 86,000TW [1]. With these statistics, solar energy would be the ultimate source of fuel due to its abundance in availability. Ultimately, solar energy would replace the dwindling fossil fuels' reserves in this new era of cleaner and more efficient energy as the world surges on to new technologies and horizons. In 2050, the world needs at least 10-30 TW of $C0_2$ free power for the survival of mankind [2]. In one hour, the sun provides 14-15 TW energy. But currently, only 0.04% of our energy consumption is solar [3].

1.2 The Solar Cell

A solar cell is a semiconductor PN junction diode, normally without an external bias, that provides electrical power to a load when illuminated [4], as shown in figure below. Solar cells or photovoltaic devices are devices that can convert the energy from sunlight into usable electrical energy.

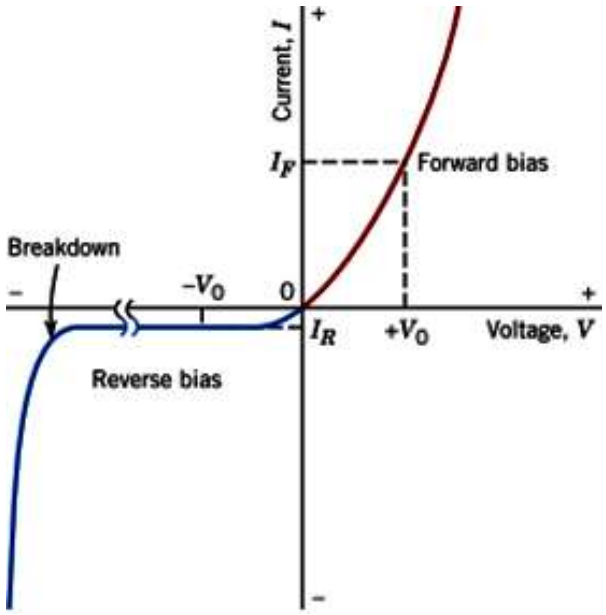

Figure 1.1: Current Voltage (IV) characteristics of a PN junction diode[5]

A solar cell under illumination would exhibit the IV characteristics of a forward bias PN junction diode as indicated in the Figure 1.2:

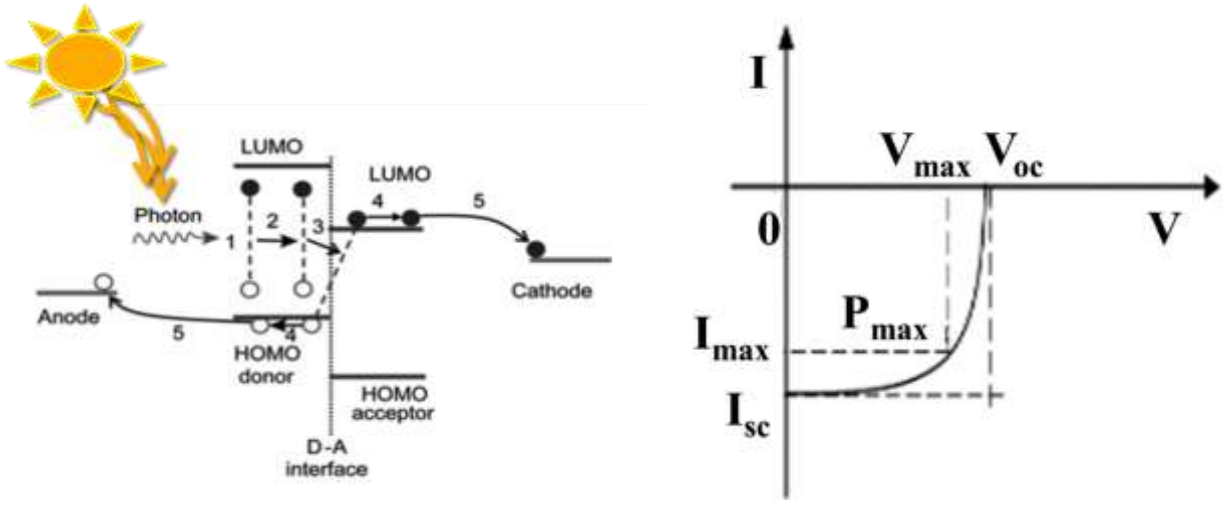

Figure 1.2: Characteristics of a solar cell under light[6]

In the dark, a solar cell would exhibit the Ohmic characteristics curve of a conventional resistor. The efficiency of a solar cell is the ratio of the electrical power it delivers to the load, to the

optical power incident on the cell. The maximum efficiency occurs when the power delivered to the load is P_{max} [7].

A solar cell could be either organically or inorganically manufactured. A solar cell made by depositing one or more layers (thin films) of photovoltaic materials on a substrate is called a thin- film photovoltaic cell (TFPV) or thin- film solar cell (TFSC). These have thickness ranges varying from a few nanometers to tens of micrometers. Various deposition methods on a variety of substrates are used to deposit many different many different photovoltaic materials. Therefore the photovoltaic material used categorizes the thin- film solar cell into inorganic and organic forms given as:

- Amorphous Silicon and other thin- film Silicon
- Cadmium Telluride
- Copper Indium Gallium Selenide

} Inorganic

- Dye synthesized solar cell and other organic solar cells [8]

1.3 Organic Electronics

The make-up of an electronic device could be either inorganic or organic [9]–[11]. Examples of organic electronics are organic light-emitting diodes (OLEDs), organic field- effect transistors (OFETs), organic photovoltaics (OPVs) and photo-detectors. Organic electronics are now applicable to photovoltaic (PV) technology to solve the growing energy challenges that will take an integral part in future energy production. However, the performance of organic electronic devices' and the lifetimes of OPVs depend critically on the properties of active materials used and their interfaces. One example is how surface energy and work-function greatly affect the

charge injection or extraction and transport in organic semiconductors. This is further explained in chapter 2. [12]

1.3.1 Advantages of Organic Electronic Devices

The organic photovoltaic (OPV) is an organic electronic device discovered in 1959, with the structure of an anthracene single crystal sandwiched between two electrodes. [13] For many years, its low efficiency, below 0.1%, prevented its commercial application. In 1986, its power conversion efficiency rose to about 1%. [14] From 1995, Yu et al. introduction bulk hetero-junction (BHJ) solar cell structures which also lead to various work that continue to increase these electronic device efficiencies. [6] Organic electronics has become a vastly developed field in the past two decades due to their promise of low cost, lightweight, versatility of chemical design and synthesis, ease of processing,[12] and mechanical flexibility as compared to inorganic solar cells. Recent improvements in efficiency from ~1% to 12% [15] have organic photovoltaic (OPV) cells commercially viable, since it is analogous to about 15% efficiency of silicon based solar cells. This suggests that organic electronic devices would evolve to be widely used in both rural and urban applications. Figure 1.3 below shows the schematics of an organic solar cell manufactured in the electronic industries.

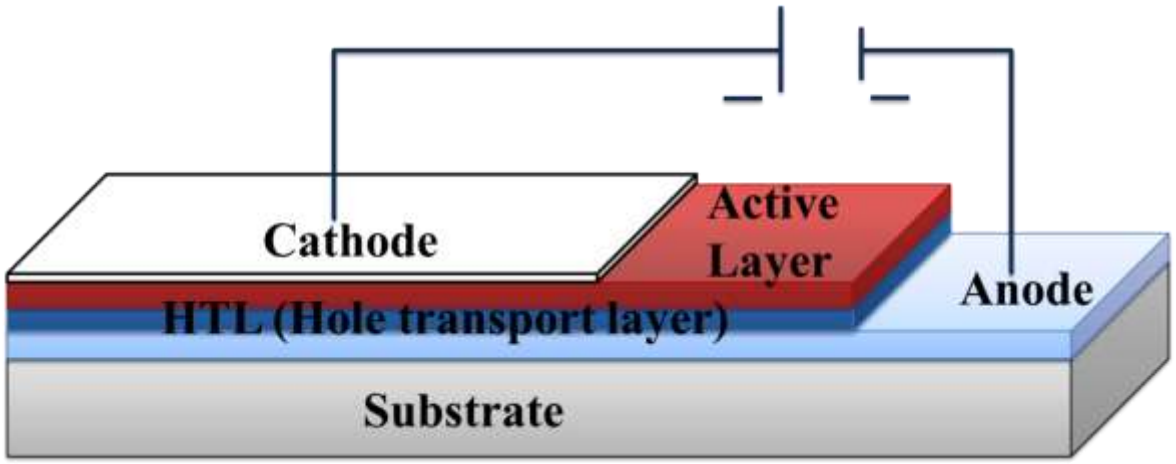

Figure 1.3: The Schematics of an organic photovoltaic cell

There has been increasing interest in the development of low cost organic electronic devices stimulated by the potential for significant processing cost reductions compared to the cost of their amorphous or crystalline silicon counterparts in solar cell and light- emitting devices [16]. The main advantages of the organic semiconductors over inorganic semiconductors in the electronic industry are: easier deposition of thin films, higher degree of sensitivity to external agents, a potential lower- cost on large scale production, higher absorption coefficient and greater flexibility [17]. However, the major merit is those very simple and low cost deposition techniques (e.g. sputtering, vacuum evaporation and spin coating) used to deposit these organic thin films on some suitable substrate.

1.4 Photovoltaic Energy Conversion and Make-Up

The ability to force electrons to move especially from the valence band to the conduction band [18] is what is termed as the potential difference or voltage. The potential difference across a conductor such as copper, silver and gold (they have one valence electron- good conductors) causes current to flow thereby providing electricity (see Figure 1.4) [19]. The conversion of

electromagnetic energy such as light (which includes infra-red, visible and ultraviolet) to electric energy in the form of current or voltage is termed photovoltaic energy conversion [7].

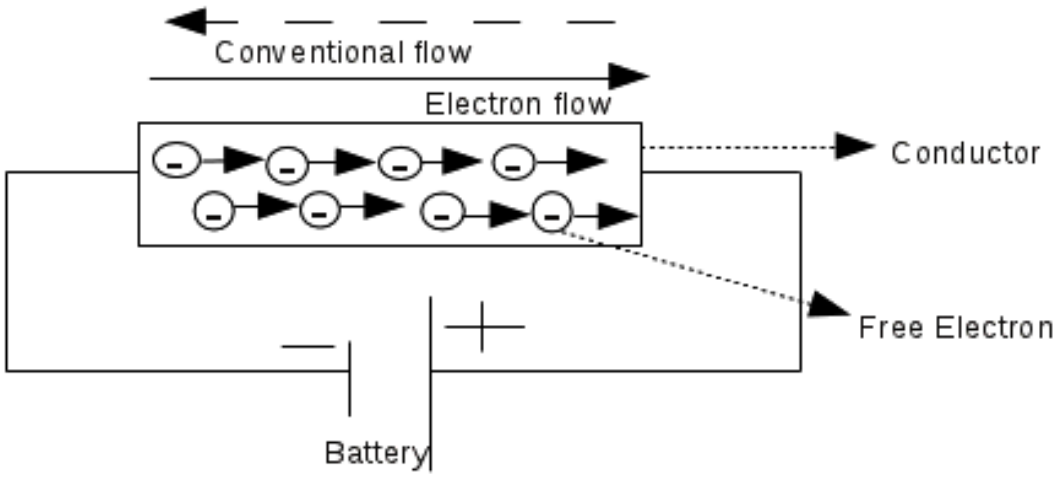

Figure 1.4: Electricity generation [19]

When the light is incident on the absorber/ material, it experiences a transition from a ground state to an excited state after which this excited state [20] is converted to free negative and positive charge carrier pairs. The free negative charge carrier moves to the cathode whiles the free positive charge carrier move to the anode. During this discriminating transport mechanism, the energetic photo-generated negative charge carriers arriving at the cathode result in electrons which move through an electric circuit losing their energy to electrical loads as they make their way back to the anode to recombine with the arriving positive charge carriers. This recombination process eventually returns the absorber back to its ground state [7].

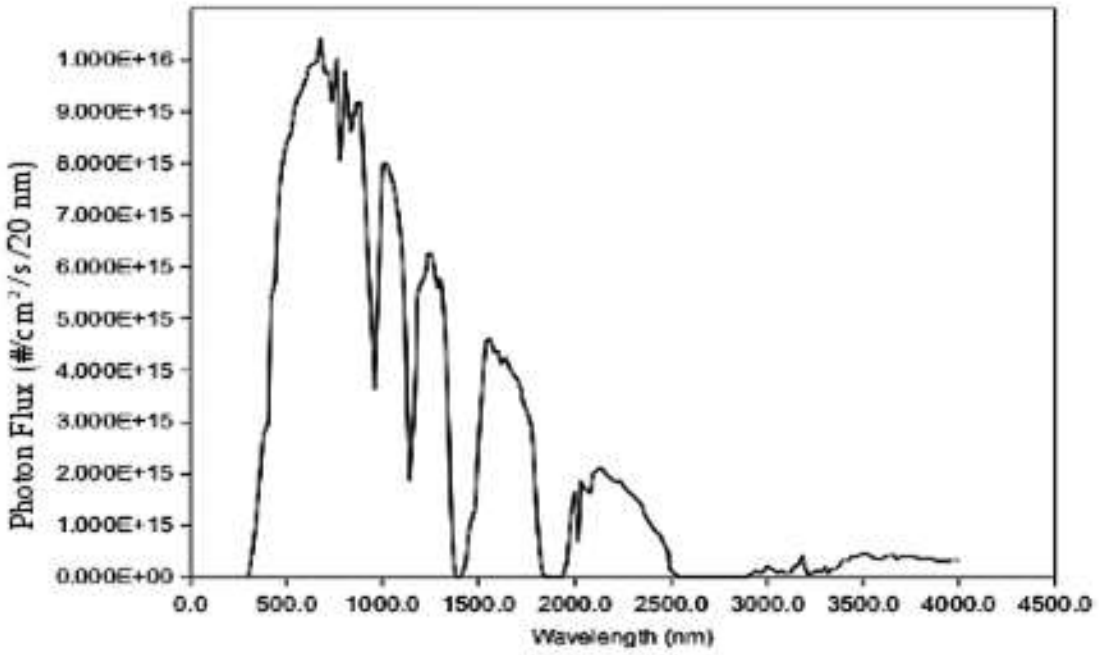

Figure 1.5: Solar energy spectra[7]

In solar cells' energy generation, photon spectra as depicted in Figure 1.5 are much preferred because in the most desirable way one photon translates to an electron- hole pair for the energy conversion (see Figure 1.6 below).

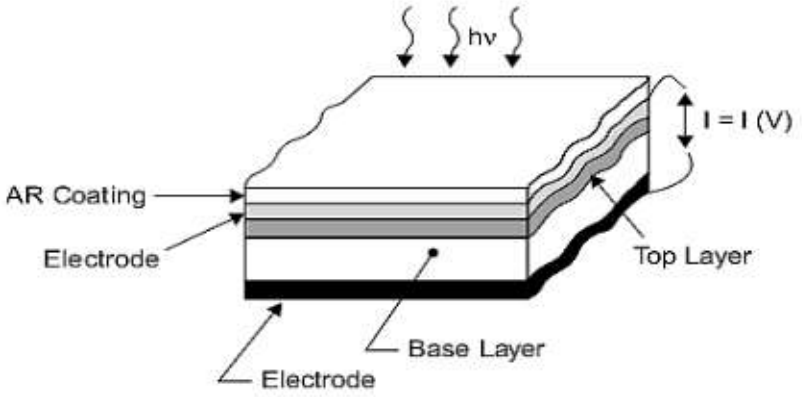

Figure 1.6: Cross-section of a typical solar cell [7]

1.5 Unresolved Issues

With so many research interests in electronic and optoelectronic system developments whose elastic response to strain far greater than 1% [21]–[31] act as the basis to addressing issues pertaining to wearable electronics [22], flexible health monitors [25], digital cameras and sensitive robot skins [23], [32]–[35]. Such device efficiency and reliability are affected in a drastic manner by the interfaces of the semi-conductor and the electrical contacts. Due to this, the electrical contacts have to be designed in a way that enables the interfaces to have low resistances, low operating voltages and stability to minimize device degradation [36].

Building electronic devices on deformable and flexible substrates is a requirement for novel large-area electronics, such as electronic textiles, electronic paper, sensor skin for robotics or medical prosthesis, and drape-able solar cells or flexible displays. [37] Amorphous silicon and other traditional solar technologies consist of brittle inorganic semiconductor device materials and as such crack easily when subjected to a significant amount of mechanical strain. There is, therefore, the need to understand the relationship between the optical performance of layered devices and that of the mechanical strain values applied to them [38]. Such strains can give rise to deformantion and cracking phenomena under flexural loading. With the knowledge of bending strains and their effects on the optoelectronic and failure mechanisms in bendable substrates, the brittle glass substrate mostly used in the manufacture of organic electronic devices, are being replaced with flexible or bendable substrates in flexible solar cells. In most cases [39]–[44], poly-dimethyl siloxane (PDMS) or polyethylene terephthalate (PET) substrates are used as stretched and bendable substrates respectively. PET is generally chosen over PDMS for flexible substrates. This is due to the former's inability to undergo stretching for being stiffer in Lu and Yang's report [45], but its flexural ability would enable the analysis of the effects of bending on

the multilayers feasible. However, there are relatively few studies [46]–[54] of the effects of bending on the performances of organic solar cells and their constituents.

Prior work has shown that for enhanced flexibility, minimizing the number of silicon chips assembled on plastic substrates and using nanostructured materials and stretchable substrates can be done [54]. Due to this, more investigations are still considered vital to access how mechanically reliable electronic devices that would not malfunction when submitted to dynamic bending cycles and how flexible these diverse technologies can be achieved.

1.6 Scope of Work

The objective of this research is to understand the effects of deformation on the optoelectronic properties of bendable organic solar cells. Following an initial study of the effects of bending of organic solar cells on PET substrates with indium tin oxide (ITO) anodes, the study focuses on the study of organic solar cells on PET substrates without ITO anodes. The effects of pre-buckled cathode/active bulk hetero-junction layers are also investigated for a range of pre-buckle geometries. The results show that the flexibility of solar cells can be improved by the introduction of pre-buckles with different wavelengths.

The thesis is divided into 7 chapters. Following the background and introduction, the relevant literature is presented in Chapter 2. The deformation of bulk hetero-junction solar cells is then modeled in Chapter 3 on flexible PET substrates with or without ITO anodes. The effects of pre-buckling are then explored in Chapter 4 before investigating the effects of impurity and pull-off technique involved in delamination process of cold welding in Chapter 5. Policy implications for

the applications of solar cells are considered in Chapter 6 before presenting the conclusion from this work and direction for future work in Chapter 7.

CHAPTER TWO

LITERATURE REVIEW

2.1 Background

The energy in light is directly converted into electrical potential energy through a physical process called the photovoltaic effect in solar cells. In 1939, Edmund Becquerel was the very first person to notice this photovoltaic phenomenon when he observed light-induced currents in a dilute acid. This phenomenon was elucidated in 1900 and 1930 by Planck and Wilson respectively via quantum concepts of light and solids. In 1954, the first solid-state photovoltaic cell also known as solar cell was designed. These cells' applications and their production rate has sky-rocketed since then and an example was when in 1991 enough photovoltaic modules was built to provide 50 MW of power. [55] "Expectations are that in the long-term, thin-film Photovoltaic technology would surpass dominating conventional solar Photovoltaic (PV) technology, thus enabling the long sought-after grid parity objective" [56]. Photovoltaic thin films initially appeared as small strips powering wrist watches and pocket sized calculators. This technology is currently obtainable in modules of very large sizes for charging systems such as vehicles and household electrical utilities. Since 1958, satellites orbiting the earth use PV cells to generate power. The Green Building Initiative (GBI) research projected thin film production to grow to 22,214 MW power in 2020.

This section delves into the literature work of others beginning from the historical evolution of the organic solar cell to the theoretical background of bendable organic solar or photovoltaic

cells. Relevant mechanisms have also been discussed to improve the lifespan and flexibility associated with organic thin film electronics.

2.2 Organic Solar Cells

Traditional organic materials, in the electronic industry, have been considered as insulating materials [57]. Photosynthesis is what inspired the earliest works using the idea of light being absorbed by chlorophyll which forms part of the Porphyrin group [58]. Electro luminescence (EL) response of organic molecular solids was first reported by Bernanose in 1955 [57]. In the 1970's, William et al. developed an organic semiconductor thin film instead of a single crystal semi-conductor films (done earlier by Pope and Helfrich [59], [60]) by vacuum evaporation and Langmuir- Blodgett method [61]. However, Tessler et al. were the first to successfully attempt to achieve lasting action from organic semi-conductor materials [62].

Currently, sensors, memories, OPVs, actuators, OLEDs, radio frequency identification devices and organic integrated circuits are various types of organic electronics under extensive investigations to improve their reliability and performance. Many of these low cost applications are the organic semiconductor based devices and as such, their efficiency and reliability needs constant improvements to enable it survive in the market [36]. Silicon solar cell electricity currently makes up over 90% of the photovoltaic (PV) market but its generated electricity is still more expensive compared to that from conventional fossil fuels. This is due to the single crystal wafers used in the manufacture of solar cells. The intent is to increase their efficiency since grain boundaries promote recombination and impede charge transport but the cost of manufacturing these single crystal wafers is very high so the need to look out for an alternative [63].

Depositing organic layers on electrode substrates followed by the deposition of a counter electrode are the basis to the preparation of organic electronic devices. In many instances metals are chosen for the electrodes and these can be doped with semi-conductor materials or conductive metal oxides. Stacking various semi-conducting materials on top of each other [64] in the bulk of the solar cell device leads to structures like p-n junctions [36]. The deposition methods and solution preparations were done according to standard techniques used as has been reported in various publications including that of [65] and [66].

The deposition methods of these layers vary significantly depending on the materials that the system used. Vacuum techniques are used to deposit small conducting organic molecules whiles printing, spin/ dip coating are used to deposit processed polymer solutions. Finally, thermal evaporation is used to deposit the top electrode layers [36].

2.2.1 Flexible Organic Solar Cells

Recently, the interest in the use of plastics as substrates for thin solar cells is increasing in order to again cut down on the costs of manufacturing by means of roll to roll deposition, aside the fact that they offer novel possibilities in building integration [67].

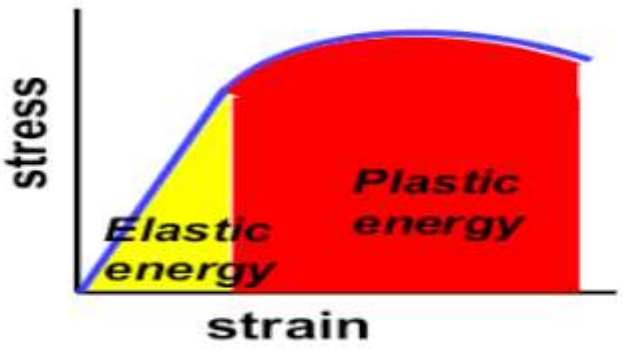

Figure 2.1: Deformation of plastic and elastic relation [68]

From Figure 2.1, it can be clearly noticed that the plastic deformation does not depend on Hook's law meaning it is a non-reversible process. Plasticity in structural design predicts the maximum load which can be applied to a body without the occurrence of excessive yielding aside the other aspect that deals with large plastic deformation requirement in changing metals into desired shapes [69].

In this thesis, PDMS or PET would be chosen as a substrate for the solar cell to be manufactured due to the attractive combination of the former's stretch- ability aside its ease of processing, and the latter's bendability [39].

The lack of the ability of PDMS to measure the angular separation of images that are close together (resolution) when used in intermediate molds propelled this chapter to use PET as the device substrate. This means that even though PDMS is ultraviolet (UV) transparent, its use in intermediate molds leads to replicas with smooth textures. Smoothing of these master textures has been demonstrated to be beneficial in solar cell application cases. Meanwhile, the detrimental or beneficial effects of replication losses cannot be guessed in general as they depend on the original or pilot textures and device configuration [67].

2.2.2 Layer Composition of the Organic Solar Cell

The bulk heterojunction organic solar cells will be fabricated on Polyethylene Terephthalate (PET) substrates with Indium Tin Oxide (ITO) anode already deposited on top via sputtering process. Poly-3-Hexylthiophene: [6, 6]-Phenyl-C61-Butyric acid Methyl Ester (P3HT: PCBM) will act as the active layer and Poly (3, 4-Ethylenedioxythiophene) Polystyrenesulfonate (PEDOT: PSS) as the hole injection layer. All the organic layers will be deposited by spin coating whiles the Al cathode will be by vacuum thermal evaporation. All these layers are

chosen because they are known to give the most desirable photovoltaic power conversion properties [70].

PET accounts for 18% of the world's polymer production making it the third most common synthetic polymer. “PET is aromatic/ aliphatic polyester which possesses very practical thermal properties that are not found in the all aliphatic commodity thermoplastics polyethylene or polypropylene. It has a glass transition temperature near 67°C and a melting temperature of 265°C”. [71] PET can exist as either amorphous (i.e. transparent) or as a semi- crystalline thermoplastic material (i.e. opaque and white). It is generally a good resistant to mineral oils, solvents and acids but very prone to bases. “The semi-crystalline PET has good strength, ductility, stiffness and hardness whiles the amorphous PET has better ductility but less stiffness and hardness” [72].

PEDOT is excellently transparent in the visible electromagnetic spectrum and is a good conductor electrically. But even though it is environmentally stable, like most conducting polymers, PEDOT is in-fusible and insoluble making it difficult to process in thin film form. Due to this, a dispersal of PEDOT in water doped with PSS has become the most promising and most extensively used hole-injecting material in organic thin film research today. [73] This thin layer of PEDOT:PSS on ITO surface increases the maximum luminance of the device, reduces the threshold voltage by more than 50% and eventually increases the lifetime by a factor of 10 [74], [75]. Lastly, the PEDOT: PSS acts as a physical barrier against the many defect sites present in the ITO [76].

Further analysis would replace ITO film with PEDOT: PSS due to its demerit in large area flexible electronic industry which includes cost and availability as well as its brittleness [77]–

[79]. This transition was confidently done in this research because of the similar photovoltaic power conversion characteristics they exhibit when used [70]. It should be noted also that using PEDOT:PSS as the hole transport layer (HTL) in the presence of ITO as the transparent conducting oxide (TCO) would etch the ITO electrode leading to a diffusion of indium into the active layer due to the acidic nature of most commercially available PEDOT:PSS [80], [81]. With PEDOT: PSS as both TCO and HTL layer, the observable degradation occurring in most Organic Photovoltaic Solar Cell (OPVSC) devices would be avoided.

Since limited absorption spectra and poor charge mobility are the main factors that affect the relatively low efficiency of organic solar cells, combining a narrow- band donor with a fullerene derivative will be an approach to solve this challenge. The most efficient fullerene derivative based donor-acceptor copolymer is P3HT: PCBM blends[82]–[84]. PCBM (fullerene derivative) plays the role of electron acceptor in many organic cells due to its high hole mobility tendency. P3HT is from the family of Polythiophene which is a kind of conducting polymer. The photovoltaic effect in the blend is due to the excitation of the p- orbit electron in P3HT [85].

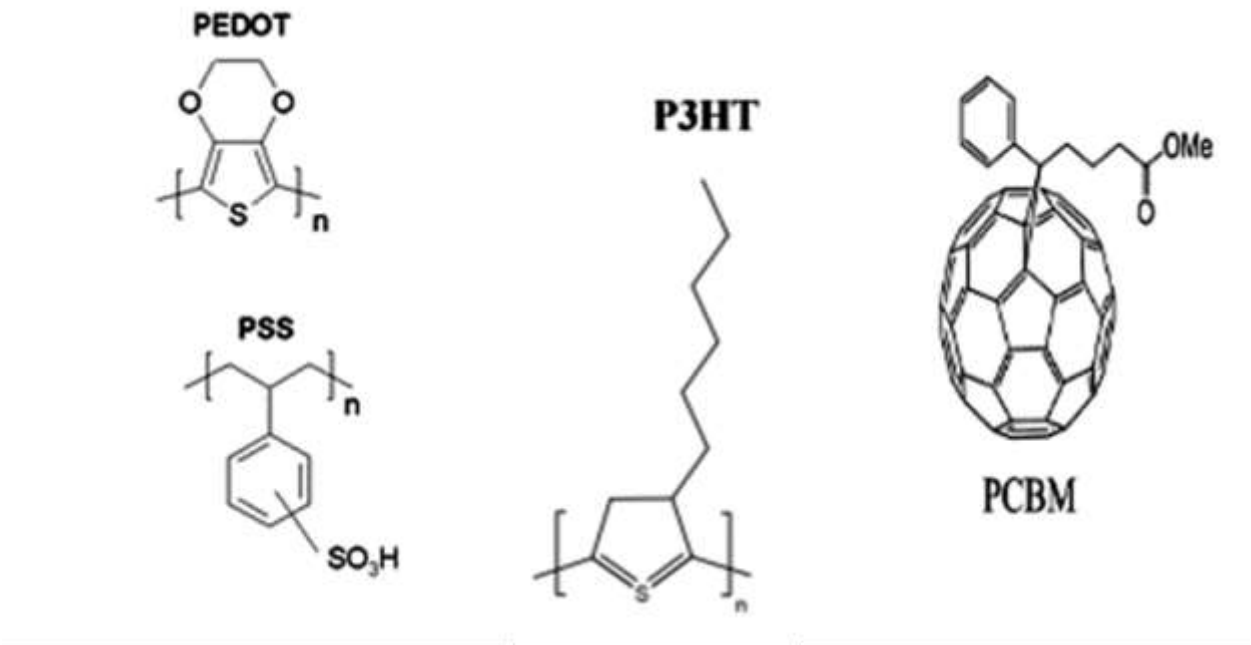

Figure 2.2: Chemical Structures of the Organic layers [86]

Figure 2.2 shows the chemical structures of the various constituents of the organic layer of the photovoltaic cell to be fabricated.

2.2.3 The Electrical Interactions at the Organic Solar Cell Interface

Abrupt and cleaner interfaces are allowed when organic semiconductors are deposited on metal.

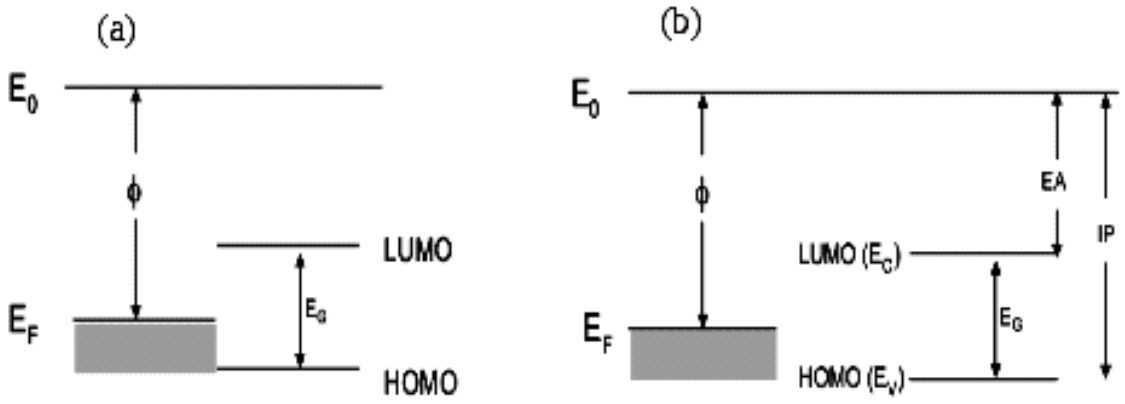

Figure 2.3: Energy level diagram of a metal and semiconductor (a) before contact (c) when contact is made.[36]

In Figure 2.3, the highest occupied state in the metal is denoted by E_F (Femi level). The minimum energy requirement for an electron to be removed from the surface of the metal to the vacuum level(vacuum of zero kinetic energy) is termed the surface work function (ϕ) whiles E_C and E_V are the valence and conduction band edges respectively. [36]

HOMO (Highest Occupied Molecular Orbital) and LUMO (Lowest Unoccupied Molecular Orbital) levels are the names given to energy bands in organic semiconductors since they are not continuous.

The difference between the vacuum level and the conduction band edge (which is a constant of the material) of the semiconductor is termed electron affinity (EA). The band gap E_G is also a constant of the material. The difference between the vacuum level and the valence shell is referred to as the ionization potential (IP). Also, the abrupt discontinuity of allowed energy states at the interface, in Fig 2.3 (b), is clear and this forms an energy barrier for charge transport and eventually affects the interface resistance. [36]

The closer energy level alignment suggests lower barrier at the interface and higher efficiency for charge injection. The rule for interface engineering is seen in matching the work function of the electrode with the EA and IP of the semiconductor. The Fermi level of a low work function metal aligns more closely with the LUMO level of the semiconductor with the assumption that the chemical potential of the metal and semiconductor do not equilibrate when in contact (as can be seen in Figure 2.4 below). Similarly, a high work function metal's Fermi level will align more closely with the HOMO level of the semiconductor. [36]

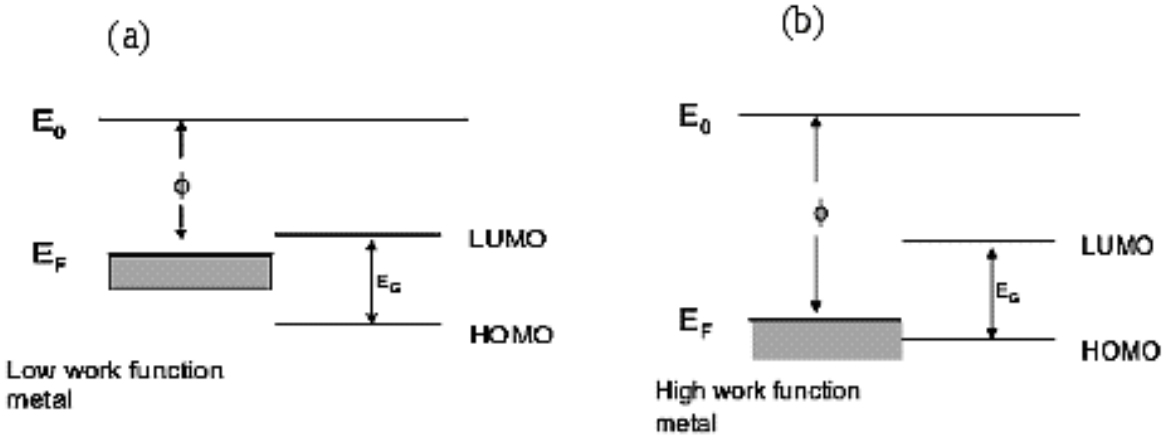

Figure 2.4: Energy offsets (a) Low (b) High [36]

In an ideal manner, there should be negligible resistance to current flow at the interface of the contact compared to the bulk of the semiconductor. So an essential task for engineering efficient semiconductor device would be to determine the energy states that contribute to the charge transfer since these states at the interface are not always energetically aligned causing a barrier for the charge transfer process. It should be noted that the charge transport process at the interfaces occurs from the de-localized states of the metal into the localized states of the organic semiconductor.

With adequate design, negligible resistance to current flow can be achieved at the metal/ semiconductor interfaces. For inorganic semiconductors, heavily local doping will provide tunneling or Ohmic contacts whiles it is not always viable for organic semiconductors. Organic semiconductor doping is an interstitial process, a substitution for inorganic crystalline semiconductors. [36]

2.3 Organic Light Emitting Diodes

Organic thin film materials vastly offer an untapped source of possible material properties useful in the semiconductor- based industries. Another organic thin film which is slightly different from the OPV is OLED (Organic Light Emitting Diode). Light-emitting diodes (LEDs) are optoelectronic devices that generate light when they are electronically biased in the forward direction. The light-emitting diodes that are made with organic materials are called organic light emitting diodes (OLEDs). Prior to the invention of OLEDs, organic-based devices could only be operated in electroluminescence mode. The first organic electroluminescence device was demonstrated in 1960s [87]. These devices were made with Anthracene single crystals doped with Tetracene (a red-emitting fluorescence dye) sandwiching between two electrodes [88]. Very high voltages were required for their operations and the efficiencies were very low. In the 1980s, a major breakthrough was made as low-voltage OLEDs were demonstrated [89]. In contrast to the first electroluminescence devices, the new OLEDs devices were based on a multilayer structure and they consisted of a transparent anode, a hole transporting layer, an electron emitting layer, and a cathode[90], [91]. During operation, electrons and holes are injected from a cathode and an anode respectively, and recombination of electrons and holes leads to efficient light generation [92]–[94]

2.4 Adhesion

Adhesion is known as a force of attraction existing between dissimilar constituent parts. These forces in nature could be diffusive, dispersive and chemical. When soluble molecules move across an interface between two adjacent materials then the adhesion is termed to be diffusive. An adhesion is dispersive when Van der Waals attractive forces exist between two joint molecules in a polar form. However, when a compound is formed by courtesy of a hydrogen, covalent or ionic bond holding two materials together, then the adhesion is chemical in nature. Contact surface area is vital when talking about adhesion strength because the bonds existing in between the interface are directly related to the strength. Here, the higher the bond strength the lesser the risk to break the two particles in contact.[95]

2.5 Fundamentals of Fracture Mechanics

The fundamental requirement of any structure is that it should be designed to resist mechanical failure through any or a combination of Elastic instability (buckling), Large elastic deformation (jamming), Gross plastic deformation (yielding), Tensile instability (necking), and Fracture. Even though most of these failure modes are relatively well understood, and proper design procedures have been developed to resist them, fractures that cause major damage in structures [96] are the least well understood. Considering strength alone in a design is unsafe since this may result in other instabilities such as buckling when dealing with trim or lean structures. Therefore failure curves for such structures would show a smooth transition in the failure mode from sections based on gross section yielding to those based on instability.

Buckling or delamination of the layers from its substrate at a strain depends on the adhesive strength between the two layers. It should however be noted that films such as ITO, due to their brittleness, are likely to crack, buckle or delaminate under compressive loading. It has also been

found out that at a strain of ~1% ITO cracks. Small cracks form prior to electrical failure. Under cyclic loading, these small cracks grow via fatigue. Akogwu, in his thesis work, made mention of how to delay the onset of ITO losing its conductivity through tension by reducing its thickness[38]. This was achieved using a non-brittle undercoat with high modulus for the ITO layer. From literature, the critical strain for cracking is similar to what is seen in ceramic films which is the reciprocal of the strain to the square root of lm thickness [38], [97], [98]. Cracking mechanisms and their effect on thin film properties has been investigated by Bouten et al. [97] who specifically considered ITO films on PET substrates.

2.6 Micro-buckling

A bar undergoing bending is described as a material leaving its equilibrium form to a state of instability. A basic thermodynamic principle is that free energy minimization occurs in the equilibrium of stable states. This principle is however hard to establish because, of the difficulty in locating a minimizer among the possible states. This is also due to the inability to absolutely define the entire possible states. In an attempt to solve this, all the modes of instability would have to be completely defined as in experiment so as not to lose any observation in the quest to make the problem formulated in class solvable. Explaining free energy wholly during instability would mean talking about buckling, wrinkling [99], crease [100], rupturing, vaporization or oxidization of solids into elementary particles. This mode of instability has been analyzed by E. Hohlfeld and L. Mahadevan. [101]–[103]

A buckle occurs at a critical value when bending states are included in restricting homogenous states on application of a compressive force. Wrinkling takes place when a bar’s width is short compared to its length. Here, the surface is perturbed since the homogeneity of the shape becomes exceedingly unstable despite the force of compression being below the critical value

that leads to buckling (Euler buckling). Rupturing takes place when the stretch is very large despite the fact that the material may not neck under tension (E.g. Rubber).

2.7 Wrinkling

A polymer substrate has the ability to stretch beyond 50% when bonded to a thin metal film. This happens because the substrate has the ability to delocalize strain when the metal film is well bonded to it causing both to elongate indefinitely till the polyimide substrate ruptures.[104]

2.8 Theory

The challenging aspect of flexible substrates in solar cell manufacturing is the extent to which it can be deformed. This can be investigated by its stress and strain relationship. For a substrate of length, L with a central or neutral line length, Lo after bending defines strain, as:

$$\text{Strain, } \varepsilon = \frac{L - L_o}{L_o} = \frac{\left(R + \frac{w}{2}\right)\theta - R\theta}{R\theta} = \frac{w}{2R} \qquad (2.1)$$

If the distance from the central line to the surface of the substrate is w/2 in this case is converted to an arbitrary number say "π", then the strain becomes; $\varepsilon = \pi/R$. Clearly, the strain is directly proportional to π, meaning that the smaller the substrate thickness the lower the strain. The results are very desirable since we seek to manufacture a solar cell of very low strain when bent. Relating this results to the stress ($\sigma = E\varepsilon = E\pi/R$) means that the deformation of the manufactured solar cell could be studied. This implies that $\sigma/\pi = E/R = M/I$; where E is the Young's modulus, R the radius of curvature, M the moment and I the moment of inertia.[38], [105]

For a thin film on a flexible substrate, the elastic stresses in the thin film are given by Brunner et al. [51] based on approximations made on Timoshenko and Reddy's work[106] for thin films on a thick substrate. For such a case where one layer is much greater than the other composites (i.e. $\sum_i t_i << t_S$), the summation term signifies the total thickness of the thin films on the substrate whiles t_s signify that of the substrate.

The solutions for this case are most useful with the biaxial description of a composite plate with different moduli in each layer taking note that the ratio t_i/t_s term which is less than unity from the first to higher order terms has been neglected for the analysis. This simplifies the position of the neutral plane, π to for structures containing N layered thin films[51];

$$\pi = \frac{t_S}{2} + \sum_{i=1}^{N} \frac{t_i E_i (1 - \nu_S)}{2E_S (1 - \nu_i)} \tag{2.2}$$

Here E and ν have their usual meaning. This equation shows that the neutral plane or line is only slightly displaced from its original position in the bare substrate (See Figure 2.5).

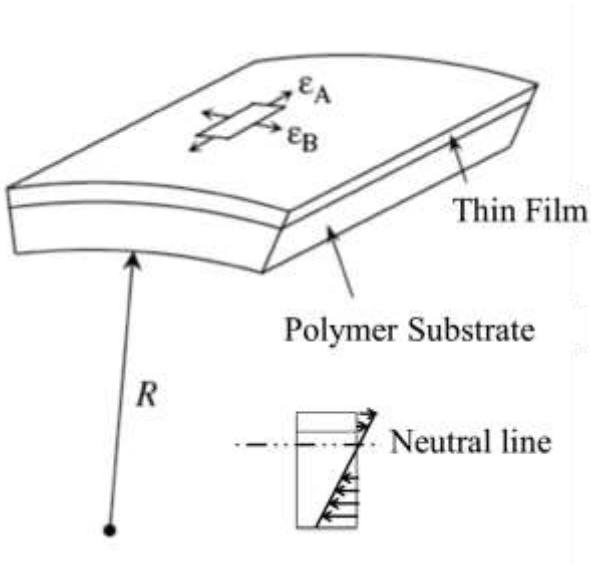

Figure 72.5: Elastic stress (i.e. $\varepsilon_A = \varepsilon_B = \varepsilon$) in thin film on a polymer or flexible substrate undergoing bending showing its radius of curvature, R and newly positioned neutral line.

2.9 Green Roofing Structures

The National Stadium in Kaohsiung, Chinese Taipei, is topped with 8,844 solar panels covering 14,155 m^2 (152,362 sq. ft.). These generate 1.14 million kWh electricity everyday which caters for 80% of the venues needs. If it this stadium was powered by traditional power stations, 660 tonnes (1.45 million lb.) of Carbon dioxide would be released annually. Designed by Toyo Ito from Japan, the stadium's shape is said to be based on that of a curled dragon leading to it ending a spot in the 2015 GUINNESS Book of Records. [107] Replacing these brittle silicon based panels with robust and flexible organic solar panels would be very vital for architects who would prefer a more robust system that can be easily integrated into their designs instead of adjusting their designs to accommodate fragile systems which might eventually ruin the picturesque setting.

OPV modules manufactured on flexible substrates and packaged with flexible low performance barriers are known from literature to be sufficiently stable for both outdoor exposure and indoor experiments. [108]

In practicality, successful OPV devices are based on relatively stable organic materials combined with some encapsulation technology in the form of a plastic with good barrier properties. In roof-top studies, plastic-encapsulated solar cells were shown to have lifetimes of at least 3–5 years, with manufacturers reporting even longer lifetimes. [109]–[111] With this information, encapsulating the OPV via cold welding would highly improve the lifetime of the device in green roofing structures.

2.10 Cold Welding

Cold welding, which is also called contact welding, is a solid state welding process that involves the joining at the interface of two distinct parts without the use of heat [112], [113]. This process makes no use of liquid or a molten phase within the interfacial joint unlike fusion welding which involves heating. This phenomenon was first recognized in the 1940s [114] as a general materials phenomenon. It was revealed then that under vacuum conditions, two clean surfaces (flat) of similar material properties (e.g. metal) would strongly adhere if brought into contact. This idea has been inculcated in nanofabrication processes due to micro [115]–[117] and nano-scale cold welding's [118] great potential. The idea for backing this mechanism is that when the atoms in contact are all of the same kind, there is no way for the atoms to discover that they are in a different material from theirs. However, it should be noted also that this breaks down only when grease, dust particles or other impurities are embedded within the interface for the cold welded joint to formulate. This brings to mind that the two flat surfaces to be cold welded should be clean to avoid interfacial failure from occurring in the welding process especially during the

pull off of the stamp used for this process. See figure below showing the two types of cold welding mechanisms.

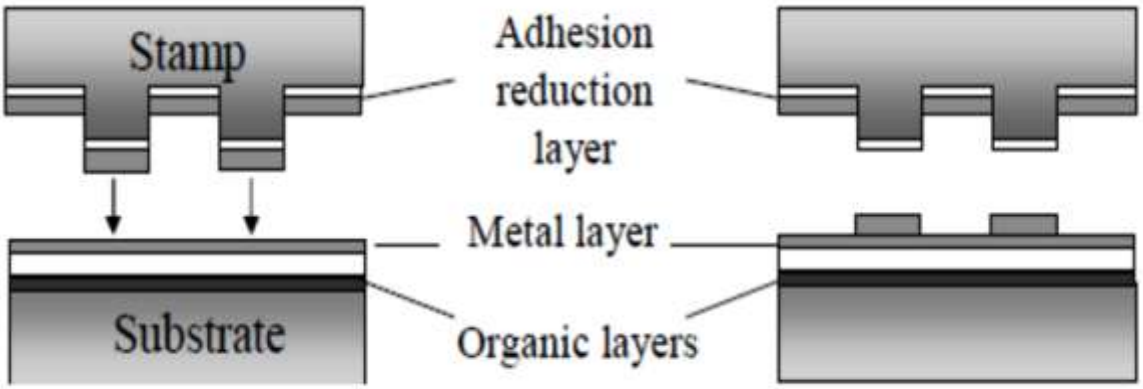

Figure 2.6: Additive Cold Welding[119]

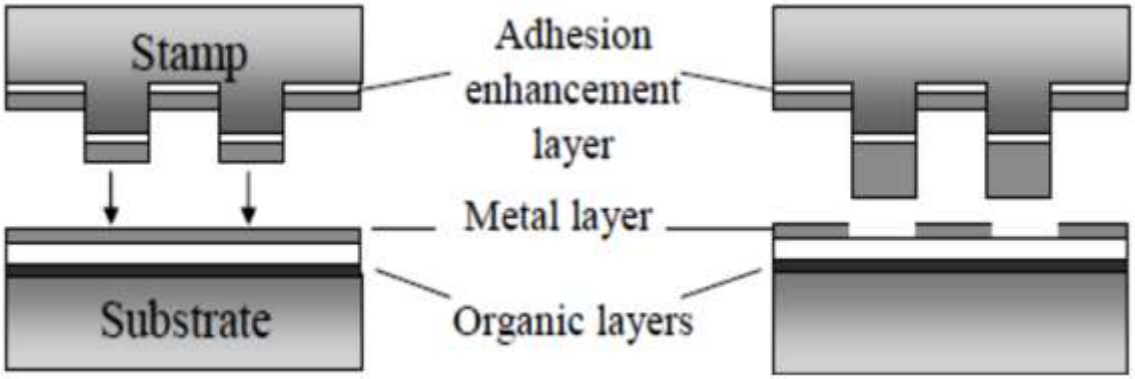

Figure 2.7: Subtractive Cold Welding [119]

The Cold welding technique is mostly used to encapsulate organic electronic devices to due to their sensitivity and reactiveness of low work-function metals used for their fabrications. The immediate use of these devices as cheap and accessible alternatives are limited in the presence of ambient moisture and oxygen so encapsulating reduces their sensitivity the environment. [120]–

[123]. Figure shows some of the applications of cold welding which include Microelectronic packaging.

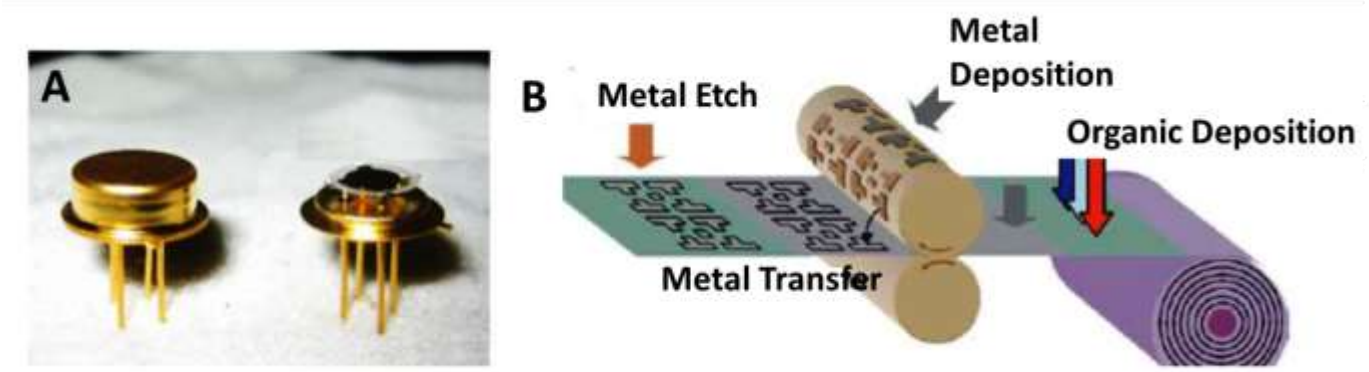

Figure 2.8: Applications of cold welding (a) microelectronic packaging (b) roll-to-roll fabrication technique used for organic electronic devices [119], [124]

"Most transfer substrate has often been made of silicon which is stiff but the device substrate material can range from modestly compliant polymers (e.g., polyethylene- terephthalate, PET and polyimide) to extremely compliant rubberlike elastomers (e.g., polydimethylsiloxane, PDMS). The wide range of device substrate stiffness (e.g., from 10 GPa to 1 MPa) and the huge stiffness ratio between the transfer substrate and the device substrate (e.g., from 10 to 105) can lead to rich characteristics of the competing delamination, which are far from well understood." [125]

CHAPTER THREE

FAILURE MECHANISMS OF FLEXIBLE ORGANIC SOLAR CELL STRUCTURES UNDER BENDING

3.1 Introduction

In recent years, there has been increasing interest in the development of flexible organic solar cells with the potential to replace silicon-based solar cells[49], [126]. The interest in organic solar cells has been due largely to their potential for lower cost [127], [128] and application in bendable [26], [129] and stretchable solar cells that can be draped over roofing tiles and flexible electronic structures [39], [130]. This is in spite of the moderate efficiencies of 12%[15] that have been achieved largely through significant efforts to develop Bulk-Hetero-Junction (BHJ) solar cells [6], [131]–[140] or Small Molecule Active Layers (SMAL) with planar structures.

However, unlike flexible electronic structures with metallic wires and surfaces in which failure mechanisms have been studied under monotonic and cyclic loading [39], there have been relatively few efforts to study the deformation and failure mechanisms layered structures that are relevant to bendable or stretchable organic solar cells [49], [66], [141]–[145]. Since such materials and layered structures can deform and fail by a number of deformation mechanisms, there is a need to develop a fundamental understanding of the possible deformation and failure mechanisms that can occur in flexible [146] organic solar cells [147]. There is also a need to develop a basic understanding of how deformation and failure mechanisms affect optical and electrical properties of materials and layered structured that are relevant to organic solar cells.

The paper presents the results of computational and experimental study of the deformation and failure mechanisms in materials and layered structures that are relevant to bendable organic solar cells. The stress and strain distributions associated with flexural loading are elucidated using analytical and computational models that incorporate the results of nano-indentation and micro-testing measurements of layered mechanical properties. The computed stress and strain distributions are then related to failure mechanisms observed during cyclic bending experiments that are conducted on model specimens with PET substrates [148]. The resulting changes in optical transmittance are also related to the observed deformation and failure mechanisms. The implications of the results are then discussed for the design of flexible organic solar cells. It should also be noted that since this work deals with thin films, plane stress conditions would be employed [105].

3.2 Modeling

3.2.1 Analytical Modeling and Finite Element Modeling of Deformation and Cracking

The stress and strain distributions in the different layers of the model organic solar cell (Figure 3.1) were computed using the finite element method. The modeling was carried out using the ABAQUS/CAE 6.12-1 software package (ABAQUS, SIMULA, Pawtuckettm, RI, USA). The model used prior measurements of Young's moduli that were obtained using Nano indentation methods [149]. These are summarized in Table 3.1 with their corresponding Poisson's ratios. The measured moduli were incorporated into finite element simulations of the linear elastic deformation of layers in the model OPV structure.

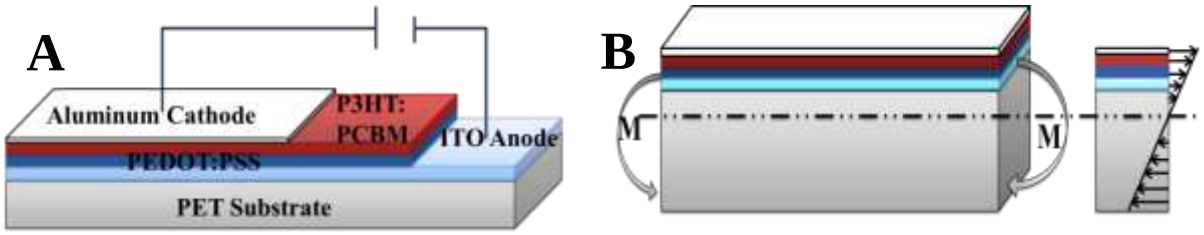

Figure 3.1: (a) Schematic of Flexible Organic Solar Cell on PET Substrate (b) Bending Moments and neutral line depiction on the Flexible Organic Solar Cell

Table 3.1: Material properties

Materials	**Young Modulus, E / GPa**	**Poisson ratio**	**Source**
PET	2.5	0.3	Ref:[149], [150]
PEDOT:PSS	1.42	0.3	Ref:[149]
P_3HT:PCBM	6.0	0.35	Ref:[151], [152]
ITO	116	0.35	Ref:[149], [153]
Al	70	0.3	Ref:[105]

The modeling with Abaqus/ CAE 6.12-1 began with the step of creating the parts as a 2D and 3D deformable shell planar, with dimensions corresponding to the physical specimen. The architecture of the multilayer system used was PET (107 µm)/ ITO (90 nm)/ PEDOT: PSS (100nm)/ P3HT: PCBM (90nm)/ Al (200nm). The material properties where defined to represent each layer using their Poisson's ratios and Young's Moduli in Table 3.1. The support effects were modeled and the boundary conditions used depicted the 3 point bend fixture as can be seen in Figure 3.2.

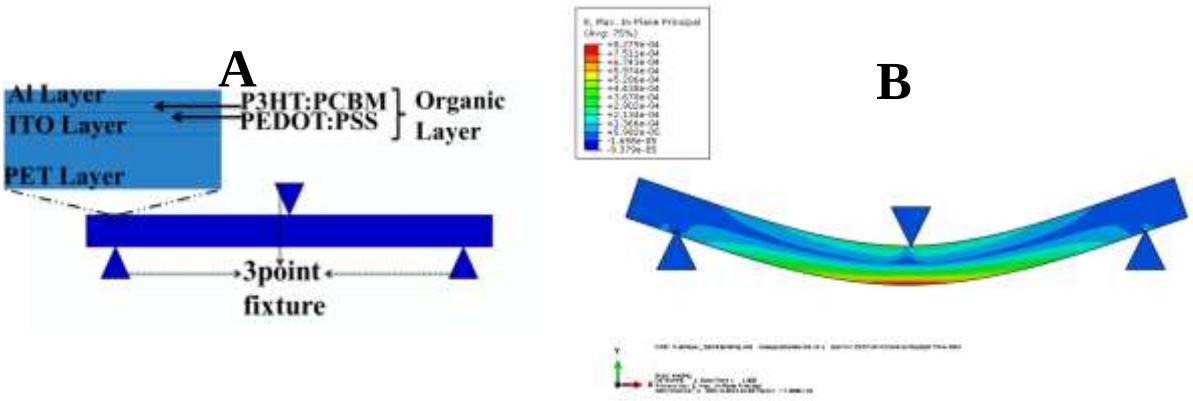

Figure 3.2: (a) Geographical view of multilayer and its 3 point bend fixture model created (b) Strain contours of OPV deformed multilayer structure at the maximum loading point of a compressive 3 point bend test just before unloading occurs in a single bend cycle.

The model is instanced and meshed as dependently followed by assigning interaction properties to all the sections in contact with the 3 point fixtures. Also, all sections were defined to have structured quad element. The boundary conditions set at the stoppers included fixing in the X, Y and Z direction (i.e. U1, U2 and U3). The middle roller was set to displace downward (i.e. move only in the U2 direction as depicted in Figure 3.2).

In the 3D model, a tunneling crack was introduced in the ITO layer to simulate its crack driving forces. The crack tips were modeled using much finer element sizes (See Figure 3.3A and 3.3B). These were used to compute the path independent J integral (J_i)/ energy release rates (G_i) using the relation for a plate deformed under three-point bending:

$$J_i = \frac{K_i^2}{E'} + \frac{2A_i}{B(W-a)} \qquad (3.1)$$

Where K_i is the stress intensity factor, B is the specimen thickness, A_i is the area under the load displacement curve, (W-a) is the remaining ligament, and E' = E for plane stress and E' = E/(1-ν^2) for plane strain for the specimen used [105]. It should be noted that plane strain was employed since the thickness of the substrate was very much greater than the multilayers deposited on it.

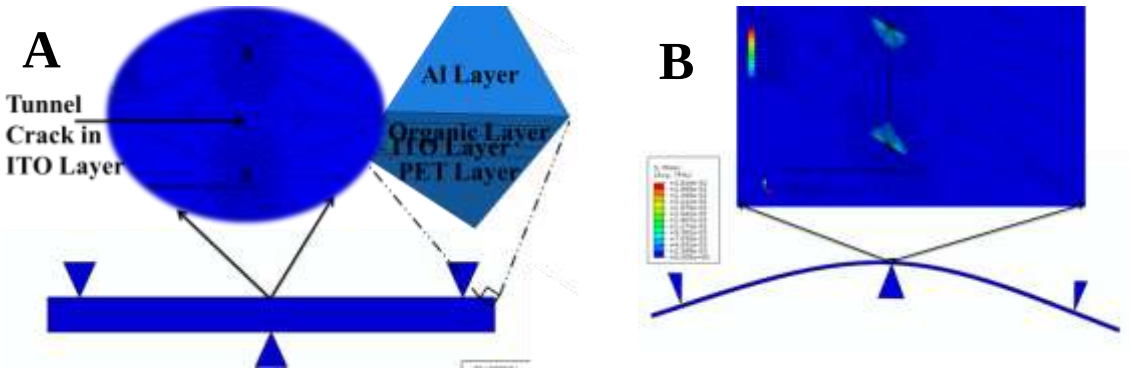

Figure 3.3: (a) 3-dimensional elemental meshing of tunnel crack in ITO layer (b) 3-dimensional simulation crack growth in ITO layer during bending of the multilayer

3.2.2 Modeling of Optical and Electrical Properties

3.2.2.3. Thickness Determination of ITO on PET

The ITO layer, with its thickness unknown, was completely covering the PET substrate. The surface profiler was used to find this thickness but scratching two places on this ITO/PET multilayer. The flexibility of the PET substrate made the results obtained inconclusive since there was likelihood that the scratch penetrated the substrate. Figure 3.4 has the scanning results which suggested that the thickness was between 7000 to 9000 Armstrong.

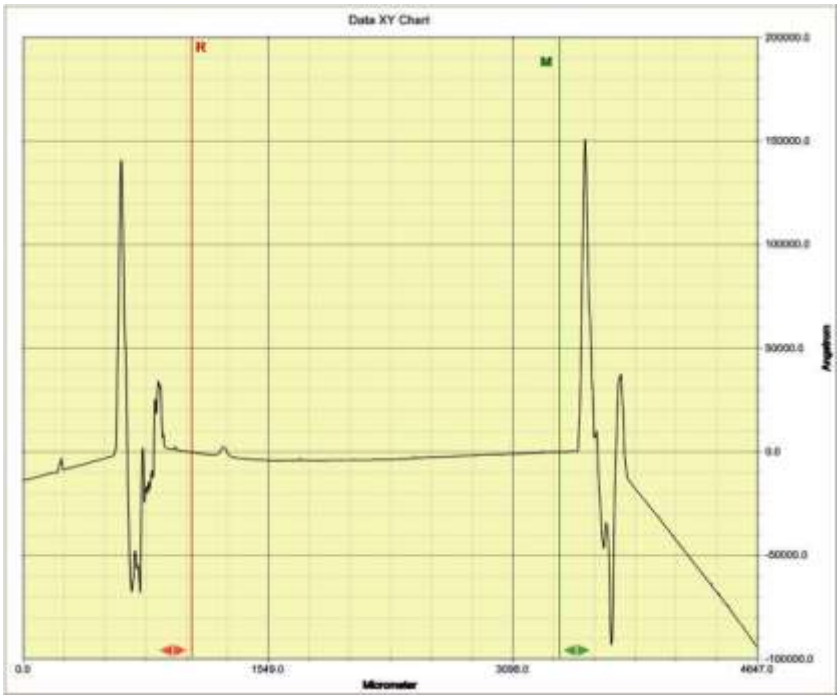

Figure 3.4: Surface Profiler results indication ITO film thickness range from 70000 to 90000 Armstrong

Confirming the thickness of ITO deposited on the PET substrate started with an Ultraviolet (UV) spectroscopy measurement of the ITO/PET multilayer light transmittance. This ITO thickness confirmation involved modifying an optical index file (see Table 3.2 and Table 3.3) created earlier by Schubert [154]. In an effort to determine and characterize the multilayer, the experimental transmittance of unbent ITO on PET (See Figure 3.5) obtained were first uploaded into the optical program and plotted merging all the important index files together. The ITO thickness range was then assumed and used to calculate the actual ITO layer thickness. To confirm the calculated thickness data, the guess was repeated and thickness estimations were repeated until the new plot from the modified optical index file coincided with the experimental plot, hence, ascertaining the guessed value of the ITO thickness. This was done assuming the experimental accuracy to be ± 2.0 % of the full scale.

Table 3.2: Format of Index file of PET saved with ".in3" extension

This is a PET Index File Format		**First row or line in text editor left blank for comments**
1000	20000	Second role has the first and last wavelengths in units of Armstrong
2		Third role indicates the number of wavelengths with their corresponding indices used
1000	1.58	First wavelength and index respectively
20000	1.64	Second and last wavelength and index data
2		The value 2 indicating 2 corresponding index and extinction coefficient data
1000	0	First coefficient data corresponding to wavelength value
20000	0	Last wavelength value with its corresponding extinction coefficient data

Table 3.3: The Data File (in ".dat" file format)

Wavelength [nm]	Transmittance [%]
300.47	0.5909
301.06	0.5703
…	…
798.88	79.32
799.44	79.385
800	79.928

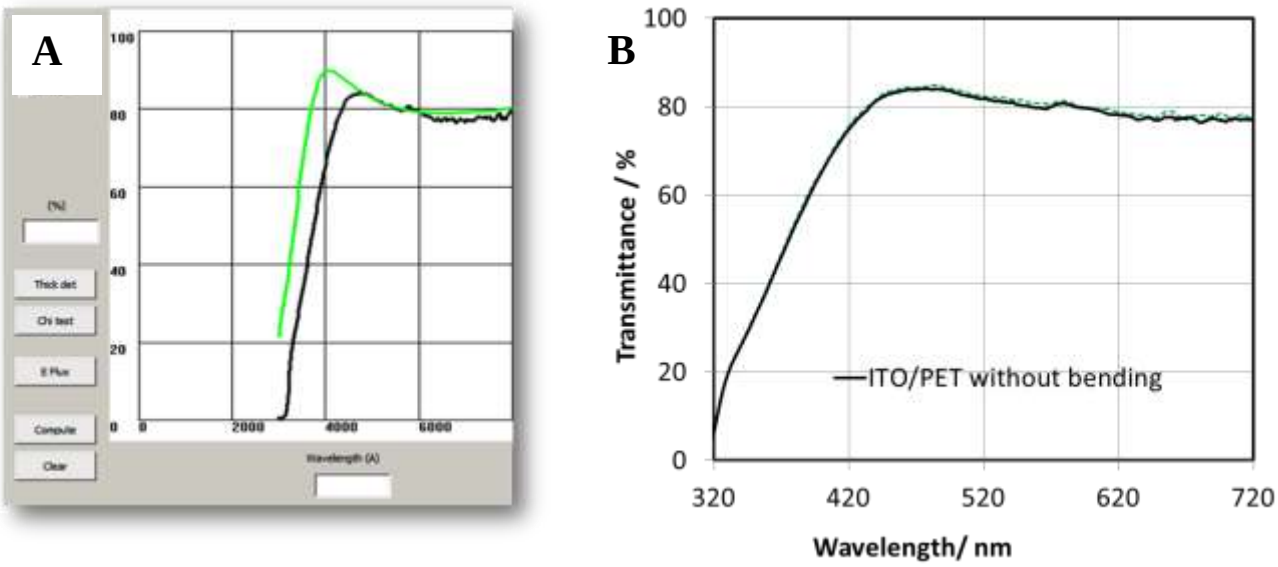

Figure 3.5: (a) Optical Simulation of results showing a mismatch between wavelengths ~ 3000 and 4500 Å (b) Experimental transmittance data file of ITO on PET

This Optical analysis of the ITO/PET layered film done based on transmittance shows that about 96 nm average thickness of ITO layer on PET substrate was needed for the optimum optical performance of flexible organic solar cells. The optical transmittance simulation data for ITO/PET multilayered film were used to explore and estimate the ITO thicknesses needed to improve the performance of flexible solar cells. Optimum ITO thickness were obtained and compared with the experimental ITO thickness values obtained from the Surface Profiler.

There is a shift between the simulated and experimental transmittance values of the ITO/PET in the spectrum with wavelengths between ~ 3000 and 4500 Å. This mismatch can be attributed to the non-idealness of the ITO or PET structure obtained from SOLARONIX as this may account for changes in optical band-gap of experimentally prepared ITO/PET material causing the observed differences[155]. Interfacial defects could also account for this shift.

After comparing this result with that from the Surface Profiler motivated the need to calculate the actual thickness using Rutherford Backscattering (RBS) Technique. ITO thickness was found to be ~90 nm, but this was assuming a composition of Indium, In = 0.333, Tin, Sn = 0.057, and Oxygen, O = 0.610 combined with an impurity composition of the same thickness of Carbon, C = 0.333, Oxygen, O = 0.08, Hydrogen, H = 0.59. This RBS measurement was done by Dr. Leszek Wielunski of Rutgers University, USA. In this work, the stoichiometric configuration of the ITO was relatively not ideal, advising an adjustment in the deposition process. Cleaning the thin film in clean room environment would also minimize impurity effects.

3.3 Experimental Methods

3.3.1 Materials Fabrication

The device configuration explored in this work is the Al / P3HT: PCBM/ PEDOT: PSS/ ITO/ PET structure (see Figure 3.1). The model OPV samples were prepared on ITO-coated PET substrates (SOLARONIX Ltd, Aubonne, Switzerland) with square cross sections of $25 \times 25\,\mathrm{mm}^2$ sheet resistance, R_s = 60 Ω/square. The substrates were ultrasonically cleaned in acetone and iso-propyl alcohol (IPA), rinsed in deionized water and blown to dry with nitrogen gas.

The transmittance and absorbance of the ITO-PET thin film multilayer were measured with an AvaLight-DHc UV-VIS spectrophotometer (Avantes Inc., Broomfield, USA) in the wavelength range 300-1100 nm. The hole injection layer PEDOT:PSS solution (H.C. Stack Inc., Newton, MA, USA) was filtered with 0.2 µm filter paper and 0.4 ml of the filtrate was deposited using a model WS 650 Hz Laurel spin-coater at rates of 500 rpm for 5 s, 1500 rpm for 3 s and 3000 rpm for 60 s. The samples were subsequently baked in a carbolite oven for 15 min at 100 ^{o}C. The

P_3HT and PCBM materials that were used in the active layers were from Sigma Aldrich, St Louis, MO, USA. Three tenth milliliter of the mixture was spin coated on the PET/ITO/PEDOT.PSS with two spin cycles at 400 rpm for 10 s, and 800 rpm for 30 s. The sample was again baked on a hot plate for 15 min at 140 ^{o}C.

The Al cathode (99.99 % pure pellets, Leskan, Philadelphia, PA, USA) of 200 nm thick was thermally deposited in an Edwards FL 400 thermal evaporator with a tungsten boat at a pressure of 2.0 x10^{-5} Pa. This was done inside an argon gas chamber flowing at a rate of 0.8 SCCM, based on the earlier procedure reported by Demirkan [36].

3.3.2 Bending Experiments

The OPV devices were tested using 3-point bending in an Instron Model 5848 Micro-tester which was operated at a ramp distance of 6 mm, and a ramp speed of 0.03 mm/sec. The applied loads were between 0 and 1.28 N. The resulting force-displacements curves were used to generate stress-strain (σ-ε) curves from the following fundamental expressions [105]:

$$\sigma = \frac{\text{Force}}{\text{Area}} \tag{3.2}$$

$$\varepsilon = \frac{\Delta L}{L} \tag{3.3}$$

where ΔL and L are the change in length and original length respectively of the thin film being analyzed.

3.4 Results and Discussion

Force-displacement curves obtained from the tests on the model flexible OPV are used to calculate stress- strain curves of both tensile and compressive cyclic bending of the various

multilayers of the OPV. From the graphs in Figure 3.6, it can be seen that the initial linear elastic deformation is followed by elastic unloading to zero force and displacement. Hysteresis losses can be identified occurring from the unloading part of the stress strain graph calculated from the force displacement results attained from the Instron micro-tester.

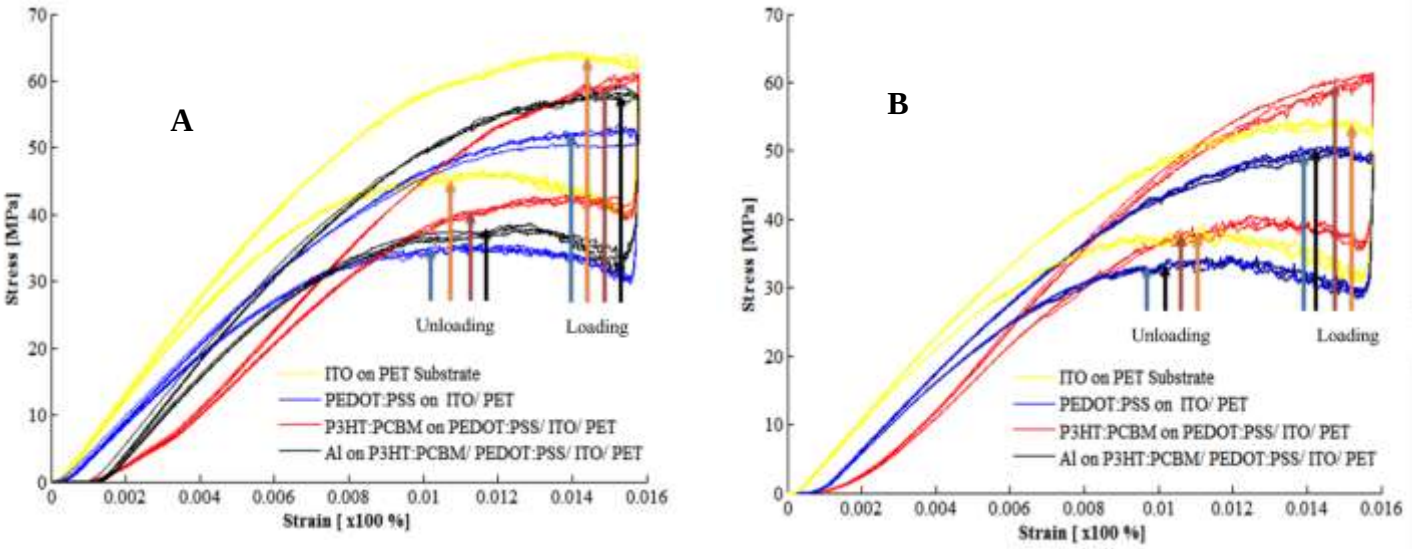

Figure 3.6: (a) Cyclic Compressive bending of various device multilayers (b) Cyclic Tensile bending indicating loading and unloading sections of the 5 cycle process for the various device layers

These loading and unloading results for the various device configurations indicate viscoelasticity of the substrate used (i.e. PET- Polyethylene terephthalate). Apart from the compressive bending being more susceptible to device failure in comparison to tensile bending, both have a maximum strain value of ~1.6%. Their stress saturation points range from 50 to 60 MPa for the compressive bending loading whiles that of tensile is between 48 to 60 MPa. These results compared with those in Figure 3.7 from the Finite element model shows that single cyclic tensile or compressive bending do not damage the multilayer thin film as would have happened

in the case of multiple cyclic bending even though the ITO layer experience the most strain which can be avoided by replaceing with another compliant TCO.

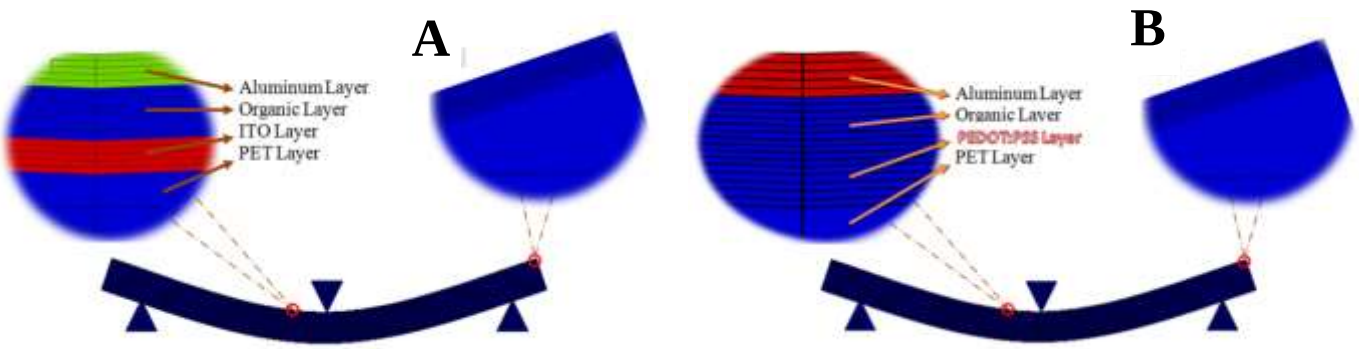

Figure 3.7: Comparing with Finite Element images; (a) OPV multilayer deformed structure with ITO (b) OPV multilayer deformed structure without ITO

3.4.1 Surface Topography

3.4.1.1 Atomic Force Microscopy

Atomic Force Microscope (AFM) tip was fitted with a 12.5 µm radius diamond tip purchased from Veeco Instruments (now Bruker Instruments) Woodbury, NY, USA to detect minute surface variations in the surface topography of the PEDOT:PSS film on the ITO/PET multilayer via scanning lengths within the ranges of 1000 and 4000 µm [130]. The topological micrographs obtained from the Atomic Force Microscopy (AFM) can be seen in Figure 3.8.

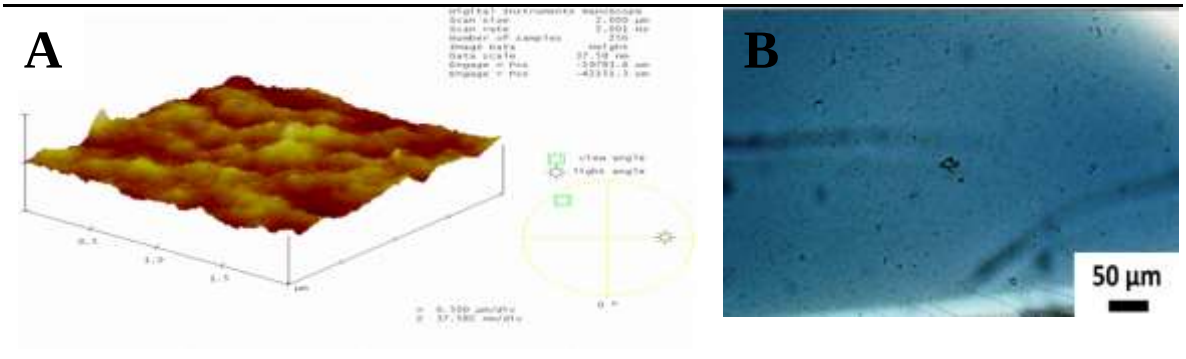

Figure 3.8: (a) and (b) are respectively, atomic force microscope and optical microscope image comparison of PEDOT:PSS on ITO/PET substrate

The surface roughness of the thin film layers in the model flexible organic solar cell thin film layers were characterized using a Veeco Dektek 150 Stylus Surface profiler (Veeco Instruments Inc., Plainview, NY, USA).

3.4.1.2 Optical Microscopy and Scanning Electron Microscopy

Initially, the PET substrate which had an already deposited layer of ITO, was optically characterized under a light microscope (Celestron LLC, Torrance, CA). It should be noted that the transmittance measurements were repeated after the flexural tests where done on the devices. Scanning Electron Microscopy (Carl-Zeiss Evo MA-10 SEM, Oberkochen, Germany) analysis was carried out on the samples to show the surface microstructural deformations of the thin-film layers before and after flexural analysis. Figure 3.9, 3.10, 3.11, and 3.12 compares the Optical images with SEM micrographs of the various multilayers before and after undergoing flexural deformations.

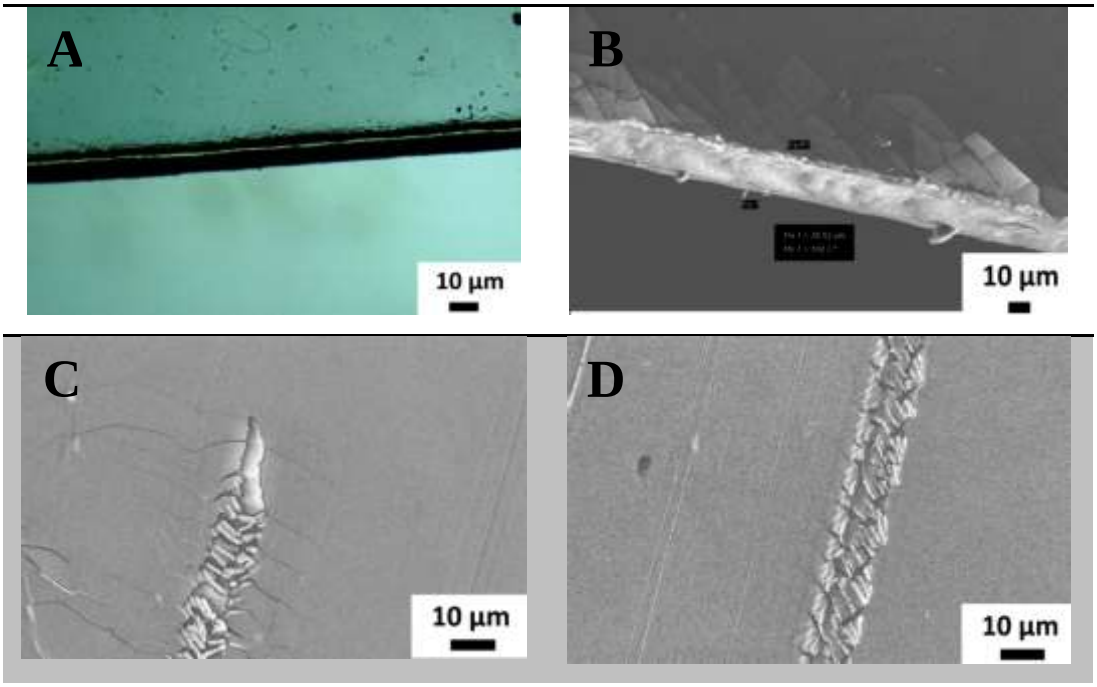

Figure 3.9: Comparison between optical microscopy image in (a) and SEM micrographs in (b), (c) and (d) of ITO on PET substrate. (c) and (d) show crack outlines due to tweezers handling by courtesy of the ITO's brittle nature.

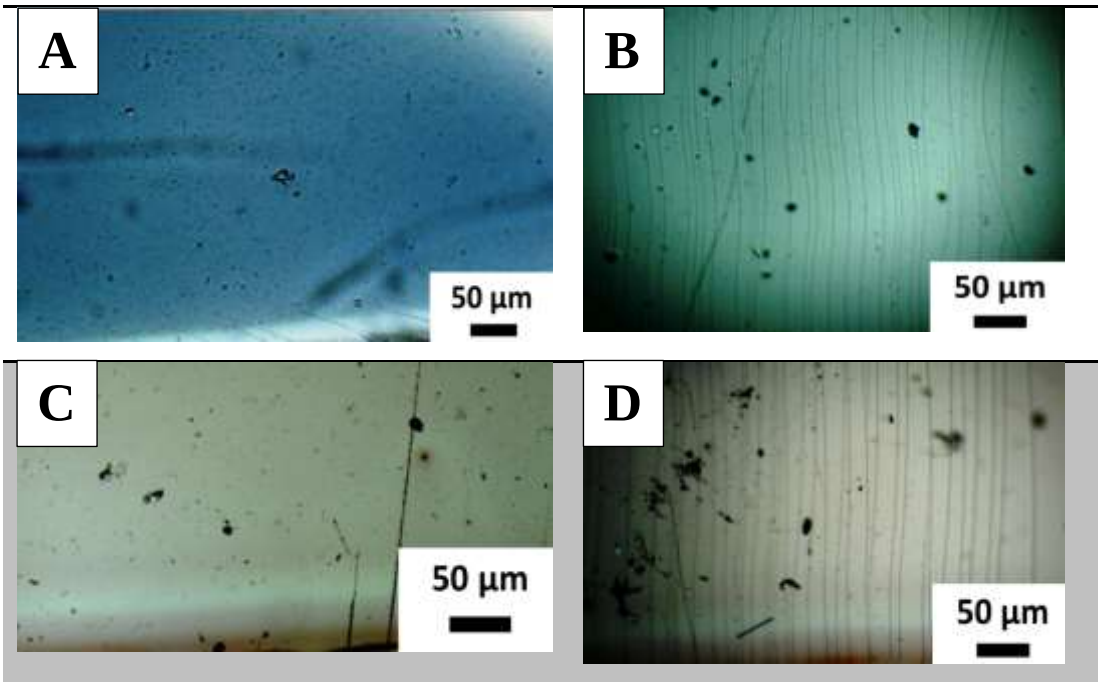

Figure 3.10: Optical images of multilayers before and after cyclic bending.(a) and (d) are images of PEDOT:PSS on ITO/PET before and after bending respectively. (c) and (d) show images of P3HT-PCBM on PEDOT:PSS/ITO/PET before and after bending respectively

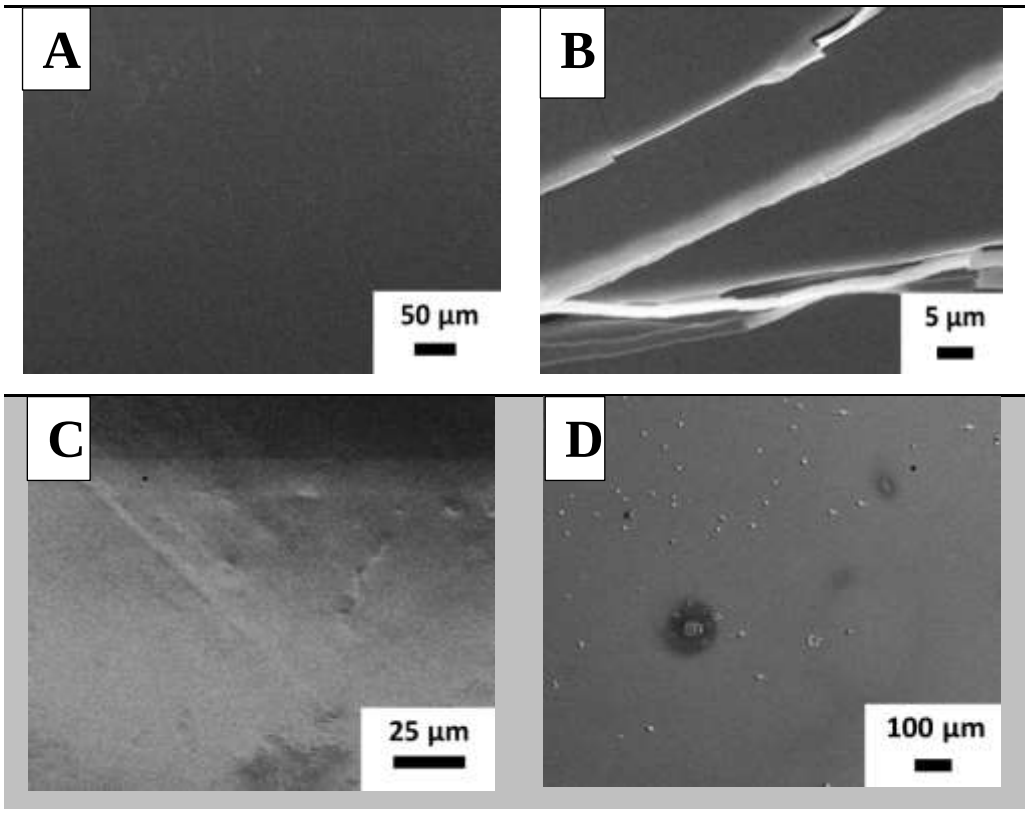

Figure 3.11: SEM Images of multilayers before and after cyclic bending (a)ITO on PET before bending (b) ITO on PET after cyclic bending. (c) Al layer on multilayers before undergoing bending (d) Al layer image after cyclic bending.

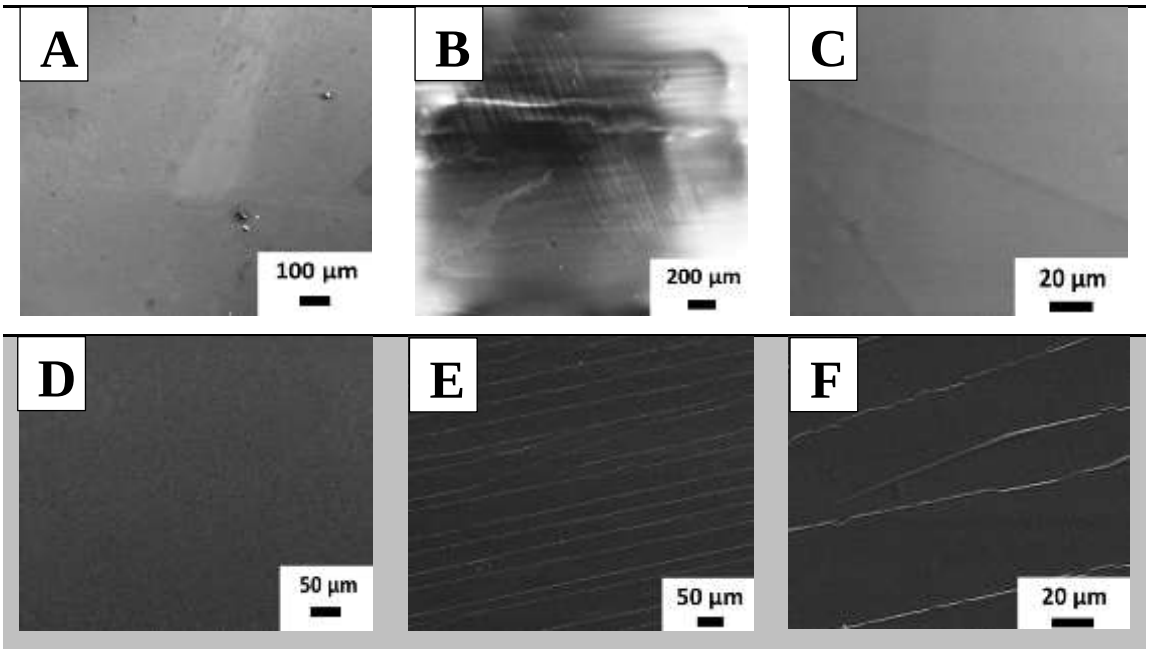

Figure 3.12: SEM images of multilayers before and after cyclic bending.(a) and (b) are images of PEDOT:PSS on ITO/PET before and after bending respectively. (c) is an enlarged view of (b) showing tunneling cracks underneath this layers as can be seen in (f) for P3HT:PCBM layer on the PEDOT:PSS/ITO/PET multilayer structure. (d) and (e) are respective images of P3HT:PCBM layer on PEDOT:PSS/ITO/PET structures before and after bending.

3.4.2 Deformation Mechanisms

For a thin film on a flexible substrate, the elastic stresses in the thin film are given by Brunner et al. [51] based on approximations made on Timoshenko and Reddy's work [106] for thin films on a thick substrate. For such a case where one layer is much greater than the other composites (i.e. $\sum_i t_i << t_S$), the summation term signifies the total thickness of the thin films on the substrate whiles t_s signify that of the substrate. The solutions for this case are most useful with the biaxial description of a composite plate with different moduli in each layer taking note that the ratio t_i/t_s term which is less than unity from the first to higher order terms has been neglected for the analysis. This simplifies the position of the neutral plane, π to for structures containing N layered thin films[51];

$$\pi = \frac{t_s}{2} + \sum_{i=1}^{N} \frac{t_i E_i (1 - \nu_s)}{2E_s (1 - \nu_i)} \tag{3.4}$$

Here E and ν have their usual meaning. This equation shows that the neutral plane is only slightly displaced from its original position in the bare substrate. With radius of curvatures 10, 20 and 30 mm, the stresses in a 90 nm thick ITO thin film on a PET substrate of thickness 175µm would be 1.418 MPa, 2.836 MPa and 4.253 MPa respectively using equation 1. Also, from equation 2, the neutral line of the complete multilayer with thickness 175.48 µm was calculated to be 92.68 µm. Similarly, the transmittances (See Figure3.13) of the film structures were also measured with an AvaLight-DHc UV-VIS spectrophotometer (Avantes Inc., Broomfield, USA) in the wavelength range 300-1100 nm (visible spectrum).

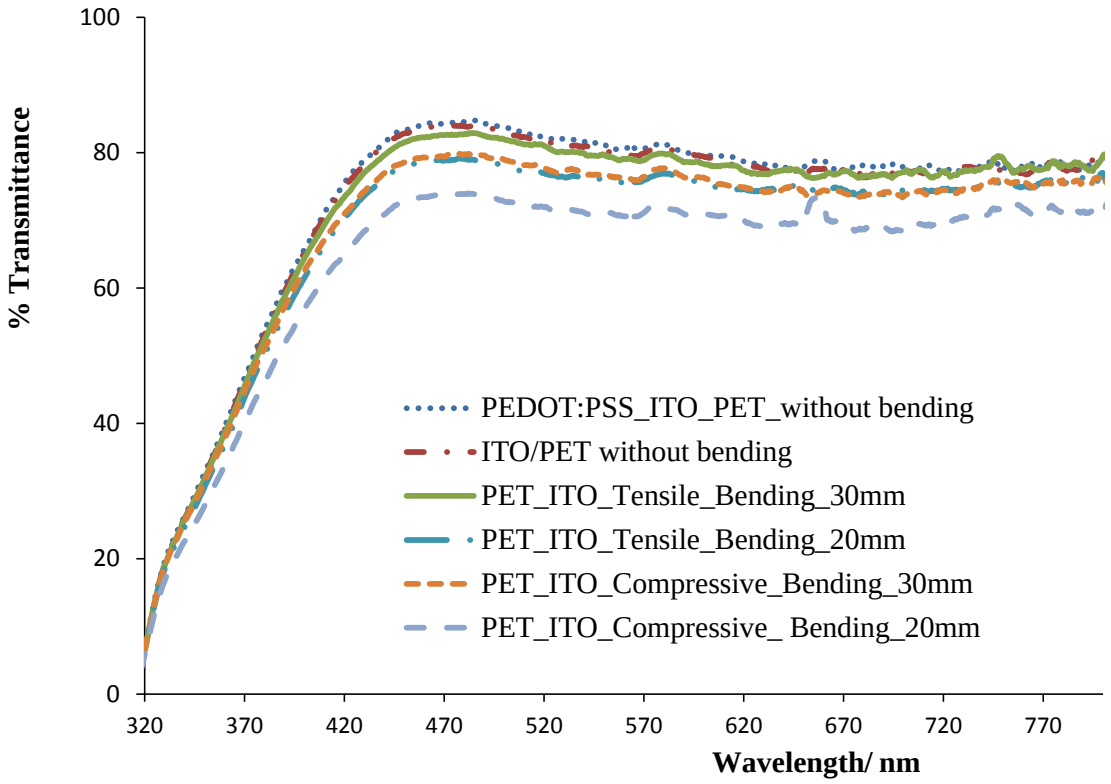

Figure 3.13: Effect of bending on the transmittance characteristics of an ITO on PET multilayer structure

The ITO anode and hole injection layer (PEDOT: PSS) exhibited 80- 85 % transmittance in the UV- VIS Spectrum. It is also clear that bending has very minimal effect on their transmittance, especially during tensile bending. Compressive bending, on the other hand, had its transmittance dropping from ~80 % to about ~70 %.

3.4.3 Stress and Strain Distributions

Most electrodes and contact materials used in electronics are metallic but those required in displays and thin film photovoltaic must be transparent and highly conductive. CdO was the first transparent conducting oxide introduced and this was in 1907. [79], [97], [98], [156]–[158] Currently, the metal oxides are widely used but the demerit in these is their brittleness. The most widely used TCO example is tin-doped indium oxide (ITO) which was originally developed for defrosting aircraft windshields. It is used in touch screens, electromagnetic shielding and displays. ITO's elastic modulus is ~116 GPa [105], [149] making it stiff and brittle so depositing it on a compliant/flexible substrate such as dc sputtering it on PET may cause cracks or even delamination during fabrication and use. [79], [97], [98], [156]–[158] The depositions on PET after taking through flexural tests characterized the effect of bending on its failure mechanisms when compared with the results from the finite element model (See Figures 3.6 and 3.7) showing ITO with the highest stress values in relation to the other layers during bending.

3.3.4 Crack Driving Forces and Mode Mixities

These SEM micrographs indicate that apart from ITO layer that undergoes severe cracking, the other layers do not due to the deference in their material properties. From the stiffness relation (i.e. K α EA/L) [105], it can be seen that the stiffness, K of a material is directly proportional to its Young Modulus, E (which is its material property). Note that A and L are the area and length respectively. Due to this, comparing the young modulus of the various layers indicate that the ITO (which holds the highest E values) would be the stiffest. This is verified in the finite element results showing that ITO has the highest recorded stress values as compared to the other layers during bending (See Figure 3.7) followed by the Aluminum cathode. This implies that the ITO layer is highly susceptible to cracking. Tables 3.4 and 3.5 summarize the J_i, K_i and G_i values obtained from the ITO crack analysis.

Table 3.4: J, K and G values of the top crack tip

J_t	K1	K2	K3	G_t
4.09267×10^{-06}	0.0001152	6.51×10^{-05}	4.23×10^{-11}	6.62×10^{-06}

Table 3.5: J, K and G values of the bottom crack tip

J_b	K1	K2	K3	G_b
9.21473×10^{-07}	0.000126	-6.9×10^{-05}	1.99×10^{-11}	4.34×10^{-06}

3.4.5 Optical and Electrical Properties

The simulation and optimization of the optical transmittance of the ITO/PET multilayer system along with their experimental data on the "Optical" Software provided was followed by the resistivity characterization of the TCO (ITO) was 60 ohms/sq. before bending and the results on bending have been summarized in Table 3.6.

Table 3.6: Electrical resistivity of ITO/PET under bending

Curvature Radius/ mm	Average Resistivity/ ohms per square
∞	60.000
30	68.172
25	46400.000
20	96400.000

This means that under tensile bending, the resistivity of the ITO increases with crack growth. The characteristics of the OPV device fabricated behaved like a perfect diode in the dark. More work is expected to be done on device optimization to improve on IV results obtained under illumination.

3.4.6 Implications

From the thickness analysis, it should be noted that subsequent thicknesses of various other thin films could be determined using their experimental transmittance data confirming the thickness simulated with RBS measurements. In this work, the stoichiometric configuration of the ITO was relatively not very good, advising an adjustment for the deposition process. Cleaning the thin

film in clean room environment was also advised to minimize the effects of impurities. Cairns et al. [98] has done lots of work on the mechanisms and effect of cracking on ITO's electrical properties when deposited on PET films.

These investigations show that, as observed in a typical ceramic film, the critical strain for cracking is the reciprocal to the square root of film thickness [97], [98]. At a strain of ~ 1%, ITO cracks beginning with the formation of small cracks that grow under cyclic loading by fatigue leading to failure especially when needed for electrical purposes. As such, the commencement of conductivity loss in the ITO under tension can be delayed by a reduction in the ITO film thickness. Other findings also suggest an introduction of a compressive pre-stress into the ITO layer or using a high-modulus but non brittle undercoat for the ITO [97], [98]. But it should also be noted that under compressive loading, the ITO film is likely to buckle, crack or even delaminate. Vital information that can be investigated further is the fact that the strain at which buckling occurs depends on the strength of adhesion between the ITO and the substrate [97], [98]. Apart from these, looking at the high reduction in the strains when the ITO layer is eliminated entirely from the multilayer as shown from the simulation results in this work, robustness is assured without compromising on the electrical conductivity of the device. Using PEDOT:PSS alone for the transparent, high- work-function electrode instead of adding or combining it with tin-doped indium oxide proved useful because ITO films are brittle [146], and from these simulations it is very clear that ITO would crack upon the application of strain as low as ~1% even though the other compliant layers included would only increase the strain to ~1.6%.

The hysteresis from the experimental cyclic graphs could be associated with the viscoelastic deformation of the organic layers and failure mechanisms that can occur within or between the layers during cyclic deformation.

It is also clear that as the bending moment increased, the bending strain increased along with the increase of cracking. This resulted in the increased absorption of light transmission between the ITO on the PET interface. Hence at higher bending strains, the organic solar cell layers absorb more light than at lower bending strains.

3.5 Conclusion

With Bert Groenendaal L description of how failure of films can occur during processing and use due to the mismatch of mechanical properties of the inorganic device layers and their polymer substrates [159], using conductive polymers in place of ITO would reduce the risk to failure drastically. From the results of this experiment, conductive polymers such as polythiophene derivatives (e.g. polyethylene dioxythiophene, PEDOT) coupled with polystyrenesulfonate when used as interconnect and contact materials in all-organic flexible electronics would have the high tendencies to eliminate the risk of failure during repetitive usage of such devices. Heeger, MacDiarmid and Shirakawa in 1976 considered doping polyacetylene with iodine oxidant for high electrical conductivity. Moreover, others suggestions such as polyaniline and polypyrrole which are used as anti-static materials would replace inorganic ITO successfully. These suggestions are highly recommended since when in these devices because whiles some function as good hole injection layers and transport layers in solar cell applications, the others excel as active material layers in polymer light-emitting diodes (e.g. polyphenylene vinylene derivatives) [159].

CHAPTER FOUR

EFFECTS OF PRE-BUCKLING ON THE BENDING OF ORGANIC ELECTRONIC STRUCTURES

4.1 Introduction

In recent years, there has been considerable interest in the development of low cost flexible organic solar cells with the potential to replace conventional silicon cells that are fabricated typically on glass substrates.[26], [160], [161] However, the rigidity of the glass substrates limits the extent to which flexible electronics structures can be deformed without inducing cracks in the rigid and brittle glass substrates.[146] There is, therefore, a need for approaches that can improve the deformation of flexible organic solar cells, without inducing cracks in the underlying substrates.[162]

Two approaches have been used in literature to improve the flexibility of organic solar cells structures.[21], [40], [129], [130], [141], [163]–[165] One involves the replacement of the glass substrates with bendable polymers, such as polyethylene terephthalate (PET)[41]–[44], [166], [167] or polydimethylsiloxane (PDMS),[37], [40], [168]–[170] while the second approach involves the introduction of pre-buckles that stretch and flatten out during deformation. The pre-buckles also increase the range of deformation that can be applied to flexible organic electronics prior to the onset of cracking and other stress/strain-induced failure mechanisms.[171]

Prior work on the deformation of flexible and stretchable organic electronics structures has been reported by Bao et al.[146], [151], Volinski et al.[172], Groenwold[173], Huang[174]–[176], Stafford et al.[143] and Sariciftci and co-workers.[77], [163], [177] Their work shows that pre-

buckles with different wavelengths can improve the flexibility of layered organic solar cell structures with different substrates. Similar reports of improved deformability have also been presented by Huang and co-workers[23], [25], [31], [176], [178], while Rogers et al.[148] and Akogwu et al.[37] have used pre-buckles to improve the "stretch-ability" of flexible organic electronic structures.

Bao et al.[146] have presented two methods that can be used to influence the elasticity of rigid materials. The first involves the dispersion of conductive materials in an elastic matrix (as exploited by Wagner[28], Suo[104], Rogers[179], Sariciftci[77]), while the second involves the pre-buckling of electronic structures deposited on elastomeric substrates. The latter have been investigated by Stafford [144], Sariciftci [180], Tarasovs and Andersons.[181] The results show clearly that the potential application of pre-buckled films (with controlled wavelengths and amplitudes) could have a significant effect on the deformability and reliability of electronic devices.

Rogers et al.[148] have also suggested that the buckle wavelength increases with increasing buckle film thickness. However, there have been only limited prior efforts to model the deformation of flexible organics cell structures under bending loads and deformation conditions[182] that are relevant to flexible organic electronics.[41]

Furthermore, the flexibility of transparent electrodes has been achieved by structurally configuring devices to accommodate most of the strain under mechanical deformation that minimizes the strains in the conducting materials. These structural configurations have been classified into out-of-plane and in-plane structures.[184]–[187] The most common out-of-plane structure is the 'wavy' structure, which is generally obtained by depositing conductive materials

on pre-strained elastomeric substrates. When subsequently released, these conductive films spontaneously form periodic wavy structures in which most of the induced strains are absorbed by the structural changes.[184] These have been likened to accordion bellows, where increased buckling wavelengths and decreased buckling amplitudes can be achieved.[184], [188], [189]

The fundamental advantage of the presented pre-buckled structure is its ability to permit large elastic deformation protecting the active layers with limited strains. Thin films fabricated this way are more compliant when compared to the bending strain which is less than that of pre-stretch. [184-190]

However, although the effects of pre-buckling have been studied,[190] there is only a limited understanding of pre-buckling on the deformation of flexible organic structures. Hence, this paper, therefore, presents the results of an experimental and computational study of the effects of this most common out-of-plane structure (pre-buckling) on the deformation and failure of flexible organic solar cell structures on polydimethylsiloxane (PDMS) substrates. The effects of pre-buckle wavelengths and amplitudes are modeled using finite element method. The stress/strain distributions and the deformation profiles associated with the bending of the pre-buckled profiles are computed for the model flexible multilayer structures deposited experimentally. The increased deformation associated with the flattening of the pre-buckles is determined for pre-buckles with different wavelengths and amplitudes. The implications of the results are then discussed for the design of flexible organic electronic structures [125], [191].

4.2 Experimental Procedure

This section utilizes un-stretched, pre-stretched and post-stretched structures in a study of the bending of model organic semiconductor layers on flexible PDMS substrates. It is important to

note that the un-stretched condition corresponds to the un-stretched PDMS substrate, while the pre-stretched condition corresponds to the stretched condition prior to the deposition of poly 3, 4-ethylenedioxythiophene polystyrene sulfonate (PEDOT:PSS) thin film layer. The post-stretched condition corresponds to the subsequent deformation of the pre-buckled structure that is formed after the release of the PEDOT:PSS/PDMS structure.

4.2.1 PDMS Substrate Preparation

The PDMS substrate was prepared from a Sylgard 184 elastomeric base and a silicone curing agent with 1:10 weight ratio, as described in our prior work.[192] Observations show that increasing the weight ratio of the silicon curing agent makes the resulting PDMS less stretchable, as expected, since silicon acts as the cross-link (hardener) agent between the polymer chains.[37] In any case, PDMS substrates with dimensions of 1.5mm and 4.5 cm × 1.25 cm were prepared by casting and curing them in an aluminum mold.

4.2.2 PEDOT:PSS Coating Deposition

PEDOT: PSS was procured from H.C. Starck Inc., Newton, MA, USA. It was filtered with a 0.2 μm filter paper before depositing 0.4 ml of the filtrate with the Model WS 650 Laurel spin-coater at an initial rate of 500 revolutions per minute (rpm) for 5 s. The PEDOT:PSS was then spin coated at 1500 rpm for 3 s and 3000 rpm for 60 s.[166] The principal challenge in depositing PEDOT:PSS on PDMS was its high water contact angle on PDMS. It was observed that when PDMS was stretched to a high degree before deposition, PEDOT:PSS deposition was possible. The pre-stretching experiments were carried out on 3D printed fixtures that were fabricated from

polylactide (PLA). These were used for the deformation of the PEDOT:PSS/PDMS structures to different levels of pre-stretch. The fixtures were used to apply pre-stretch levels of 35% and 50% by varying the PLA stands (Figure 4.1a).

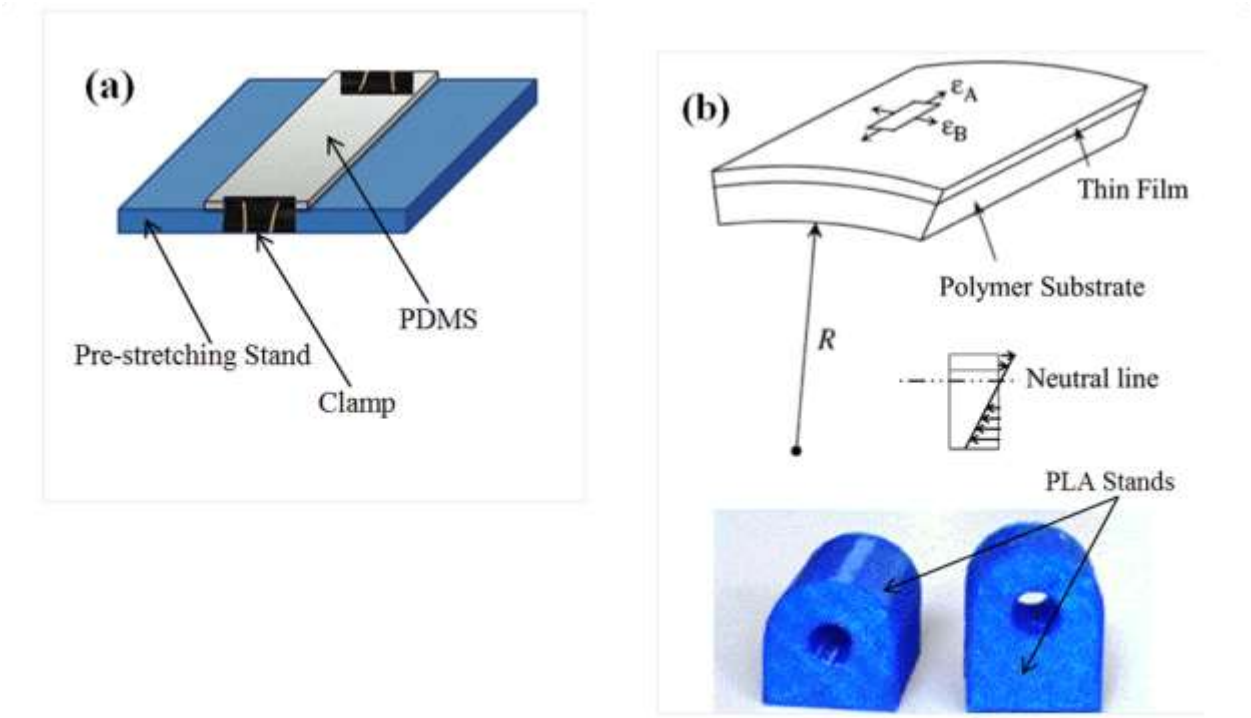

Figure 4.1: (a) PDMS clamped to a pre-stretching stand made of PLA. (b) PEDOT:PSS thin film on a polymer substrate (PDMS) undergoing bending showing its acquired radius of curvature, R when placed on PLA stands with different diameters. [4], [193]

PDMS was pre-stretched by clamping to the PLA stands. PEDOT:PSS was spin coated while the PDMS is pre-stretched. Afterwards, the clamps were carefully removed to introduce the buckling. Since PDMS is not rigid enough to compensate the force of the water-air-surface tension perpendicular to the surface, a ridge is pulled up around the edge of the water drop,

locally increasing the surface roughness and thus hysteresis via pre-stretching enhancing the PEDOT:PSS deposition.[194], [195]

4.2.3 Surface Characterization and Bending Experiments

Microscopic observations of the surfaces were made with atomic force microscopy (AFM) and optical microscopy (OM). The latter was performed under different stretching conditions. After pre-stretching, the PDMS substrates were spin-coated with PEDOT:PSS. They were then mounted on 3D rollers with different diameters (Figure 4.1b). Rollers with different diameters were used to apply different bending strains to the pre-buckled/wrinkled PEDOT:PSS on PDMS substrates.

Deformation was applied until the thin film flattened out on the substrates (Figure 4.1b). Atomic force microscopy (AFM) images of the coated and uncoated surfaces were then obtained in the contact mode, using a Bruker Instruments Nanoscope IIIa atomic force microscope (Bruker Instruments, Plainview, NY, USA). The three dimensional (3D) printed rollers with diameters of 20, 18, 16, 15, and 12 mm used to apply controlled bending strains of 0.0375, 0.0417, 0.0469, 0.0500 and 0.0625, respectively. The axial strains were determined using the following expression:[4], [105], [196]–[198]

$$Strain = \frac{(\frac{Thickness - of - PDMS}{2})}{Diametter - of - Roller} \tag{4.1}$$

AFM was then used to characterize the wavelengths of the surfaces of the wrinkled/buckled PEDOT:PSS layers on PDMS. This was done after pre-stretching and bending to different strain levels. AFM imaging was carried out in the contact mode using a Bruker Instruments Dimension 3000 atomic force microscope (Bruker Instruments, Plainview, NY, USA).

4.3 Modeling

Finite element simulations where used to model the effects of bending on the pre-buckled films. The structures were modeled undergoing three-point bending, after introducing pre-buckled profiles with different wavelengths. Finite element modeling was carried out using the ABAQUS software package (ABAQUS CAE 6.12-1, Dassault Systèmes, Pawtuckett, Rhode Island, USA). A 2D (two dimensional) plane stress model was built (Figures 4.2a and 4.2b).

The thickness of the PDMS was 1.5 mm in the model. This corresponded to the thickness of the PDMS substrate that was used in the experiments. It should be noted that the pre-buckles were simulated using profiles of PEDOT:PSS that were in partial contact with the PDMS substrates prior to the application of bending (Figure 4.2a). The deformation of the pre-buckled structures then resulted in the flattening of the layers as the bending strains were increased (Figures 4.2b and 4.2c).

The mechanical properties of the individual layers (Young moduli and Poisson's ratios) that were used in the simulation are presented in Table 4.1.[105], [149], [150], [153] Linear elastic deformation was also assumed in each of the layers. Structured quadrilateral meshes were used in the finite element model, along with standard bi-linear plane stress elements with incompatible modes. The two aluminum stoppers at both ends were fixed in the X, Y and Z directions (i.e. U1, U2 and U3, respectively). The middle roller was constrained to displace upward (i.e. move only in the U2 direction) upon the application of pressure.

The above procedure was repeated for the other layered structures in which the anode layer (ITO), the active layer (P3HT: PCBM), and the cathode (Aluminum) were pre-buckled and deformed on the relevant layers in model organic photovoltaic structures.[44], [97], [166], [167],

[199]–[202] The layer mechanical properties that were used in the simulations are summarized in Table 4.1.

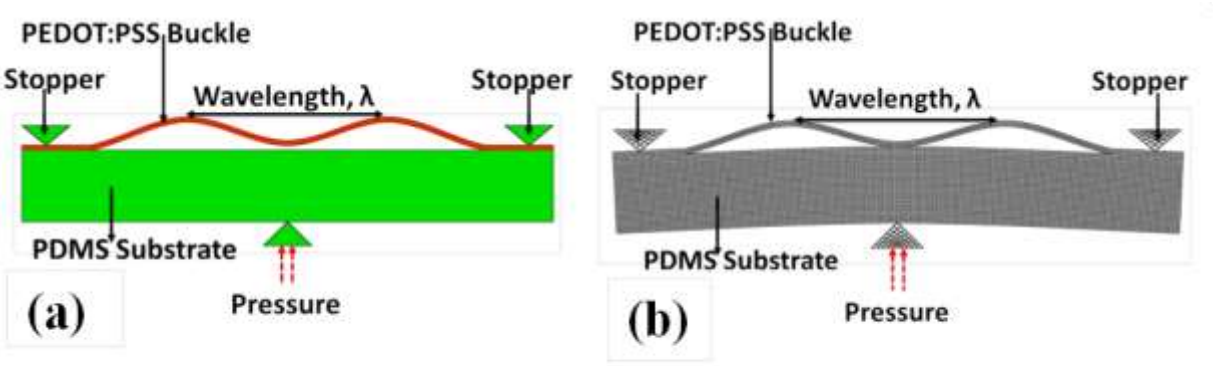

Figure 4.2: (a) Schematics of multilayer parts designed for the finite element analysis taking into consideration the experimental parameters and (b) elemental view of buckle on PDMS

Table 4.1: Material Properties

Materials	Young's Modulus, E/ GPa	Poisson's ratio	References
PDMS	0.003	0.48	[149], [193], [203]
PEDOT: PSS	1.42	0.3	[149]
Al	70	0.3	[105]

4.4 Results and Discussion

4.4.1 Effects of Pre-Stretching on Surface Topography

The AFM images revealed the presence of buckles, following release from small pre-stretches of 18%, 25% and larger pre-stretches of 35% and 50% (Figure 4.3a-4.3d). These show clearly that the wavelengths of the resulting buckles decreased with increasing pre-stretch. Optical Microscopy images of the surfaces of the PDMS and PEDOT:PSS/PDMS structures also revealed similar trends in the pre- and post-stretched conditions (Figures 4.4a-4.4c)). These

images also showed that the surface roughness (wavelengths) decrease with increasing pre-stretch.

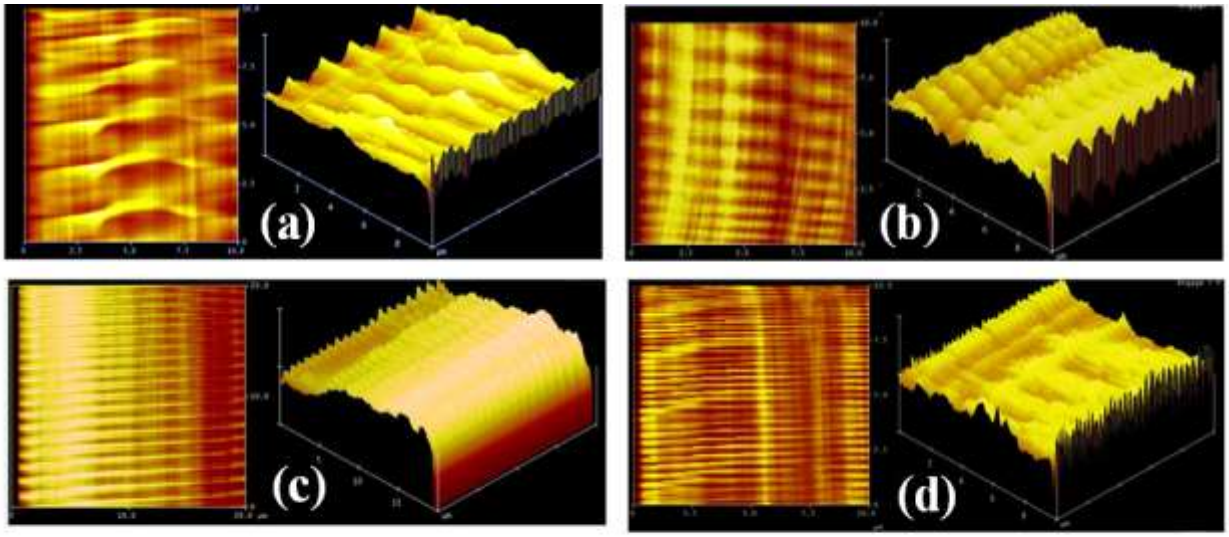

Figure 4.3: AFM images of micro-wrinkles observed with pre-stretched PDMS substrates after PEDOT:PSS deposition. (a): 18% pre-stretch. (b): 25% pre-stretch. (c): 35% pre-stretch. (d): 50% pre-stretch. [Note that the wavelength decreases in this order: (a) > (b) > (c) > (d)].

Plots of the wavelengths of the buckled profiles (obtained from the contact mode AFM images) are presented in Figure 4.5. These were obtained for surfaces that were subjected to different levels of pre-stretch. These show clearly that the wavelengths of the pre-buckled profiles decrease with increasing pre-stretch. Similar results have been reported by Oyewole et. al. [170] for the formation of pre-buckles on the surfaces of pre-stretched and released Au films on PDMS substrates.

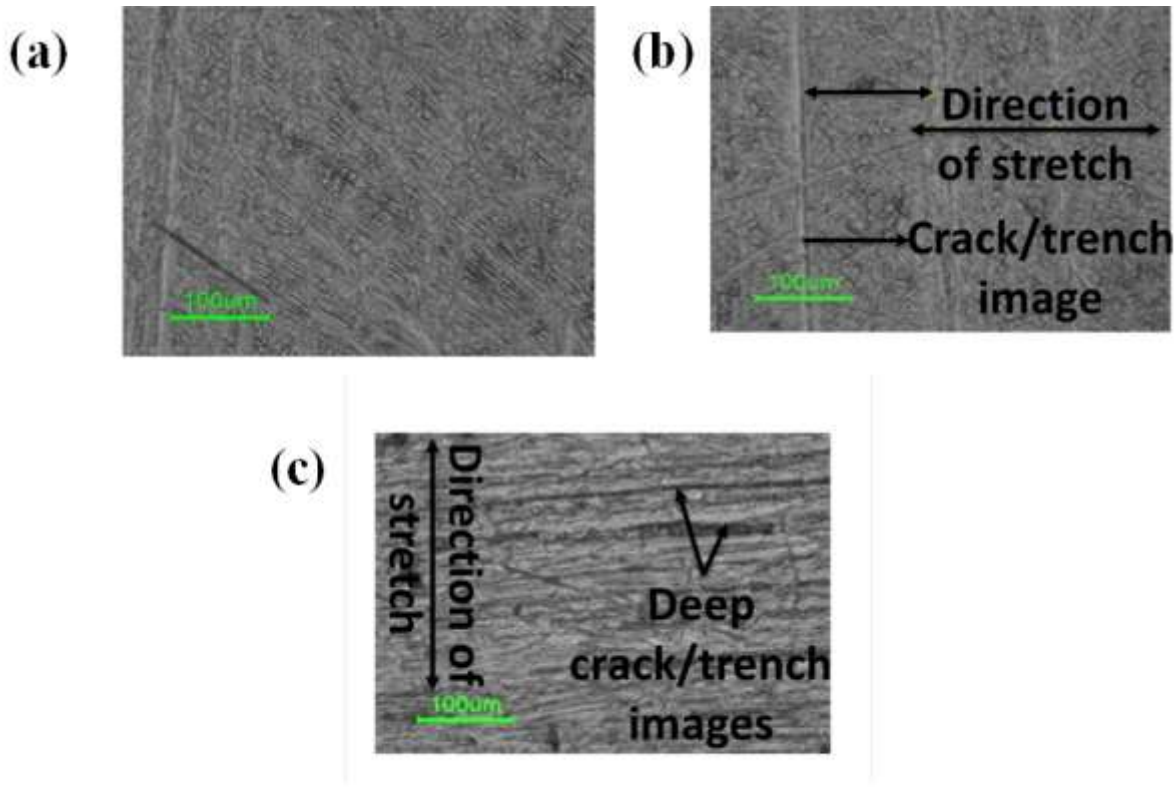

Figure 4.4: Optical Microscopy images of the surface topology of PDMS and PEDOT:PSS/PDMS structures; (a) is an optical image of un-stretched PDMS substrate; (b) 35% post-stretched PDMS substrate with PEDOT:PSS deposition, showing less wrinkles, and (c) 50% post-stretched PDMS substrate with PEDOT:PSS deposition showing deep crack/trench images observed as surface features indicating more wrinkles

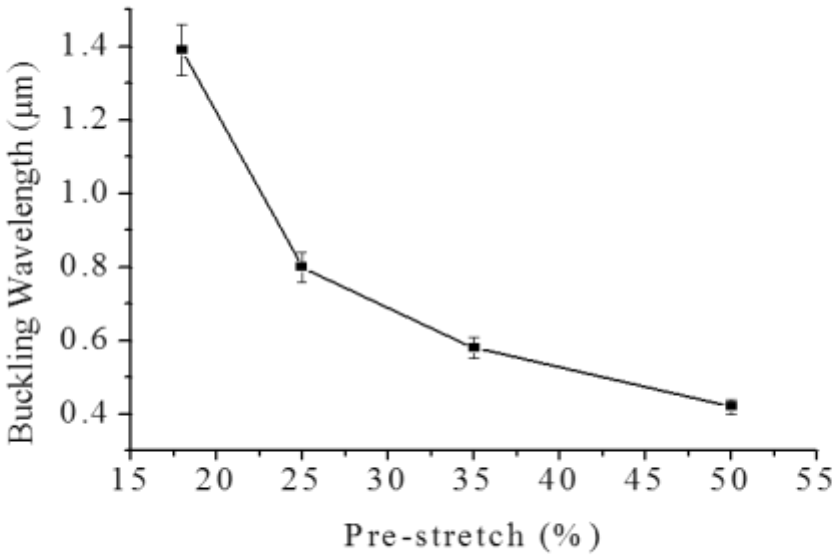

Figure 4.5: Buckling/wrinkling wavelengths changes as a function of pre-stretching percentage.

4.4.2 Effects of Deformation on Surface Topography

In general, increased pre-stretch resulted in a reduction in the wavelengths of the pre-buckled profiles (Figures 4.3 and 4.5). However, upon subsequent bending of the pre-buckled structures, the surfaces of the pre-buckled structures flattened out (Figures 4.6a and 4.6b). In the case of the samples produced after 50% pre-stretch, the initial pre-buckled surfaces had wavelengths of about 0.13 microns. The surface wavelengths increased to 0.4545 microns, after applying a bending strain 0.0417. This is consistent with a tendency to flatten out the buckles with increasing applied strain. In the case of the samples that were subjected to a pre-stretch of 70%, the initial PEDOT:PSS/PDMS structures had pre-buckles with a wavelength of about 16.7 nanometers. However, upon applying a bending strain of 0.0417, the surface wavelengths increased significantly to about 1.67 microns (See Table 4.2).

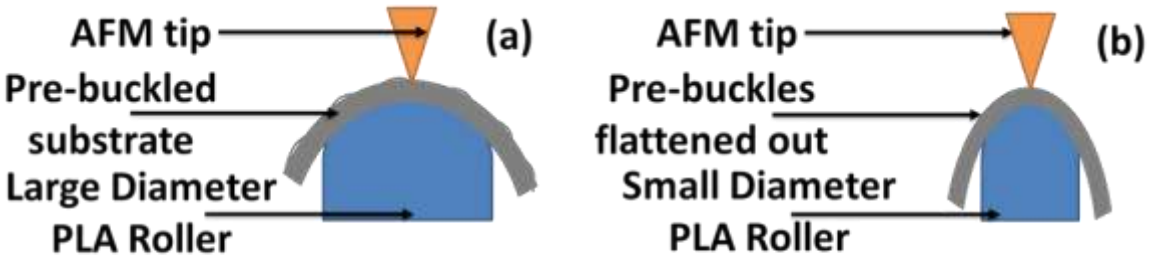

Figure 4.6: Schematics of an AFM tip measuring the wavelength of a substrate with wrinkles/buckles undergoing bending on different PLA rollers; (a) Buckles exhibit small wavelengths due to less bending strains applied by courtesy of larger diameter PLA roller used, (b) Buckles flattened implying very high wavelength values due to large bending strain achieved on a small diameter PLA roller.

Table 4.2: Pre-buckled wavelength before and after bending

Pre-buckled Wavelength before Bending/ µm	**Pre-buckled Wavelength after Bending/ µm**
0.1300	0.4545
0.0167	1.6700

4.4.3 Finite Element Simulations of Three-Point Bending

The finite element simulations of the deformation of the pre-buckled PEDOT:PSS profiles on a PDMS substrate are presented in Figures 4.7a-4.7c. These show the progression of stress and deformation profiles from the initial pre-buckled states to the conditions at which the buckles

become flattened out due to the application of tensile stresses through bending. The results clearly show that the stretching of the surface layers flattens out the initially sinusoidal profiles.

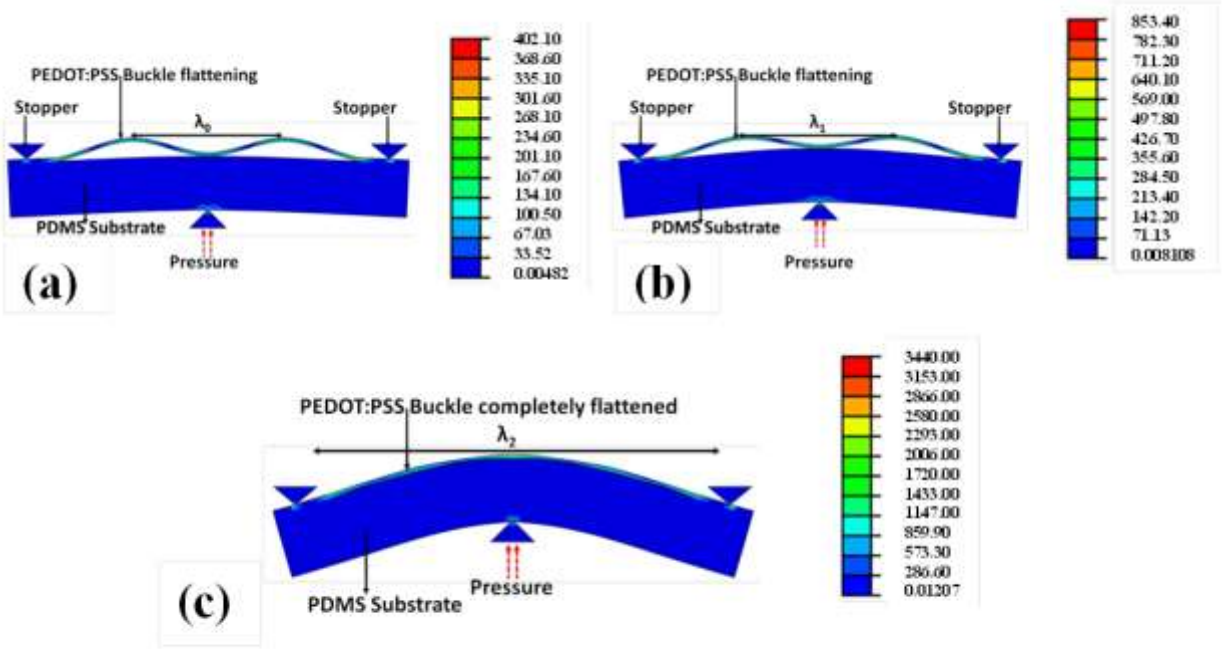

Figure 4.7: Pre-buckled structure of PEDOT: PSS on PDMS with von Misses stress distribution at the onset of flattening for various wavelengths; (a) buckle with wavelength, λ_0, at 15 N/mm^2 pressure (b) buckle wavelength gradual increase on further application of bending moment to λ_1 due to the stretching of the buckle at 37 N/mm^2 pressure, and (c) complete flattening of buckle on PDMS substrate on applying 50 N/mm^2 pressure

The finite element predictions of the initial pre-buckle flattening conditions confirmed results presented in Table 4.2, along with the experimental measurements of the forces per unit width required for the flattening of the pre-buckles. These forces were observed to increase with decreasing pre-buckle wavelength. Hence, increased pre-stretch of the films, which gives rise to decreased pre-buckled wavelengths, is likely to increase the apparent film "deformability".

Furthermore, the computed von Misses stress distributions obtained for the deformed pre-buckled films were used to characterize the deformation in multilayered structures (Al/P3HT:PCBM/PEDOT:PSS/ITO/PDMS and Al/P3HT:PCBM/PEDOT:PSS/PDMS) that are relevant to organic solar cells. The results are presented in Figures 4.8a and 4.8b. These show that the bending of the films (for different initial pre-buckle wavelengths) results in increased von Misses stresses that can lead ultimately to the onset of plastic deformation in the Al cathode layers and the polymeric layers within the model organic solar cell structures.

Hence, the deformation that occurs, prior to flattening, is likely to extend the deformability of the flexible multilayer structures, while the deformation that occurs, after the flattening can result in the build-up of stresses until the onset pf plasticity or fracture. Interfacial failure can also occur between the layers, depending on the adhesion between the layers.[16], [130], [204]

Finally, it is important to discuss the potential effects of transparent indium tin oxide (ITO) layers that are often used as the anode of organic solar cells. Since these layers have relatively high moduli (Table 4.1), they can result in higher stress distributions and elastic strain energies in flexible model solar cell structures (Figures 4.8a and 4.8b). These can lead ultimately to the cracking of the ITO layer, as observed in earlier work.[43], [49], [97], [205] There is, therefore, a need to avoid the use of ITO layers in the development of flexible organic solar cells.

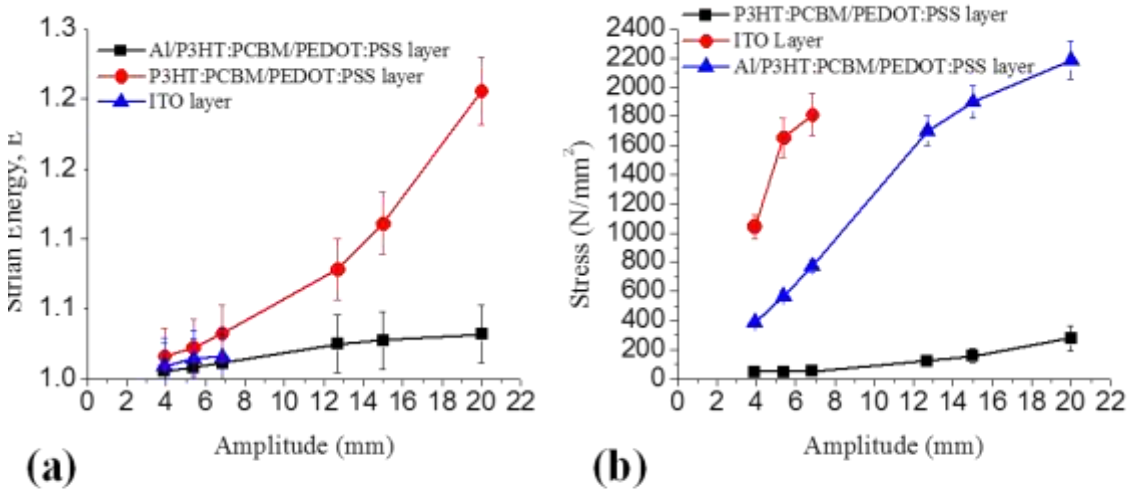

Figure 4.8: Maximum strain and von Misses stresses in the different films for different amplitudes at constant wavelength with effects of indium tin oxide layers in the pre-buckle structures; (a) strain energy variations and (b) stress distribution in the different layers.

4.5 Implications

The implications of the results are very significant. First, they show that pre-buckling can be used to increase the deformability of flexible organic solar cells (see Figures 4.8a and 4.8b), prior to the onset of failure by the plasticity or fracture of the film constituents. The improvements in flexibility can also be enhanced by the control of initial buckle wavelengths and amplitudes, which can be achieved by the use of pre-stretching methods (as done in the experimental section of this paper).[187], [206]

However, increased pre-buckle wavelengths can also result in higher film stresses that can induce failure within the layers or between them. A balanced approach is, therefore, needed to determine the pre-buckled configurations that improve flexibility/deformability, without compromising the conditions for final film failure.

Furthermore, from the literature[163], [183], [185], [207], [208], it is clear that further flexibility can be achieved by fabricating the devices on ultra-thin polymer substrates and laminating them unto a pre-strained elastomers such as PDMS. The application of such ultra-thin substrates could decrease the bending strains. However, the compliance of these structures would also be increased significantly. In any case, the model PEDOT:PSS transparent electrode, explored in the current work is consistent with the work of Drack et al.[185] and Kim et al.[207] who have produced flexible devices in which resistance increases to ~30% after 10,000 cycles of stretching to strains of 50%.[185], [207]

Furthermore, the current work suggests that improvements in the flexibility of pre-buckled organic electronic structures can be estimated by considering the ratio of the strains to flattening of a pre-buckled structure to the strain to failure of a non-pre-buckled structure. This means that the surface area of the device (if it is a solar cell) would have more wavy characteristics that could improve the harnessing of sunlight for photo-conversion to electricity.

The fabrication of the above organic solar cell structures could be achieved by the use of roll-to-roll printing[44], [52], [209] and lamination processes.[149], [210] The optimization of such manufacturing processes could lead to the future scale up of emerging approaches for the design and fabrication of flexible solar cells.[66] The flexible organic solar cells could also be integrated into roofing tiles[211] and electronic textiles[127], [212], [203] in which significant bending strains can be applied during fabrication and service.

4.6 Summary and Conclusion

This paper presents the results of an experimental and computational study of the deformation behavior of pre-buckled thin films structures that are relevant to the deformation of flexible organic electronics. The results show that the additional strain to flattening (of the pre buckles) enhances the deformability/ flexibility of the films. The strains to flattening also increase with increased pre-buckle wavelength. However, such increased pre-buckle amplitudes and wavelengths may also induce failure by film plasticity, fracture or delamination. A balanced approach is, therefore, needed for the design of robust pre-buckled layers for potential applications in flexible organic electronic structures.

CHAPTER FIVE

COLD WELDING OF ORGANIC LIGHT EMITTING DIODE: INTERFACIAL AND CONTACT MODELS

5.1 Introduction

There has been significant interest in the fabrication of organic electronic structures using cold welding techniques.[213]–[218] Cold welding or cold pressure welding has been described as a process by which clean surfaces are brought together to achieve intimate contact, and thereby form strong bonds at the resulting interfaces.[219] It has attracted widespread attention due to its potential for low-cost fabrication of organic electronic devices.[123]

The initial step in cold welding involves bringing together the surfaces of two different thin film materials at room temperature.[112] In most cases, the contact occurs around dust particles that are present in the clean room environment.[220] These include materials such as silicone, silicon, silica and organic materials. The contacts are enhanced by the application of pressure,[203], [215], [221]–[224] which is often applied through compliant materials such as poly-di-methyl-siloxane (PDMS). Such compliant layers improve the contacts between the cold welded layers. However, increasing pressure can lead to excessive sink-in of dust particles[224] and the damage of the organic electronic device.[149]

There is, therefore, a need to control the pressure that is applied during the cold welding of organic electronic structures. Similarly, the transfer of one metal film to the other (that occurs during cold welding) requires careful control of the interfacial fracture processes that can occur

in any of the interfaces with the organic electronic structures. Also, depending on the interfacial and layer fracture energies, fracture may occur by interfacial or layer fracture, or a combination of both.[225], [226]

Prior work on cold welding [112], [118], [123], [224], [227], [228] [149], [192], [218] of thin film organic electronics has been carried out by Cao et al., [215] Kim et al. [216] and Akande et al. [214] These studies have identified the role of interfacial impurities in the cold welding of gold-gold and gold-silver thin films that are relevant to OLEDs. They have also focused largely on the effects of stiff impurities on contacts induced by the application of pressure. However, it is quite possible for the moduli of interfacial impurities (silicon, silicon oxide and organic materials) to vary significantly.[229] The adhesion energies and layer dimensions may also affect the surface contacts and pull-off forces associated with the lift off stage of cold welding, which may be considered as an interfacial fracture process, as in recent work on the lamination of organic electronic structures.[215], [229]–[232]

Hence, in this paper, we present the results of a study of the pressure-associated contact and lift-off stages that are associated with the cold welding of Au, Ag and other organic layers used in OLED structures. The effects of impurity Young's moduli are elucidated, along with the role of layer thickness and interfacial adhesion energy. These are explored using finite element models. The paper is divided into five sections. Following the introduction, surface contact and pull-off theories are presented in section II. The experimental methods are then described in section III before discussing the results in section IV. Salient conclusions arising from the study are presented in section V.

5.2 Modeling

5.2.1 Surface Contact Model

The deformation of a thin film around an interfacial impurity particle can be identified by the displacement of a cantilever beam (Figure 5.1a).[192], [204], [233], [234] As the beam deflects, the cantilever beam (layer 2) makes contact with the adjacent layer (Layer 1), as shown in Figure 5.1b. This results in surface contact that increases with increasing pressure (Figure 5.1c). The corresponding void length, S, also decreases with increasing pressure[149] (Figure 5.1c). Furthermore, the deformation of the sandwiched particle depends on the weight of the film, the pressure of the stamp and the combined (effective) Young's moduli of the particle and the film.

In an effort to model the contact between the two cold-welded layers, Zong et al.[235] have shown that the total energy, U_s, stored in the film (due to the bending) is given by:

$$U_s = \frac{6E_f Ih^2}{s^3} - \gamma(L-s)a, \tag{5.1}$$

where a is the width of the film, E_f is the Young's modulus, γ is the adhesion energy between the two cold-welded layers, I is the second moment of area of the beam, h is the height of the particle and L is the length of the beam.

However, before bending, the dust particle (illustrated in Figure 5.1) can penetrate or indent the film or beam (layer 1), depending on the elastic nature of the dust particle (and that of the beam). Assuming that the dust particle is rigid, the dust particle can be idealized as a rigid indenter that penetrates the film or beam during the application of external pressure. Therefore, the Young's

modulus in Equation 5.1 can be replaced by the effective or combined modulus, E_{eff}, of the dust particle and film:[236], [237]

$$\frac{1}{E_{eff}} = \frac{1-(\upsilon_d)^2}{E_d} + \frac{1-(\upsilon_f)^2}{E_f} \tag{5.2}$$

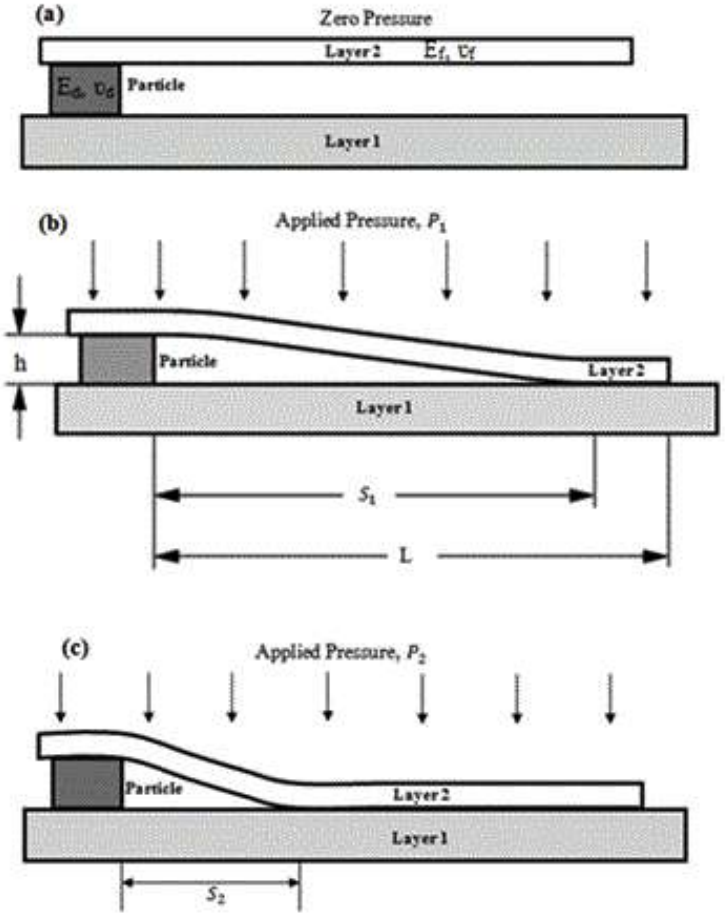

Figure 5.1: Elastic deformation of a cold-welded film layer around a particle (a) the layer is in contact with the particle with zero pressure applied (b) small pressure is applied on the film layer (c) additional pressure applied on the film layer. The length, s, of the void decreases with increasing pressure. E_d and E_f represent the Young's moduli of the dust particle and film or beam, respectively. υ_d and υ_f also represent the Poisson's ratios of the dust particle and film or beam, respectively

$$E_{eff} = \frac{E_d E_f}{E_f[1-(\upsilon_d)^2] + E_d[1-(\upsilon_f)^2]} \tag{5.3}$$

where E_{eff} is equal to the combined modulus of the film (beam) and the dust particle, E_d and E_f represent the Young's modulus of the dust particle and the film, respectively, υ_d and υ_f represent the Poisson's ratio of the dust particle and the film (beam), respectively. Therefore, Equation 1 becomes (i.e. E_f changes to E_{eff}):

$$U_s = \frac{6E_{eff} Ih^2}{s^3} - \gamma(L-s)a. \tag{5.4}$$

Taking the derivative of Equation (4) with respect to *s* gives:

$$\frac{dU_s}{ds} = -\frac{18E_{eff} Ih^2}{s^4} + \gamma a. \tag{5.5}$$

The minimum value of the total energy of the film occurs at a corresponding equilibrium $(dU_s/ds = 0)$ value of s. Hence,

$$s = \left(\frac{18E_{eff} Ih^2}{\gamma a}\right)^{\frac{1}{4}} \tag{5.6}$$

Defining the second moment of area as $I = \frac{at^3}{12}$, Equation (5.6) can be written as:

$$s = \left(\frac{3E_{eff} t^3 h^2}{2\gamma}\right)^{\frac{1}{4}}. \tag{5.7}$$

where t is the thickness of the film.

Equation (5.7) can be re-written as:

$$s = \left(\frac{3\left(\frac{E_d E_f}{E_f\left(1-(\upsilon_d)^2\right)+E_d\left(1-(\upsilon_f)^2\right)} \right) t^3 h_{eff}^2}{2\gamma} \right)^{\frac{1}{4}} \tag{5.8}$$

Similarly the contact length can also be written as a function of the applied pressure (the detailed derivation is presented in Appendix 5.1) as:

$$\frac{L_c}{L} = 1 - \left(\frac{3\left(\frac{E_d E_f}{E_f\left(1-(\upsilon_d)^2\right)+E_d\left(1-(\upsilon_f)^2\right)} \right) t^3 h_{eff}}{2PL^4} \right)^{\frac{1}{4}} \tag{5.9}$$

where L_c is the contact length, P is the applied pressure, h_{eff} is the effective height of the particle, and L is the length of the structure, as shown in Figure 5.1. The above analytical model (Equation 5.8) presented here was verified using the experimental study of adhesion in cold-welded Au–Ag interfaces obtained by Akande et al.[214] The results obtained from the finite element simulations were also validated by the experimental results[214] and the predictions obtained from the analytical model (Equation 5.9).

Hence, if the geometry and Young's modulus of the film are known, the interfacial adhesion energy between the cold-welded films can, therefore, be determined using force microscopy[130] or interfacial fracture mechanics methods, while the film Young's modulus can be obtained from nano-indentation. [229], [238] In the case of non-rigid particles, the applied

pressure will also induce the deformation of the trapped particles, as shown schematically in Figures 5.2a – 5.2c for stiff, semi-rigid and compliant particles, respectively. In such cases, finite element simulations were used to model the contacts and the deformation of the differential types of particles.

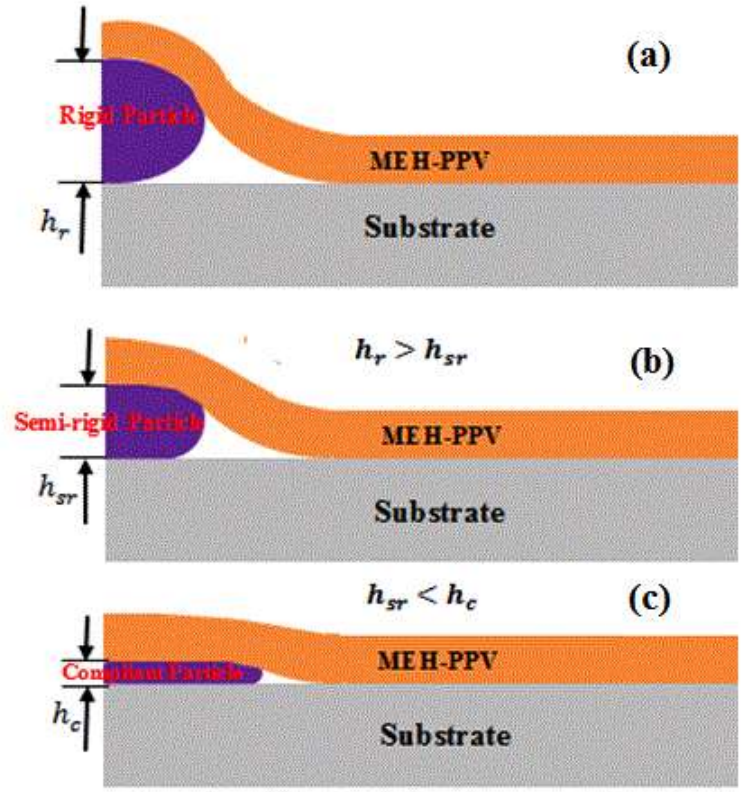

Figure 5.2: (a) – (c); Schematic diagram of cold-wedded MEH-PPV on substrate with different sandwich particles. The heights of the rigid, semi-rigid and compliance particles are h_r, h_{sr} and h_c, respectively

5.2.2 Computational Modeling of Surface Contact

In an effort to further understand the surface contact during the pre-cold-welding process and interfacial fracture during lift-off process, several finite element simulations were carried out using the ABAQUS^{TM} software package (Dassault Systèmes Simulia Corporation, Providence,

RI). First, the effects of the sandwiched/trapped particles (on surface contact) were simulated. Axisymmetric models were developed for the pre-cold-welding of MEH-PPV onto PDMS substrates (Figure 5.2). A four-node elemental mesh was used, similar to that in our prior work (Figure 5.3).[149], [170], [192], [214], [215] Fine mesh were used near the particles and the contact surfaces, where the stress and displacement levels were higher. The bottom boundary of the substrate was also fixed to ensure stability during the simulations. A uniform pressure was applied to the top of the stamp to simulate the application of pressure during cold welding. All the materials were assumed to be isotropic. The models were used to simulate the deformation of the layers and particles, as well as the contacts between the layers.

5.2.3 Computational Modeling of Lift-off as a Fracture Process

The lift-off stage of the cold- welding was modeled as an interfacial fracture process. This involved the interfacial fracture between bi-material pairs with impurity nanoparticles trapped between layers. Nanoparticles with different elastic properties were assumed to be present between these layered interfaces. Such nanoparticles have been revealed by Akande et al.[214] in prior transmission electron microscopy studies of focused ion beam cross sections of cold welded Au-Ag layers. Edge cracks were also idealized between layered interfaces [stamp/layer (top) and/or layer/substrate (bottom) interfaces]. A schematic of the lift-off process is presented in Figure 5.4.

The energy release rate at the tips of the edge cracks at the interfaces between the cold-welded film and the substrate are given by:[192]

$$G = f\left(\frac{\overline{E}_s}{\overline{E}_f}, \frac{t_s}{t_f}, \frac{d_b}{t_f}, \frac{d_t}{t_f}\right)\frac{\sigma^2 t_f}{\overline{E}_f} \tag{5.10}$$

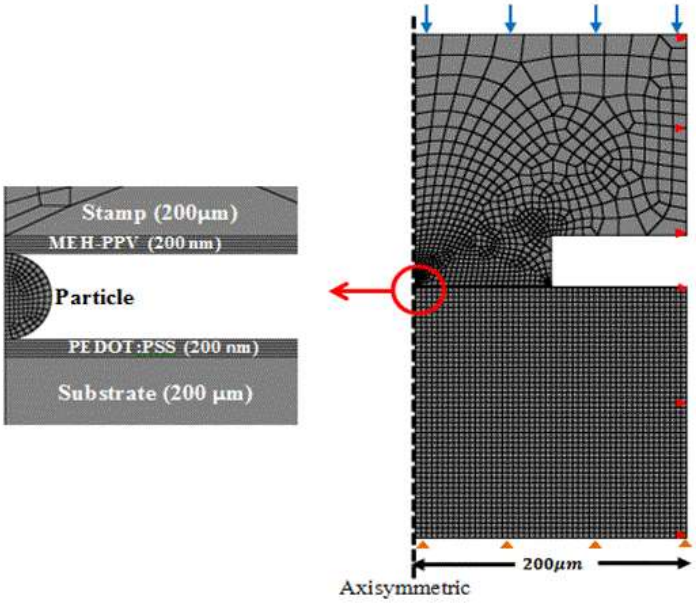

Figure 5.3: Geometry and mesh of finite element model of surface contact during cold-welding process [192]

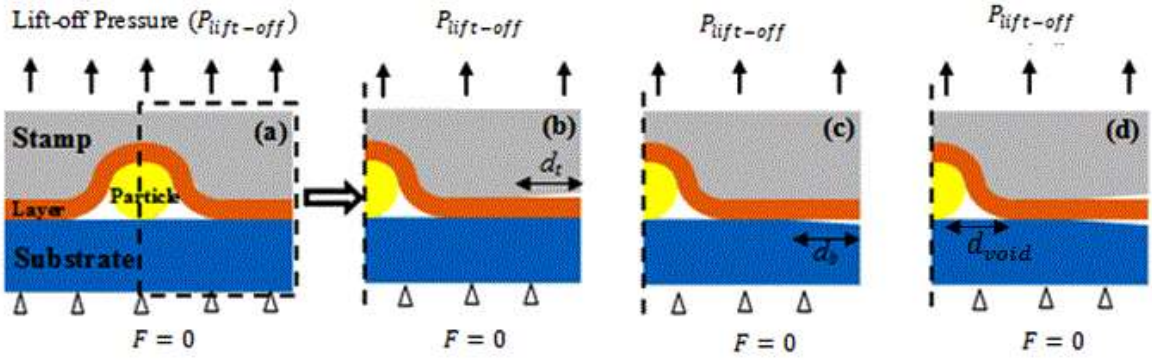

Figure 5.4: Schematics of micro scale models of interfacial fracture during the lift-off process of the lamination (a) model of the lift-off process after the press down of the layer on the substrate, (b) axisymmetric model of successful lift-off (note that d_t is the length of a top edge crack), (c) axisymmetric model of unsuccessful lift-off (note that d_s is the length of the bottom edge crack), and (d) axisymmetric model of partial interfacial fracture (note that d_{void} indicates the length of the bottom crack or the crack created by the particle) [192]

where $\overline{E}_f = E_f/(1-\nu^2)$ and $\overline{E}_s = E_s/(1-\nu^2)$ are the plane strain elastic moduli of the film and substrate, d_t and d_b are the lengths of top and bottom interfacial cracks, t_f and t_s are the thicknesses of the film and substrate, respectively, and σ is the lift-off stress.

The simulation of interfacial fracture (during the lift-off stage of the cold-welding process) was carried out using the ABAQUS^{TM} software package (Dassault Systèmes Simulia Corporation, Providence, RI, USA). The interfacial energy release rates at the tips of the edge cracks along stamp/MEH-PPV (top) and MEH-PPV/substrate (bottom) interfaces were computed as J-integrals. Four-node elemental meshes were used. A uniform lift-off pressure was applied to the stamp, while the bottom surface was fixed, as shown in Figure 5.4. The material properties that were used in the simulations are summarized in Table 5.1. These were obtained largely from the work by Du et al.[149] and Akande et al.[214]

5.3 Results and Discussion

5.3.1 Analytical Model and Verification

TEM images of cold-welded Au–Ag interfaces obtained by Akande et al.[214] were used to analyze and estimate the void lengths in the vicinity of carbon dust particles. Carbon steel was the dust particle material that was used to verify the current analytical model since the work reported by Akande et al.[214] attributed the presence of carbon steel[214] as one of the dust particle at the cold-welded Au-Ag interfaces.

The void length observed from the theoretical model was compared with quantitative estimates in the presence of carbon steel dust particle between the Ag and Au surfaces observed from Akande et al.[214] (Figure 5.5). The TEM image reveals the presence of dust particles at the cold

welded interface. The calculated void lengths are in agreement with the experimental results of Akande et al.[214]

Table 5.1: Material Properties

Materials	Young Modulus, E / GPa	Poisson's ratio, υ	References
PDMS	0.003	0.48	[203], [149], [193]
PEDOT:PSS	1.42	0.3	[149]
MEH-PPV	11.5	0.3	[149]
ITO	116	0.35	[149], [153]
Al	70	0.3	[105]
Carbon Steel	205	0.29	[239], [240]
Au	78	0.44	[241]
Ag	83	0.37	[242]
Low Density Polyethylene (LDPE)	0.2	0.3	[105], [239]

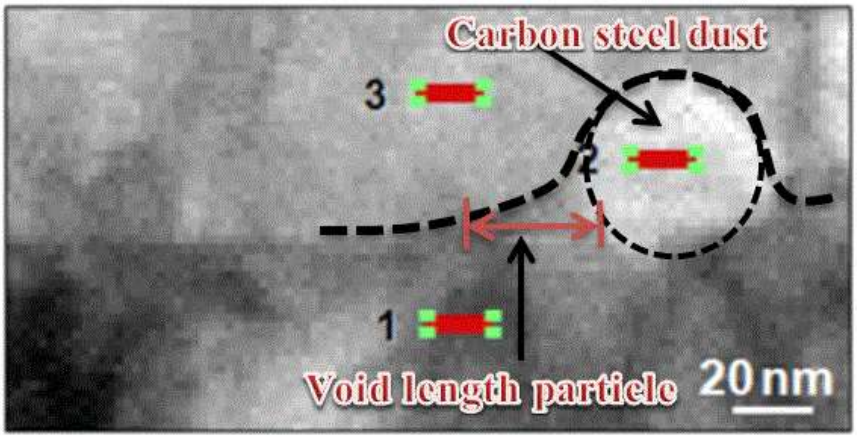

Figure 5.5: TEM image showing interfaces of as-deposited and cold-welded Ag–Au thin 1$\boldsymbol{\mu m}$ [214]

5.3.2 Deformation and Contact around Trapped Particles

Unlike prior work by Akande et al. [214], Kim et al.[227] and Cao et al.[229], in which the trapped particles were assumed to be rigid, the finite element simulations that were performed in the current work considered the elastic deformation of stiff, semi-rigid and compliant dust particles (i.e. aluminum, plain carbon steel and low density polyethylene, respectively) with Young's moduli of ~ 70 GPa, 205 GPa and 0.2 GPa,[149], [214] respectively. In the case of the rigid particles, the contact lengths predicted by the analytical models are presented in Figure 5.6a. The predictions obtained from finite element simulations (that included the actual deformation of the trapped dust particles) are presented in Figure 5.6b.

In both cases, the percentage of contact area increased with increasing applied pressure. However, the contact area was lower in the case of the stiffer layers e.g. Aluminum, as expected from prior work that showed that stiffer layers result in reduced contact lengths, for the same applied pressure.[149], [214], [233] In any case, increased pressure resulted in increased contact area, and the percentage of contact approached a plateau, as the pressure was increased, for each bi-material pair (Figure 5.6a and 5.6b).

The contact lengths also increased with increasing particle compliance, due to the increasing deformation of the particles, which resulted ultimately in improved film/surface contact. The modeling of particle deformation is, therefore, important for the modeling of contacts with compliant or trapped nanoparticles. These can give rise to larger open voids, in the case of more rigid particles, or closed elongated voids in the case of more rigid particles, or closed elongated voids in the case of compliant trapped particles. These two types of defects can affect the subsequent lift-off stage of cold welding, when the direction of the loading is reversed. Further details on the pull-off process are presented in the next section.

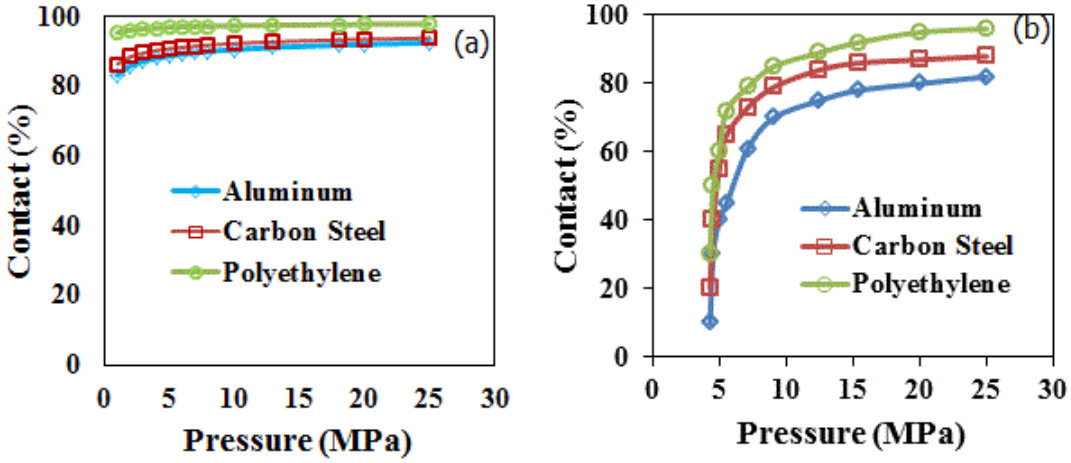

Figure 5.6: FEA results effect of pressure on the various contact percentage for (a) analytical and (b) computational models

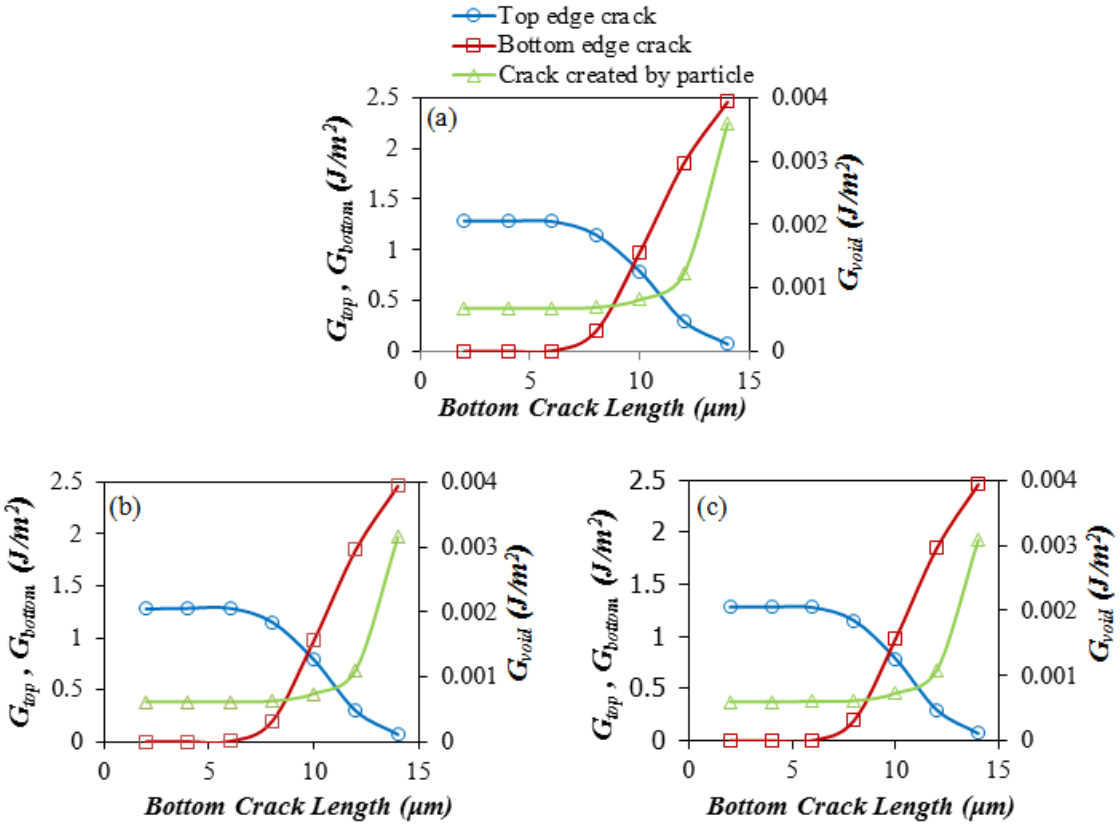

Figure 5.7: Interfacial fractures during lift-off; (a) compliant nanoparticle (E~ 0.2 GPa), (b) semi-rigid nanoparticle (E~10.2 GPa), and (c) rigid nanoparticle (E~ 70 GPa)

5.3.3 Modeling of Pull-off as a Fracture Process

The energy release rates associated with the pull-off stage of cold welding are presented in Figures 5.7a-5.7c, for lift-off around compliant nanoparticles (Figure 5.7a), semi-rigid nanoparticles (Figure 5.7b) and rigid nanoparticles (Figure 5.7c). The rigidity of the nanoparticles did not have a significant effect on the energy release rates that were computed for the top edge cracks (Figure 5.7a), bottom edge crack (Figure 5.7b) and the cracks created by the particles (Figure 5.7c). Hence, in all cases, the trends in the computed energy release rates were similar.

In order to understand the implications of the computed energy release rates, it is important to compare the computed results with prior measurements of adhesion energies that were obtained for the relevant bi-material pairs in prior work.[16], [44], [130], [204], [214], [243] Prior measurements of adhesion energies are presented Table 5.2 and Figure 5.8. These show that the computed energy release rates (Figure 5.8) can exceed the measured adhesion energies (Figure 5.7) obtained in the interfaces that are present in OLED structures.

However, since the crack driving forces are strongly dependent on crack length, initial crack growth for small cracks is more likely to occur along the top edge crack than the bottom (Figure 5.7). Also, a gradual transition to interfacial crack growth is likely to occur, as the bottom crack length increases beyond ~5 μm (Figure 5.7). Finally, the voids associated with partial contact around impurities are more likely to induce crack growth, as the bottom crack length increases beyond ~10 μm (Figure 5.7). It is important to note that as the crack extends by a kink at the interface, it smoothly follows the interfacial paths of small kink angles for which mode mixities vanishes at all times.[244]–[248]

Table 5.2: Adhesion Energies. [105], [204]

Tip Coating	Substrate Coating	Average Force (nN)	Adhesion energy (J/m^2)
Aluminum	MEH-PPV	10.00±1.20	0.8±0.05
MEH-PPV	PEDOT:PSS	59.00±6.00	15.00±3.00
ITO	PEDOT:PSS	30.00±6.70	1.70±0.38
ITO	Glass	58.24±14.33	9.31±1.20

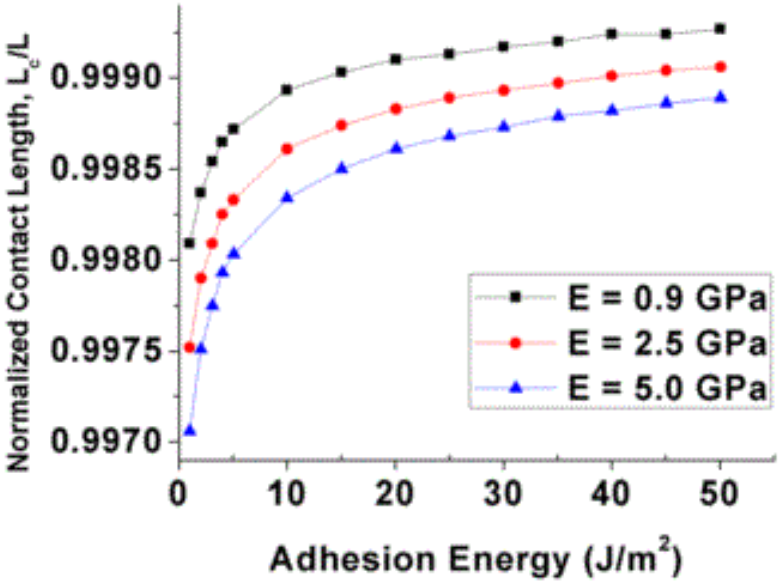

Figure 5.8: Adhesion energy against contact length for different Young's moduli [204]

5.3.4 Dependence of Interfacial Energy on Void or Particle Height

The dependence of the energy release rate on the initial void length, S, is presented in Figure 5.9. The results show that the energy release rates decrease with increasing void length. Also, since

the void length increases the crack driving forces, increased void lengths are likely to result in higher crack driving forces that are more likely to exceed the interfacial fracture energies (Figure 5.8 and Table 5.2). Hence, larger voids and partial contacts are more likely to result in favorable conditions for lift-off during cold welding.

5.3.5 Implications

The implications of the above results are quite significant for cold welding processes. First, they suggest that cold welding process can be idealized as a two stage process in which the first stage involves evolving contacts with adhesion, while the second stage involves interfacial fracture processes. Since the crack driving forces vary with changes in crack lengths, the initially favored cracks may not be the ones that propagate ultimately to failure.

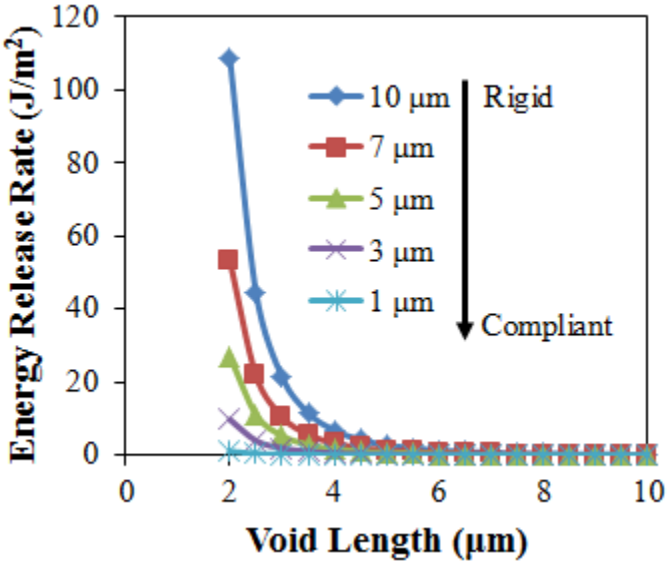

Figure 5.9: Effect of dust particle moduli on void length and interfacial energy release rate

Furthermore, the conditions for layer cracking may become lower than those required for interfacial cracking in some scenarios.[249]–[252] In such cases, the cracks may kink in-and-out of interfaces, depending on the prevailing crack driving forces and mode mixities.[231], [250],

[253], [254] Such kinking may also be favored when the microscopic fracture mechanisms (in the layers) favor micro-void coalescence, as shown in prior work by Rahbar et al.[255]

In any case, the current work shows that contact, during cold welding, is enhanced by compliant stamps and impurities, applied pressure, and increased adhesion energies. However, increased contact also makes it more difficult for lift-off to occur. Hence, a balance is needed between improved surface contact (for improved charge and light transport[256]) and lift-off for interfacial separation of the stamp from the cold welded structure. This can be facilitated by the use of a layer with low adhesion energy between the stamp and the cold welded layer.[257] Further work is clearly needed to develop process design maps for the design of such low adhesion layers during the contact and lift-off stages of cold welding.

5.4 Conclusion

This chapter presents the results of a combined analytical and computational study of the contact and lift-off stages associated with the cold welding of Au and Ag thin films. The study shows that the surface contacts improve with increased pressure, reduced film thickness and reduced interfacial nanoparticle stiffness. However, improved contacts result in higher lift-off forces for interfacial separation during the pattern transfer stage of cold welding. Increased pressure may also lead to sink-in of dust particles, which may lead to device damage. An intermediate pressure range is, therefore, needed for the effective cold welding of Au-Au and Au-Ag layers. Also, the analytical model shows that the void length is dependent on the effective modulus and height of the dust particle. The range void sizes observed is similar to the ranges observed in prior experiments on Au-Au[192] and Au-Ag[214] films.

APPENDIX 5.A:

Analytical Calculation of Contact Length as a Function of Applied Pressure for Cold Welding

The surface energy between the film and the substrate is the product of pressure (P), surface contact area $(L_c \times a)$ and effective height of the particle (h_{eff}).[22] This is written as:

$$U_e = -P \times (L_c \times a) \times h = -PahL_c \qquad \text{5. A1}$$

Since $L_c = L - s$, the total energy in Equation 1 can now be written as:

$$U_s = \frac{6E_{eff} Ih^2}{s^3} - Pah(L - s) \qquad \text{5. A2}$$

Differentiating Equation (A2) with respect to s gives:

$$\frac{dU_s}{ds} = -\frac{18E_{eff} Ih^2}{s^4} + Pah \qquad \text{5. A3}$$

The length of the void can be calculated from Equation (A3) at the equilibrium, $dU_s/ds = 0$. This is given by

$$s^4 = \frac{18E_{eff} Ih^2}{Pah} = \frac{18E_{eff} Ih}{Pa}. \qquad \text{5. A4}$$

Defining the second moment of area as $I = at^3/12$, equation (A4) can be written as:

$$s = \left(\frac{3E_{eff} t_f^3 h}{2P}\right)^{\frac{1}{4}} = L - L_c \cdot \qquad \text{5. A5}$$

Hence,

$$\frac{L_c}{L} = 1 - \left(\frac{3E_{eff} t_f^3 h}{2PL^4}\right)^{\frac{1}{4}} \qquad \text{5. A6}$$

Introducing the effective modulus and changing h to h_{eff} gives:

$$\frac{L_c}{L} = 1 - \left(\frac{3\left(\frac{E_d E_f}{E_f\left(1-(\upsilon_d)^2\right) + E_d\left(1-(\upsilon_f)^2\right)} \right) t^3 h_{eff}}{2PL^4} \right)^{\frac{1}{4}} \quad . \qquad \text{5. A7}$$

CHAPTER SIX

STUDY OF SOLAR POWERED LED: IMPLICATIONS FOR POLICY

6.1 Introduction

In recent years, there has been increasing recognition of the need to formulate effective evidence-based policies that can result in the delivery of electricity to the roughly 2 billion people that live in off-grid areas in the developing world [258]–[261]. Since the cost of conventional power plants and grid connections is prohibited in the short term [262], the need to use alternative power supply systems has become apparent to those engaged in providing electricity to the rural/urban poor [263]. This has resulted in the use of solar energy [264], wind energy [265], small hydro-power [266], [267] and biomass [268] in the provision of clean alternative energy sources that could increase the access of the rural/urban poor to electric power [269].

Portable solar powered lanterns (Roy Solar, Shanghai, China) represent one approach that can be used to provide electricity to the rural/ urban poor that live on incomes of ~$1-2/ day. For such people, the cost and financing of solar lighting are just as important as the social, health and technological impacts of the lighting technologies [261]. There is, therefore, a need to explore the influence of these factors on the adoption and diffusion of solar lantern technologies before formulating evidence based energy policies that can be used to facilitate the scale-up and diffusion of solar lanterns to the 2 billion people that currently lack access to electricity [258], [261].

This chapter presents the results of a questionnaire study of the factors that influence the adoption of solar lanterns into a rural off-grid village, Mpala Village, in the Laikipia District of Kenya. These include: social, economic, technology, cultural and aesthetic factors that influence the adoption and diffusion of solar lanterns. The study was conducted on a village with 53 homes that purchased the solar lanterns through financing schemes that were administered by the local employer (Mpala Research Center) in Mpala. The study identifies the key factors that contribute to the adoption and diffusion of the technologies. It also provides some new insights for the development of financing strategies and evidence-based energy policies that could provide access to solar energy for people living on $1-2/ day in off-grid rural/ urban communities. The implications of the results are discussed for the formulation of evidence-based policies and the development of public-private partnerships that can help to deliver energy solutions to the rural/ urban poor.

6.2 Project Goals

The following four inter-related goals were established for the project:

6.2.1 Study the Geographic and Temporal Diffusion of Solar-Powered Lanterns through an Electrically off-grid Community

This study is intended to continue a line of diffusion studies [270]–[275] that study how the distribution of technology can be made more efficient and effective; not only is there a lot of ground to cover – both in terms of market and geographic size – but technology adoption relies on physical and financial access, in addition to branding and consumer awareness and confidence. So, for example, network effects that can be studied by mapping the diffusion of technology can be useful in seeing how a desire to imitate peers in a network influences one's

decisions, or if peer reviews influence or inform one's purchasing model. Similarly, it is useful to see how news and information is spread geographically in order to capitalize on new distribution models outside of traditional vendors (e.g. mobile health clinics, and schools).

6.2.2 Identify Key Factors and Motives that Influence the Decision to Purchase, Decline, or Share the Solar Lanterns

Since the adoption of a new technology involves both a direct purchase and a behavioral change, this study is intended to identify the factors that drive the sale and adoption of the technology. Many studies show that aspirational marketing can be one of the best ways to foster a behavioral change [276], [277]. But since this involves health levels, children's education, and potential financial savings, one must determine if aspirational marketing is even needed or if the facts speak for themselves. This information is important for businesses in developing effective marketing schemes. Policymakers can also use this information for public campaigns to promote technologies with demonstrated societal benefits.

6.2.3 Identify Key Barriers to Entry for This and Other Solar Technologies

If there is a demonstrated problem and a proven solution, then what is standing in the way? There are a lot of questions that must be answered. For example: Is it the initial cost? How does the role of financing options play into the affordability? Or is it running/maintenance cost? How can repairs be facilitated and warranties implemented? Is it physical access? How can the products increase their geographic coverage? Is it knowledge/understanding/trust of solar? How can market spoilage and consumer confidence be maintained? Is it government policies? How can they foster an enabling and supportive environment for these organizations or companies? Is

it technological competition? How do solar lanterns compete for market share against kerosene or electric lights in off-grid communities? Is it sun coverage? How does geographic location/environment play a factor in the feasibility or even cost of use?

6.2.4 Determine a Feasible Scale-Up Strategy to Promote the Diffusion of Technology in Rural Communities in Developing Regions

Once the factors that drive the adoption of solar lanterns and the barriers to their entry are identified, a strategy can be developed to expand upon the results and model posed in this study to bring the technology to other areas. This will undoubtedly require an entrepreneurial model operated in an environment with favorable policies.

6.3 Hypotheses

The following four primary hypotheses in mind were tested in this study.

6.3.1 The Solar Lanterns Would Have a Positive Impact on Social, Education, and Health Statuses and Levels

Since the solar lanterns are meant to take the place of traditional kerosene lanterns, it is hypothesized that the removal of smoke-inducing kerosene will reduce the incidence of upper respiratory infections. Similarly, the whiter and more reliable light will make it easier for children to read at night to complete their studies. Finally, the lantern will be seen as a status symbol, the ownership of which denotes access to modern and advanced technology.

6.3.2 Despite a High Up-front Cost (~USD 52), the Negligible Costs of Maintaining and Charging the Solar Lanterns Would Result in Significant Long-Term Cost-Savings for the Community Members

It is hypothesized that the $52 is a worthwhile initial cost to bear because off-grid communities are overpaying for their lighting and energy services compared to their electrified counterparts. The time and money savings offered by the solar lanterns should provide a return on the investment within roughly one year.

6.3.3 Allowing for Monthly Installment Payments Would be an Attractive Financing Option That Would Increase the Adoption of the Lanterns in the Community

Nevertheless, $52 represents nearly half a month's salary for the average worker at Mpala. This is clearly a significant expenditure that may be difficult to fit into one's budget. To facilitate the purchase of the lanterns, a monthly financing scheme will be introduced that is hypothesized to ease the burden of the payments and make it easier for consumers to repay. This should be easier than alternatives that require full payment before the lanterns are received, such as trying to build meaningful savings towards this expenditure or purchasing on layaway.

6.3.4 Barriers for Entry Would Center Primarily on Questions of Access (Affordability and Distribution) Rather Than a Lack of Interest or Use for the Product

It is hypothesized that off-grid communities are acutely aware of the high price that they are paying – both literally and figuratively. It is therefore predicted that communities will be receptive to solar lanterns for their lighting needs. However, this is not to say that they will immediately welcome the technology without question. Nonetheless, it is expected that concerns

about product function and performance will be outweighed by more tangible problems such as financial and physical access, given the costs of the lanterns as well as the geographic remoteness of many off-grid communities. This is particularly true in a country like Kenya, which has already established a strong solar-based market [278].

6.4 Project Design

6.4.1 Sample Population

The research was conducted over a period of two years. The investigation involved a year-long impact assessment of solar-powered lanterns in an electrically off-grid village (Mpala Village in Laikipia District) in rural Kenya. This was followed by a year-long follow-up survey in the same community. The community represented one of three communities of staff members for a wildlife research center, the Mpala Research Centre (henceforth, Mpala or MRC), in the Laikipia district of central Kenya (Figure 6.1). While these community members are guaranteed to have at least one household member with fairly stable employment, the village is nonetheless located one hour by car from the nearest outpost town, Nanyuki. This remoteness translates into restricted access to infrastructure (power lines, paved roads), disproportionate use of resources (time, money) to access basic supplies, and a lack of information and technology transfer.

Originally, kerosene was the overwhelming fuel choice for lighting in this community. This was in spite of problems of access, cost, and adverse health side-effects (pulmonary problems). The goal of the study was, therefore, to create and administer a community-wide survey before and

after the introduction of solar-powered lanterns[1] in order to determine both the factors that influenced the adoption of the technology and the health, socio-economic, and education impact of the lanterns. Solar lanterns were also chosen over other types of solar power generation technologies – particularly, Solar Home Systems (SHSs) – because their price points were much lower. Moreover, the solar lanterns address a more fundamental need (lighting) that was seen to be more accessible and relevant to both the upper and lower income brackets in the village.

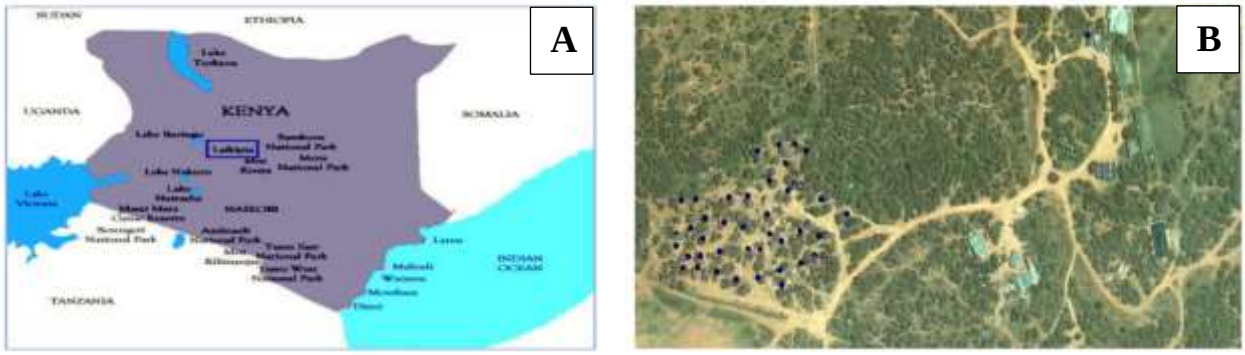

Figure 6.1: Map of (a) Kenya and (b) Aerial view of the MRC staff village. MRC Research facilities have green rooftops. Blue dots correspond to households of survey participants. SOURCE: Google Earth

6.4.2 The Solar Lanterns

The solar lanterns used in this study were purchased from a Shanghai-based supplier, Roy Solar (Roy Solar, Shanghai, China). This lantern (Model SRY-101L) was one of the earlier solar lanterns on the market. It was chosen for its ability to provide consistent room lighting at a reasonable price. Despite a design that closely mirrors traditional hurricane-style lamps as shown in Figure 6.2, these portable lanterns are quite different in function and utility. While the

[1] NB: The solar-powered lanterns will also be referred to as solar lanterns or, simply, lanterns. This is in contrast to the traditional kerosene or hurricane lamps or lanterns, which the community previously used. These lanterns will always be specified

kerosene lanterns emit hazardous fumes, these solar lanterns are safe and environmentally friendly.

They can also be transported or used anywhere in the world that receives ample amount of sunlight. The lanterns consist of LED lights that are powered by a 6 V battery and are connected to a 3 W crystalline silicon solar panel, as shown in Figure 6.3. The rugged system provides enough energy to provide 5 – 10 hours of lighting and/or cell phone charging, or an hour of radio listening each night.

Figure 6.2: Comparison of a Roy Solar Lantern with a traditional hurricane kerosene lantern

6.4.3 Financial Options

One crucial provision of this research study was that the community members be treated as customers rather than charitable recipients. The lanterns were, therefore, sold at a cost, for 3900 kshs per unit.[2]

Table 6.1 Exchange rates between the Kenyan Shilling and US Dollar at six month intervals

Exchange Rate kshs : 1 USD				
Jan 2010	**Apr 2010**	**Jul 2010**	**Oct 2010**	**Jan 2011**
75.7714	77.2572	81.3903	80.6604	80.9976

[2] Due to an unstable exchange rate, it is difficult to go back and forth between Kenyan Shillings (kshs) and US Dollars (USD or $). The two currencies will be used as appropriate, with a conversion rate based on the average January 2010 or 2011 value, as dictated by OANDA (www.oanda.com). Table 1 contains a list of the different exchange rates used over the course of this research study. The difficulties associated with this sliding exchange rate will be elaborated in more detail under the section on Product Pricing

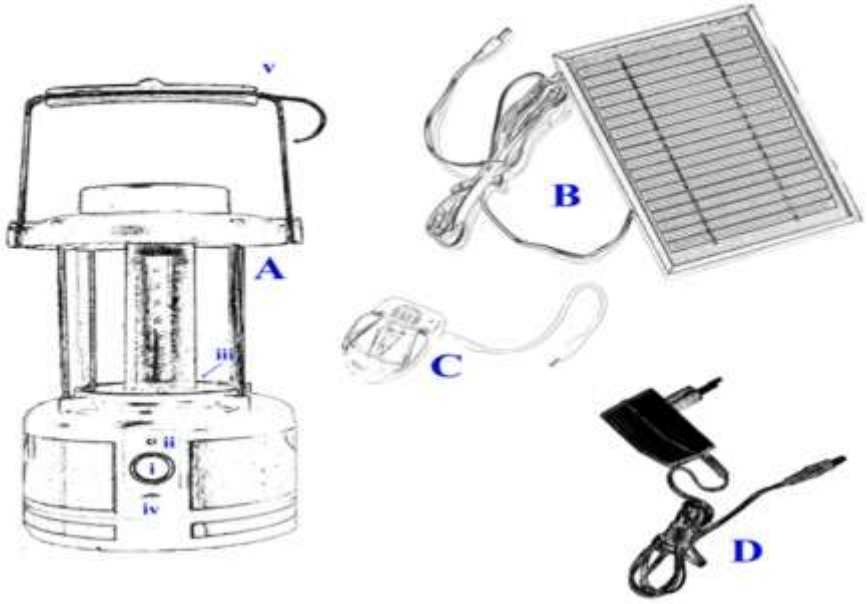

Figure 6.3: Components of the Roy Solar Lantern: (A) solar lantern with (i) ON/OFF switch; (ii) battery charge indicator light; (iii) port for mobile phone connection; (iv) port for solar panel connection, and (v) hook to hang the lantern; (B) 3W solar panel; (C) universal mobile phone charger, and (D) AC wall charger

This was important for three reasons: first, it has been demonstrated in multiple studies that an attempt to introduce a new technology to a community can be more successful if the community members associate value with the technology or product itself [279]–[282]. Secondly, such a study can only be useful for entrepreneurs and policymakers, if the decision-making process and cost-benefit analysis mirrors that of consumers at large. Finally, the money, once repaid, was used to maintain the financial sustainability of the project.

Nevertheless, it was recognized that 3900 kshs often represents a prohibitively high financial barrier that is out of reach of many of the "base of the pyramid" (BOP). These are the consumers

that are the exact demographic that could benefit the most from such technology. It was, therefore, important to provide a financing scheme that would make the lanterns more affordable to the community. It has been shown that a new behavior or service is most easily adopted when it is seamlessly integrated with prior practices [280]. Those who chose to purchase the lantern were given the option of paying in full or in monthly installments.

The lowest payment, at 325 kshs a month, was, therefore, on par with the typical costs (270 kshs) that these families already paid for kerosene. Yet, unlike the purchase of kerosene, the payment for these lanterns did not demand hours of travel to continuously replenish supplies. To further provide a smooth transition, payments were deducted directly from people's paychecks through an agreement with the MRC staff management. While this is not always a possible financing option, there have been many previous examples of similar initiatives that work with employers, unions, or cooperatives to offer financial assistance through similar types of transactions [283].

6.4.4 Timeline

Following an initial pre-assessment of the community in March 2009, the formal study began in January 2010. 100 lanterns were ordered and shipped to the MRC in November 2009. After the completion of the surveys, which are described in further detail in the section under Survey Design, the lanterns were distributed to the community following a priority system: in return for participating in the survey, households had up to one month to make a decision whether or not to purchase the lantern. Moreover, a household could establish a "credit history" by paying off its first lantern and in turn gain the ability to purchase an additional lantern, if desired. A follow-up survey was then administered after a full year of use (January 2011). Finally, a return visit was

made in August 2011 to check up on lantern performance and work with local stakeholders to determine a sustainable scale-up strategy.

6.5 Survey

6.5.1 Survey Design

The survey study was designed to collect quantitative data and qualitative feedback at both the household (HH) and individual level. Household-level questions were divided into four sections: demographic information; income/asset assessment; lighting sources and habits, and factors for adoption (in Survey 1) and feedback from lantern use (in Survey 2). Meanwhile, individual-level questions targeted physical health levels (particularly for signs of upper respiratory illness), health treatment routines, and study habits. The surveys were anonymous, with each household and individual assigned a unique numerical code for identification. Two local assistants were trained and employed to help administer the survey in Kiswahili or Turkana, as necessary. The respondents were not compensated, but rather were placed on a guaranteed priority list, in return for participation.

Whenever possible, the head of the household was interviewed for the household-level survey questions. Each individual family member was also interviewed for their personal health and study habit-related questions. However, the work and school schedules of many of the family members often prohibited the entire family from being present at once. So, with discretion, the head of the household or their spouse were allowed to answer questions on behalf of absent family members. Given the small quarters (each house was max. 12 ft. in diameter) and cultural

openness between family members, it was determined that this was a reasonable logistical accommodation.

6.5.2 Differences between the 2010 and 2011 Surveys

While the two surveys were largely similar, there were several notable differences. For instance, relative income levels were initially evaluated by indirect indicators, such as assets and standard of living. However, because of the high degree of standardization of the staff housing, more direct questions on average income ranges were included in the 2011 survey. Meanwhile, the respondents were asked to provide more formal qualitative feedback describing their experiences using the solar lanterns, in addition to rating the lantern and its components across a variety of dimensions. The respondents were once again asked to report their average kerosene expenditures. However, without requiring them to keep a monthly log, these values must be treated as rough estimates.

Finally, there were a number of households that were interviewed in 2010 that could not be reached for interviews in 2011. In two instances, separate couples had since gotten married and moved into a single household. There were four additional instances of households that had either left Mpala in the previous year or who were away for their annual leave. Meanwhile, there were a number of lantern users who had not been included in the initial survey, but had been using the lanterns for at least 6 months. 11 of these households were given mini-surveys, with a particular emphasis on sections such as survey feedback and prior verses current kerosene expenditures. This retrospective data is included in the calculations of kerosene and lighting expenditures, but should be noted for its susceptibility to memory error. Altogether, data from 53

households was used in this survey. However, the 42 households, for whom there are complete and temporally accurate datasets, will occasionally be treated separately and referred to as "before-and-after households."

6.6 SURVEY FINDINGS AND DISCUSSION

6.6.1 Community Demographics:

In the 2011 survey, households ranged from 1-8 people, with an average size of 2.5. This is down from the 2010 average of 3.1, but does not, however, tell the full story; due to space constraints, many individuals now act as migrant workers, separated from a spouse or older children, who live elsewhere. Household sizes defined in terms of financial dependency were, therefore, larger than those reported. Of the 42 before-and-after households, the male-to-female ratio in the community stayed at around 62:38. However, there were only 48 children in 2011 compared to 61 in 2010. A total of 4 households were headed by women in 2010; 5 households were led by women in 2011. The average adult education level was Grade 7 (6.28), but 19 adults were completely illiterate and only 9 had any sort of diploma or higher education degree. A snapshot of community demographics is presented in Table 6.2. Table 6.3 provides a similar snapshot of the community's happiness and financial indices. The majority of households earned incomes between 5000-10000 kshs/month (Figure 6.4a), which roughly translated into $2.15-$4.30/day or $774-$1548/year. Yet the distribution was uneven and, based on income brackets for the year 2000, as reported by Jacobson (Jacobson 2007:144-162), incomes in this village would range from the 2nd to 10th decile for rural household incomes (Figure 6.4b). When asked to rate their general happiness on a 1 (low) to 5 (high) scale, most people indeed said that they

were “happy.” Meanwhile, the community tended to think that things were “a little better,” compared to a year ago, and would continue to get “a little better” in the coming 3 months.

Table 6.2: Community demographics

Household Demographics (for the 42 before-and-after households)

	Total Members	**No. Male**	**No. Female**	**No. Spouses**	**No. Children**	**Avg. HH Size**
2010	130	80	50	20	61	3.1
2011	103	64	39	19	36	2.5

Table 6.3: Financial snapshot

Happiness and Financial Index Averages, 2011

Income Bracket	Happiness Now	Happiness, Compared to Last Year	Optimism About the Next 3 Months	Finances, Now	Finances, Compared to Last Year	Financial Optimism About the Next 3 Months
2.6	4.1	4.0	3.9	3.7	4.0	3.6

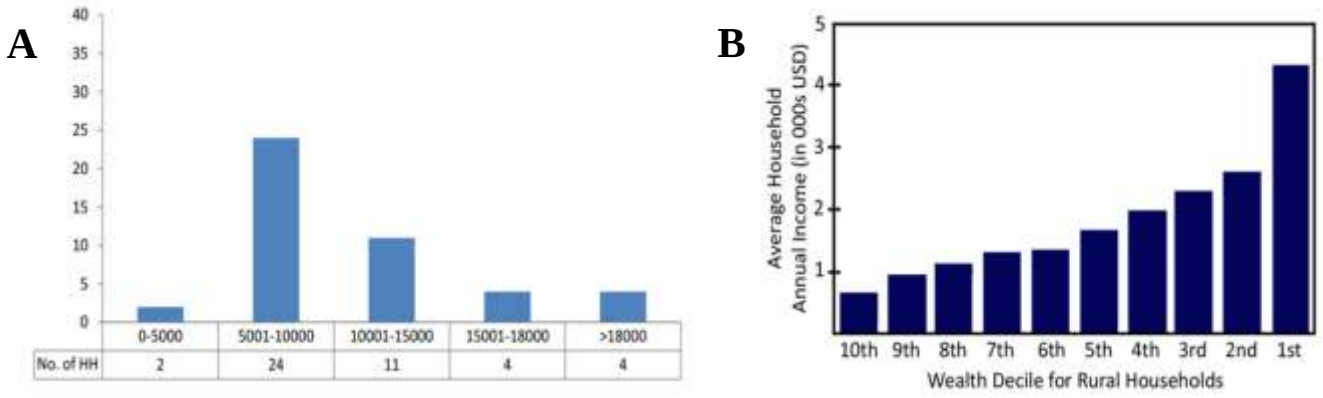

Figure 6.4: (a): Average monthly income levels in 2011, kshs (note: 77.53 kshs: 1 USD). (b): 2000 Statistics for distribution of income by wealth decile for rural households in Kenya (using an exchange rate of 76.3 kshs:1USD) ([284])

As for their financial state, on average people said they were fairly "comfortable," though many professed they were "just getting by." While housing and living conditions were fairly standardized, with some basic infrastructure (shelter, latrines, access to a central diesel generator) subsidized by the MRC management, there was still a fairly wide range of asset ownership amongst the households. Nevertheless, the selection of items retained at the MRC still revealed glimpses into each household's daily needs and preferences. All but two households owned a mobile phone, with almost 40% owning two or more. After a charcoal stove, the next most common possession was a radio, followed by a handful of chickens. Just under half of the households owned a TV (color or black & white). Social and interconnection-motivated possessions were, therefore, high priority items. This is in line with previous research on consumer needs of rural populations [276], [284]. An inventory of common assets is compiled in Table 6.4.

Table 6.4: Common asset ownership (53 total households)

(a) Households Reporting Ownership of Various Assets		
	2010	**2011**
Electricity	8	7
Refrigerator	0	0
Oven	1	4
Stove (charcoal, wood, or kerosene)	43	45
Stove (electric)	2	0
Sewing Machine	1	3
Fan	0	0
Radio	39	45
TV (color)	9	11
TV (black & white)	11	10
VCR	2	2
DVD/VCD Player	12	8
Computer	0	0
Animal-drawn cart	0	0
Bicycle	9	9
Motorcycle/Moto Scooter	0	1
Car/Truck	0	2
Chickens	26	27

(b) Mobile Phone Ownership per Household					
No. of Mobile Phones	0	1	2	3	4
No. of HH	3	27	21	2	1

Before the introduction of the solar lanterns, power generation sources fell into a small variety of forms: 14 households relied heavily on simple disposable AA or D-cell batteries for portable electronics, with 12 households claiming this as their primary "energy" source. On the other end of the spectrum, 8 households reported reasonably reliable access to electricity, which was supplied by the MRC's main generator (a combination of diesel and solar). However, the vast majority of households relied on larger battery-based electricity, charged either by the MRC's main generators or by small-scale solar panels that were fitted on top of their homes. In fact, 11 households had already purchased solar panels for their homes, though many complained of the poor quality of the low-cost panels that they had bought in town. Such feedback is again consistent with previous research on market spoilage and the high proliferation of cheap or imitation solar panels in Kenyan and other emerging markets. These panels threaten to undermine the long-term diffusion of solar-based technologies in off-grid areas [285].

As for lighting sources (Figure 6.5), the hurricane-style kerosene lantern was by far the most popular style, with 45 units counted and 33 households reporting this as their primary source of lighting. 5 households were unable to afford the ~380 kshs that it cost to purchase the hurricane style lamp, and instead had homemade variants of a kerosene/paraffin-based lantern. While owners of the hurricane-style lantern frequently complained of the daily maintenance required to clean and refill the lanterns, as well as the dangers that the smoke and hot glass posed to their family members, owners of these homemade lanterns bore an even greater challenge as they frequently had to bear flames in their homes that were completely open and unprotected altogether.

Figure 6.5: (Color online) Different lighting sources in the community in 2010. CW from top left: Electric light; hurricane-style kerosene light; homemade kerosene lantern; wick kerosene lantern; a small Christmas light coupled with a CD to better-disperse the light

Despite the prevalence of kerosene-based lighting, a number of homes chose to use their battery-based energy systems to power electric compact fluorescent lights. Yet even in these cases, respondents frequently indicated a strong interest in the solar lanterns because of: (a) their portability and (b) the ability to save up precious battery life to power a radio or TV instead. Prior ownership of an electric light, therefore, did not seem to present a significant barrier for technology adoption. In fact, when comparing the 2010 and 2011 statistics for primary versus total energy and lighting sources (Table 6.5 and Figure 6.6), it can be seen that the number of households claiming an electric light as their primary lighting source in 2011 dropped from 15 to 11, despite the number of battery-based households remaining fairly constant. Altogether, 38 households now claimed the solar lantern as their primary lighting source.

Table 6.5: 2010 vs. 2011 energy and lighting sources (53 Total Households; families could own multiple sources of energy or lighting)

(a) Energy Source Comparison

	2010		2011	
	No. Units	**No. Primary Units**	**No. Units**	**No. Primary Units**
AA Batteries	14	12 (86%)	13	12 (92%)
MRC Gen (only)	8	8 (100%)	7	7 (100%)
MRC + Battery	23	18 (78%)	27	20 (74%)
Solar Panel + Battery	11	10 (12%)	12	9 (75%)

(b) Lighting Source Comparison

	2010		2011	
	No. Units	**No. Primary Units**	**No. Units**	**No. Primary Units**
Hurricane Lantern	45	33 (73%)	9	4 (44%)
Homemade Kerosene Lantern/Candle	5	3 (60%)	0	0
TV	3	2 (67%)	4	0 (0%)
Electric Light	16	15 (94%)	15	11 (73%)
Solar Lantern	0	0	52	38 (73%)

Perhaps most notable, however, was the statistic relating to kerosene lamp usage: The number of hurricane or homemade kerosene lamps owned by the community plummeted from 50 to 9, with the majority of these unused lamps having been given to family members back home. Moreover, only 4 households claimed these kerosene lanterns as their primary lighting sources. The reasons for persisting with their kerosene lanterns tended to revolve around physical problems with the solar lanterns themselves, such as dying batteries, loose wires, or broken bulbs. These issues, though by no means trivial, still point to the overall success in the solar lanterns in playing a substitutive rather than additive role in household's lighting portfolios.

A

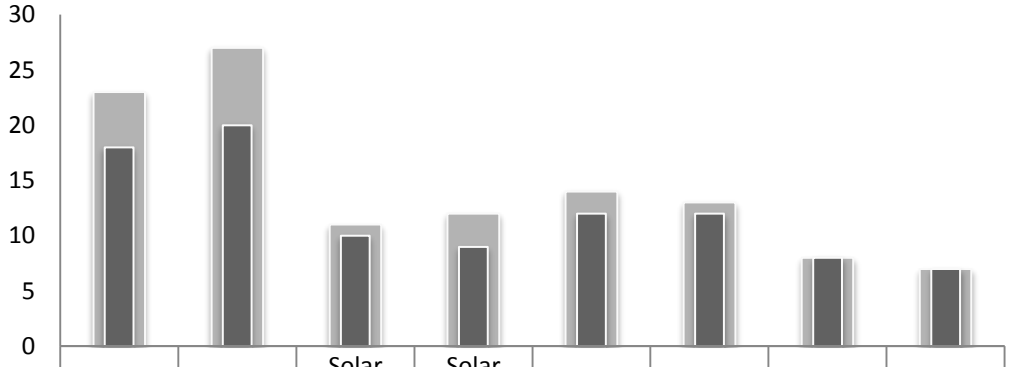

	MRC gen + Battery (2010)	MRC gen + Battery (2011)	Solar Panel + Battery (2010)	Solar Panel + Battery (2011)	AA Batteries (2010)	AA Batteries (2011)	MRC Gen (only) (2010)	MRC Gen (only) (2011)
No. Total Units	23	27	11	12	14	13	8	7
No. Primary Units	18	20	10	9	12	12	8	7

B

	Hurricane Lantern (2010)	Hurricane Lantern (2011)	Home made Kerosene Lantern /Candle (2010)	Home made Kerosene Lantern /Candle (2011)	TV (2010)	TV (2011)	Electric Light (2010)	Electric Light (2011)	Solar Lantern (2010)	Solar Lantern (2011)
No. Total Units	45	9	5	0	3	4	16	15	0	52
No. Primary Units	33	4	3	0	2	0	15	11	0	38

Figure **6**.6**:** Different lighting sources in the community in 2010. cw from top left: Electric light; hurricane-style kerosene light; homemade kerosene lantern; wick kerosene lantern; a small Christmas light coupled with a CD to better-disperse the light

6.6.2 Technology Diffusion throughout the Community

The lanterns were only distributed upon completion of the first survey to ensure fairness and minimize peer influence on the responses. Survey respondents were placed on a priority list, with lanterns guaranteed for availability within a purchase period of one month. 50 of the 52 households in the original sample community purchased the lanterns, with 49 choosing some sort of installment payment option. 98% of these purchasing households reported that this financing option was helpful in making the lanterns affordable to them.

As news of the lanterns spread throughout the duration of the survey period, members from a neighboring and affiliated ranch community (henceforth, the Mpala Ranch) expressed strong interest in the lanterns. These sales accounted for the remaining 45 lantern sales and a second order was soon placed to fulfill the overwhelming demand. Lantern adoption by the community was very rapid, with 60 of the lanterns distributed and accounted for within the first four days of availability (Figure 6.7). The vast majority was sold to residents of the Mpala Research Centre and Ranch. However, a number of local visitors and affiliates, such as health workers at a nearby medical clinic, also asked to be put on the waiting list.

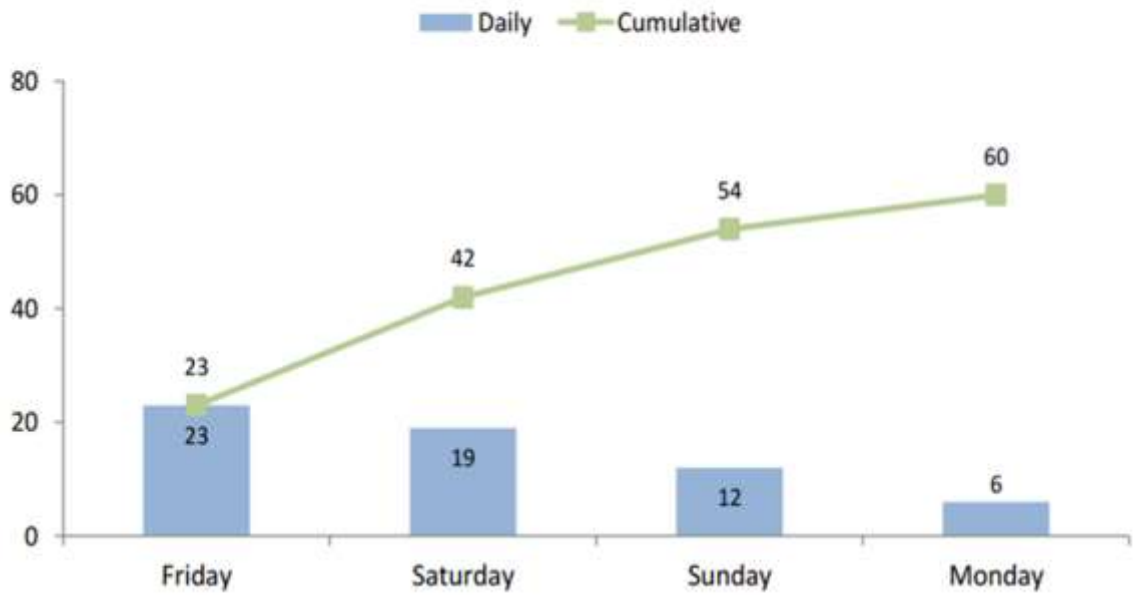

Figure 6.7: Lanterns sold, by day, before departure

Upon return in 2011, the second shipment was deployed and roughly 55 lanterns were distributed to the Mpala Ranch community members. Meanwhile, a number of the MRC community members expressed a strong interest in purchasing a second lantern. In the vast majority of cases, they explained, they had brought their lanterns back to their home villages over the holidays but realized that their families needed the lanterns more than they did. Rather than revert back to kerosene, they wanted to purchase a second lantern for their personal use at the MRC. A time-

lapse of the geographic distribution of the lanterns throughout the communities – comparing sales during the first five weeks of 2010 with sales in 2011[3] – is presented in Figure 6.8.

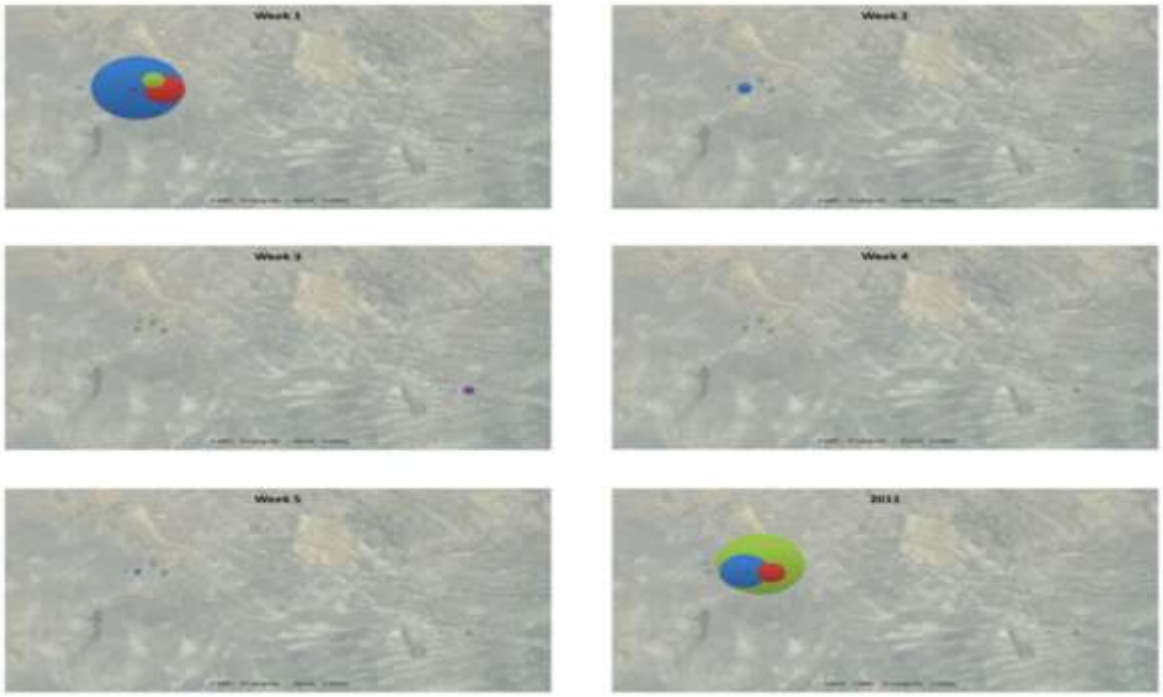

Figure 6.8: Geographic and temporal diffusion of the solar lanterns during the first 5 weeks of 2010 and 2011, between the MRC, Campsite, Ranch, and Other (primarily Nanyuki) residents.

When asked to list the motivating factors that drove their decision to purchase the lanterns, "need" was the most common response, followed by "education" and "health." Table 6.6 shows a collection of responses that were given, including order of priority, when asked "what were the most important factors that you considered in purchasing the lantern?" Some of these responses

[3] For logistical reasons, the lanterns were brought to the Ranch community members in 2011 based on pre-orders. This differed from the model in 2010, when members were allowed to purchase the lanterns at their own pace

are overlapping in intent (e.g. “safety” and “risks”; “need” is a somewhat all-encompassing term) but reflect the diversity of opinions and driving factors taken into consideration by the community. It should also be noted that the second lantern shipment was financed by the repayments made by the Mpala villagers for the original 100 lanterns.

While the villagers were given the direct contact and ordering information of the lantern supplier, only one or two of them would have been able to pay the high up-front costs required to make the international transaction. Creating this renewable financing fund made the project sustainable in the long-term because the funds derived from the sales and financing were being used to provide additional solar energy solutions for members of the Mpala community. This model, therefore, has the potential for larger-scale impact in rural villages across the world and demonstrates the critical role that microfinance and other lending institutions may play in facilitating technology adoption and diffusion.

Table 6.6: List of considerations taken into account for lantern purchase (53 Total Households; respondents were asked to list as many factors, in order of priority, as came to mind)

	Need	Education	Health	Price	Convenience	Desire	Lantern Make	Social	Economics	Helpfulness	Safety	Communal	Light Lifetime	Risks
Rank														
1	20	9	4	3	2	0	1	1	0	0	0	0	0	0
2	3	3	5	0	0	0	0	0	1	1	1	1	0	0
3	0	7	1	0	0	1	0	0	0	0	0	0	0	0
4	0	0	1	0	0	0	0	0	0	0	0	0	1	0
5	0	0	0	0	0	1	0	0	0	0	0	0	0	1

6.7 Impact Assessment

The respondents were asked to rate their opinion of the impact of the solar lanterns on their socio-economic status, health, and education on a 1 (low) to 5 (high) scale. Across all dimensions, the results were positive or at least neutral, which are explained in more detail as follows:

6.7.1 Socio-economic Status

Figure 6.9 shows the results of their responses, kerosene use was virtually eliminated, with an overall drop in monthly kerosene expenditures, for both cooking and lighting needs of over 70.5% (average monthly household savings: 190 kshs) by the end of the year. This value is increased to an impressive 83.9%, when considering kerosene for lighting alone. After factoring

in total lighting system costs, including those of the solar lanterns themselves, annual lighting-related expenditures were still estimated to drop by a combined 14.7%, with an average household savings of 646 kshs, during the first year of solar lantern use (Table 6.7)

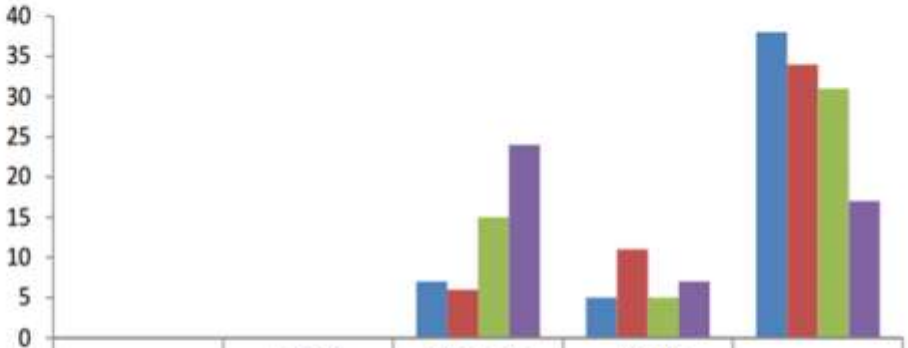

	Much Worse	A Little Worse	About the Same	A Little Better	Much Better
Health	0	0	7	5	38
Income	0	0	6	11	34
Education	0	0	15	5	31
Social Status	0	0	24	7	17

Figure 6.9: (Color online) Survey responses on the impact of the solar lanterns on Health, Income, Education, and Socio-Economic Status.

Table 6.7: Average cost savings for lighting needs (kshs)

(a) Average Annual Lighting Expenditures, including Energy Sources[4].

2010 Combined Total	2011 Combined Total	Total Combined Savings	Combined Savings/2010 Expenditures (%)	Avg. HH Savings	Range of HH Savings
232,841	198,620	34,221	14.7	646	[-6700, 7312]

(b) Average Monthly Kerosene Expenditures

	2010 Combined Total	2011 Combined Total	Total Combined Savings	Combined Savings/2010 Expenditure (%)	Avg. HH Savings	Range of HH Savings
Incl. Cooking Fuel	14285	4210	10075	70.5	190	[-600, 600]
Not incl. Cooking Fuel	14285	2300	11985	83.9	226	[-150, 600]

Furthermore, by factoring in the 2 hour return trip to Nanyuki, made twice a month, to purchase the kerosene itself, it is clear that the solar lanterns provide a number of substantial socio-economic benefits over the traditional kerosene-based lanterns. Although only 63% of households reported that they "felt that the price of the lanterns was reasonable", 34 households

[4] Note: the following assumptions were used in calculating energy costs: Lifetimes: 1 year – Electric Lights; 2 years – Solar Lantern; 5 years – Solar Panels, Deep-Cycle Batteries, Hurricane Lanterns. A TV was assumed to constitute half the total energy draw and a 6W Compact Fluorescent Light was assumed to constitute ~1/5 of a TV's energy draw, given that a 12" B&W TV draws about 20W

felt that the solar lanterns made their income levels much better and 17 felt that their social status greatly improved. 11 and 7 households felt that the lanterns led to moderate improvements in income and social status, respectively. Many also reported using the lanterns to socialize with friends at night.

6.7.2 Health

Respondents were very aware that the solar lanterns were far safer than the kerosene lanterns. In addition to the lack of smoke, respondents were also pleased that the lanterns did not get hot or break like the hurricane lanterns. A few respondents did complain that the lights were too bright for their eyes, which had grown accustomed to years of dim light from the kerosene lanterns. However, this was not a common complaint, and far more respondents indicated a desire for brighter lights than the reverse. Overall, 38 households reported that the use of the solar lanterns made their health much better, 5 households reported minor improvements, and 7 did not claim to see much of an effect.

Initial attempts to quantify indoor air pollution levels through air quality and dust particulate level monitoring were not successful. This is because the monitoring equipment was too invasive in the respondents' homes, given the cramped quarters. Meanwhile, health data on upper respiratory tract infections from the local Mpala Health Clinic was inconclusive because much of the data for the community was aggregated with other surrounding communities. It should also be noted that the houses in this community had vaulted roofs, which helped improve air circulation, particularly when compared to other types of low-income or traditional housing

designs. Nevertheless, anecdotal observations from the local health care workers did indicate that overall respiratory health had improved since the introduction of the lanterns.

6.7.3 Education

31 households (61%) felt that the use of the solar lantern improved the education and study habits of the household by enabling them or their children to study better at night. This meant more reliable (not dependent on kerosene procurement), better quality (luminance, light temperature, etc.), and/or safer (no smoke or burn risk) light as opposed to previous methods of reading after nightfall. 5 households (10%) felt the lanterns only had a moderate effect and 15 households (9%) said that the education status was "about the same".

It should be noted that since not all households included children. Hence, this question was not always applicable. In some of these cases, respondents extrapolated based on their experiences using the solar lantern either in their home villages or when their children were visiting the MRC. In other cases, the respondents admitted that it made no difference, since nobody in the household studied at night. Moreover, older high school or college aged children, who would presumably have more substantive homework assignments, did not live at the MRC as there were no schools at these levels in the immediate surroundings.

So referring to the 17 households that did have at least one child studying at night all noticed a definitively positive impact of the lanterns on their children's education: 13 of the households (76%) agreed that the lanterns made the children's education "a lot better" and 4 households (24%) felt that the lanterns "made it a little better." The responses of these 17 households also tended to be more satisfied with the light quality and strength than the general population. So

whereas only 76% of households who did not have children studying at night "loved" the "light quality", 88% of households with children reported that they "loved" the quality of light. When asked the same question about 'light brightness', 79% of those households without children studying at night "loved" the brightness, compared with 82% of those households with children studying at night. It is, therefore, suggested that seeing the tangible impact of the light on children's studying habits may lead to increased satisfaction with the product.

6.7.4 Knowledge and Understanding of Solar Technology

All but one household claimed that their experience with the solar lantern changed their interest in solar technology overall. Many expressed pride in owning the lantern and being able to know how it worked – and even show them off to other curious friends or family members. At least three households also expressed a desire to purchase larger solar home systems, as a result of this experience, so that they could charge larger devices. 38 of 41 responding "before-and-after" households would recommend the lantern to a relative or friend. The community demonstrated that they were able to pick up the technology quite quickly. When asked how easy or difficult it was to use the lanterns, 27 households said it was "okay," 6 households said it was "easy enough," and 18 households said it was "extremely easy" (2 households did not respond). Community members found themselves explaining or describing the lanterns to friends and family members in many different ways. Some highlighted the financial savings, while others appreciated the ease of use and reliance on natural resources rather than kerosene.

There were also differences in terms of function. Most households used the lantern as a portable room light, much as it had been intended. There were a few households, however, who preferred a more central and permanent fixture, and so dismantled their lanterns to connect the bulb to the ceiling directly. As for creative uses of the light, one gentleman even extolled the lantern's

virtues in scaring off cheetahs or leopards that may try to attack his cattle at night! It was, therefore, evident that people adapted the lanterns to a variety of needs and functions and that there was a low barrier to understanding the technology. As for non-lighting capabilities, these functions were not as widely adopted. Although the lanterns were able to be configured to charge a radio, only five households professed to having tried to do this. They observed that this setup drained the battery quickly and so none of them tried to do this on a regular basis. Even the cell phone charging function was rarely used, with only 13 of the households admitting to using this function on a regular basis.

However, this should not be interpreted as saying that the cell phone charging function was not appreciated. This community's unique circumstances and access to the Mpala Research Center meant that households were already accustomed to charging their phones using the research center's generators, without paying a fee. Coupled with the fact that this lantern was outfitted with a universal charger (Figure 3C) that was difficult to use and required users to remove the battery from the cell phone in order to charge, it is not surprising that the community members were reluctant to adopt this new charging technique.

Nevertheless, of 50 responding households, 36 households said that they loved having the cell phone charging feature available, 4 said they liked it, 8 said it was average, and only 1 household said that they hated the charger – while 1 household said they never tried the charger at all (and therefore couldn't comment on it). Within the solar lantern industry, there is a trend towards using a cable, equipped with a number of mobile phone adapters, which would allow individuals to charge their phones by plugging them into the lantern directly, not unlike a standard cell phone in a wall outlet. This is a positive trend and the inclusion of this design should be expected to increase cell phone charging usage.

6.8 Project Challenges and Recommendations

6.8.1 Product Reliability

While the lanterns were very popular in the community, a number of individuals faced various problems with their solar lanterns. Prior to the 2010 distribution, a number of community members expressed interest in purchasing the lanterns contingent upon the availability of spare parts. This demand had not been anticipated at the time and so parts were not initially available. To address the immediate concerns, 5 lanterns were set aside to be dismantled for their parts. An order for individual components – primarily bulbs, batteries, and solar panels – was then placed and shipped to the community.

As it turned out, lantern failure became a more serious problem than had been initially predicted. Despite prior use before the project had been carried out, test conditions back in the US could not replicate the extreme environmental conditions of the equatorial climate. Nor could they replicate continuous use for a year by an entire family. As a result, mundane problems, such as loose wires, burned out bulbs, or dead batteries, threatened to severely limit the lifetime and, hence, the value of the lanterns. While some of these components, such as batteries or wires, were available in Nanyuki for trivial costs, other components, such as the proprietary LED light bulbs or solar panels, had customized specifications and were, therefore, only available from the supplier.

The LED light bulbs proved to be the biggest source of complaint, as a number of people had 2-4 of their 28 LEDs die during the course of the year (Figure 6.10). Although this did not substantially diminish the overall quality of light, it became an eyesore and source of frustration

for a household who had spent almost a half month's wages on this product. However, bulb replacement required one to dismantle the lantern, disconnect the original bulb, and re-solder the new bulb. Though well within the skill range of the electricians and mechanics in the community, this had simply never been attempted, because people were reluctant to tamper and play around with such an expensive and valuable possession.

Figure 6.10: A security guard at the MRC displays his lantern's burned out light-bulbs

Formal training with a spare lantern was, therefore, provided to 3 of the community members. They were taught how to diagnose, dismantle and reassemble the lanterns (Figure 6.11). Further work was then done to incorporate locally-available components as much as possible.

Figure 6.11: (Color online) (a) Local community members are trained to diagnose and repair the lanterns. A large number of lanterns required only simple maintenance such as (b) the re-soldering of wires.

This eventually led to the creation of a converted hurricane lantern, where all but the solar panel itself was assembled through parts available in Nanyuki (Figure 6.12).

Figure 6.12: (Color online) Locally-purchased components, including a (a) hurricane kerosene lantern, (b) motorcycle battery, (c) compact fluorescent light-bulb, and (d) metal switch were collected and assembled. (e) The light-bulb, for example, was put into the place of the wick. (f) These modifications resulted in a converted solar-powered hurricane lantern.

This experience empowered the community, while giving them a sense of ownership over the lanterns themselves. The process of repairing, or even creating, solar lanterns also provides opportunities for income generation and points to the significant potential of developing locally-based solar technology production and manufacturing capabilities.

Nevertheless, the problems faced with the reliability of the lanterns could have proven insurmountable had the proper training not been provided. This case study, therefore, serves as a warning to solar lantern producers to take issues of device reliability very seriously. By extension, this case study demonstrates the importance of proper product testing, such as the micro-scale tests on LED and solar cell materials. While manufacturers cannot be held responsible for the heat, dust, and even abuse of their products (e.g. children throwing the lantern around), there are steps that can be taken to mitigate these risks. For example, the epoxy that was used to connect the wire box to the solar panel melted in a few instances because the panels were placed on hot tin rooftops to charge. This is a reasonable and common practice and should be accounted for in epoxy selection. Furthermore, it should be assumed that people will often ignore (or not be able to follow) warnings to place their lanterns under shaded areas at all times and, therefore, batteries that are fairly common and easily replaceable should be used.

Figure 6.13: (Color online) Examples of brightly colored plastic solar lanterns on the market [286]

Another trend observed in many solar lanterns is their plastic packaging in bright colors (Figure 6.13). While this is often done in an effort to increase the durability of the product, this packaging also introduces a number of problems: First, it makes the product look like a toy and becomes all the more susceptible to children abusing the products. Second, the plastic product is often manufactured elsewhere, thus eliminating the prospect of a locally-created or produced product. Third, bright colors may not always be well-integrated with the local décor or design sensibilities. While many BOP customers have grown accustomed to similarly-packaged products, such as jerry cans for water, it is not entirely convincing that this is truly the best approach to the introduction of solar-powered lanterns. Similarly, while the Roy Solar lantern had an easily identifiable battery case, mysterious casing, as seen in other products may dissuade owners from trying to fix their lanterns by themselves.

6.8.2 Product Pricing

One key challenge inherent in the distribution and sale of a product targeted for BOP consumers is setting a reasonable price point that is both affordable to the customer, yet financially viable for the supplier. In the case of the solar lanterns, the customer is making a decision based on a combination of financial and non-financial considerations: cash and time savings against status quo fuel source procurement, health benefits, light quality and reliability, technological adaptation, and personal prestige. When the traditional fuel source is a natural resource, such as wood for a fire, for example, the availability and vulnerability of these resources imply that time may become a strong driver for seeking alternative fuel sources. However, only one of these factors, cash savings against status quo fuel source procurement, can be directly measured and compared on a dollar-for-dollar (or shilling-for-shilling) basis.

The customer must, therefore, take into consideration his or her current fuel expenditures and adjust for future price volatility. Given that kerosene is a petroleum derivative; its price is strongly tied to global crude oil prices [287]. These prices are notoriously unstable and fluctuating. Additional costs associated with distribution from the trading ports to the last mile only increase customers' vulnerability to price variations outside their control. On the supplier side, a number of considerations must be taken into account. BOP customers often have meticulous budgets that absorb very little risk and must be carefully managed to the last detail because of uneven and unreliable pay periods [276]. It is, therefore, very difficult to sell a product at a price that is considerably higher than what a family may have budgeted for in their weekly or monthly lighting/energy allowance. Unless the seller is willing to wait indefinitely for customers to amass meaningful savings, financing options that allow customers to pay for the

product over an extended period of time are virtually a requirement for big ticket items to sell within any reasonable time frame.

In this case, installment payments may need to be adjusted to take into account factors such as a sliding exchange rate. Figure 6.14 shows the steady devaluation of the solar lantern over the year-long pay-back period; the initial purchase price of $51.50 was converted to 3900 kshs at a rate of 75.77 kshs: 1 USD on January 1, 2010 (Table 6.1). However, the reasonably stable shilling dropped considerably over the course of the year, leading to a loss of $3/lantern by year's end. While the initial goal was simply to break even, it can be seen that this contractually-set price determined in local Kenyan Shillings gradually put the project at a net loss. Pricing based on a higher profit margin or implementing a tiered payment plan (that would have incentivized up-front payments by offering a discount or, conversely, charging higher interest rates for an increased pay-back period) would have been more financially viable pricing strategies.

Figure 6.14: (Color online) Devaluation of the solar lantern, which was sold for 3900 kshs/unit based on a 76:1 exchange rate in January 2010. The lantern originally cost $52/unit. In 2010, the lantern value ranged from $47.92 to $51.47, with an average value of $49.18

6.8.3 Data Collection:

This project differs from many other studies that poll existing users or use focus group feedback, shorter trial periods of just a few months or simply ask people to play around with some lanterns and give their impressions. Instead, this study provides a broad overview of an entire village before and after an entire year of use. This project, thus, attempts to create a commercially-realistic product adoption scenario and obtain information on real, long-term, usage patterns.

However, there were a few challenges with the data collection process that could have been changed to strengthen the study. First, the solar lanterns were far more popular in the sample village than expected, with a 96% adoption rate. As a result, there was not a significant control group to compare the results against, and it was difficult to determine what network effects

existed and influenced the decision-making process. Second, by playing the role of both lantern surveyor and distributor, it was difficult to determine how candid the respondents truly were; care was taken to distance the two aspects as much as possible – for example, the translators took over the majority of the data collection in the second survey – but the two roles were still intertwined. There is, therefore, a real concern that social desirability bias, whereby respondents may answer questions to please the interviewers, may be present. That being said, the candid feedback with respect to specific problems and concerns that individuals had about various aspects of the lanterns does reveal a strong degree of comfort in providing honest responses.

Finally, key data, such as kerosene and other lighting expenditures, was collected rather informally; instead of simply asking respondents to estimate their monthly expenditures, it may have been better to track expenditures through validated weekly or monthly logs. This could have provided more accurate information but would also have been significantly more difficult for both surveyors and respondents to maintain and regulate.

6.8.4 Creating a Long Term Model

One of the primary goals of this study is to use the implications to scale-up and build a long term model. The ideal vision is to have the diffusion of the lanterns grow organically from village to village, with the community members taking it upon themselves to create an autonomous supply chain (whether directly, through the "creation" of local entrepreneurs or indirectly, through applied pressure on existing merchants). This presents an interesting challenge whereby the project's success would only be achieved, once the project component itself was removed from the equation.

One of the most common questions, however, has been how relevant the results of this study are, considering the unique circumstances surrounding the village and its relationship to outside research institutions. The relative certainty of a steady wage, employee benefits, and access to computing infrastructure, for example, did in fact set this village apart from the majority of other rural villages.

However, the reality is that the geographic isolation and lack of crucial infrastructure, such as electricity and running water, coupled with what is still a low wage in absolute terms, means that this community also shares many of the same challenges that universally plague off-grid communities, particularly in rural areas, all over the developing world. The fact that the lanterns were still observed to have a measurable impact on indicators, such as income, implies that many of the results of this study are still relevant for use in building an evidence-based strategy for scale-up. In order to supplement the findings from this case study, there is also a desire to replicate this study in other countries, regions, and settings. Such replication would provide additional data points to further validate the findings from Mpala, and the similarities and differences in conclusions may illustrate the effect that such community variations have on the technology's impact – information that is clearly valuable, for entrepreneurs and policymakers alike.

In terms of directly scaling up in Mpala, trying to remotely establish a distribution channel led to logistical complications. Ultimately, a return trip in August 2011 was made with the goal of finding locally-based suppliers who could help establish a direct distribution model. Eventually, the local supplier, Sollatek (Sollatek, Mombasa, Kenya) for the D.Light lantern (D.Light Design, San Francisco, CA), was identified as being the optimal partner with whom to enter into the next phase of the project. The D.Light lantern has won numerous industry accolades but the majority

of community members were hesitant to work with a new and unknown supplier. Without a straightforward method of shouldering the up-front cost for these new lanterns, this hesitance, in turn, prevented the rest of the community from using their collective purchasing power to bargain the price down. People were, therefore, unable to pay for new lanterns and have yet to arrange for a third shipment of lanterns.

6.9 Assessment of Project Hypotheses and Goals

6.9.1 Validation of Project Hypotheses

In order to determine the success of this study, it is useful to revisit the initial project hypotheses and goals that were set out at the beginning:

As discussed under the section on impact assessment, the lanterns were indeed seen to have positive or non-negative impacts on the community's social status (and social life), study habits, and respiratory health. The majority of this impact was determined through the community members' responses to direct questions about each indicator.

Similarly, the lanterns were indeed seen to have a significant impact on households' savings and expenses. The lanterns led to an overall 70.5% drop in average kerosene expenditures alone, and a 14.7% drop in overall annual lighting-related expenditures. This is in addition to the time savings from not having to travel to buy kerosene. The lanterns are therefore able to pay for themselves in less than a year, assuming that they are able to be properly cared for and maintained in the stressful environment.

All but one household opted for a monthly financing option. This fact demonstrates the popularity of the financing option. This point was further emphasized when respondents were asked why they chose this financing option. All but one household directly attributed this financing option to enabling their ability to pay. As one respondent explained, monthly budgets are very exact and often prepared well in advance. It is, thus, difficult to factor in such a large and unanticipated expense into their calculations. Given that the monthly payments were at par with typical kerosene expenditures, there was, therefore, a worry-free transition to this new lighting source. This evidence supports the findings presented by Collins et al. [276].

As the community's responses to questions on interest in and understanding of solar technology demonstrate, the community did not have much trouble in understanding the utility and purpose of the solar lanterns, despite never seeing this particular technology before 2010. The difficulty that ensued, however, in continuing and scaling up the distribution channel after the completion of the formal research project demonstrates how crucial easy access to physical and financial channels to the lanterns is in their ability to diffuse through a community.

6.9.2 Achievement of Project Goals

The four originally-set project goals were met with mixed results:

Figures 6.7 and 6.8 show the temporal and geographic diffusion of the lanterns at the MRC, nearby campsite and Ranch communities. It was seen that in the first week, the highest number of sales occurred in the first four days, with the number of lanterns sold decreasing each day. Similarly, the first week had a higher number of sales than any of the subsequent weeks before the lantern stocks were depleted. Meanwhile, it was shown that interest in the lanterns did diffuse

to other regions based on word-of-mouth and peer recommendations. However, the lanterns were distributed in a controlled manner with pre-orders being considered before purchase and quotas set for each community. Moreover, since the lanterns were not available for sale until after the completion of the survey study, there was ample time to generate interest. These measures were undertaken, both because of exceeding demand and logistical considerations. However, this fact also makes it more difficult to establish the patterns of organic and uncontrolled product diffusion.

Through the survey responses, this study was able to comprehensively identify different motives and rationales for purchasing the lanterns. Some of these drivers for technological adoption could be inferred, while other drivers could be ascertained through direct questions and answers, such as those presented in Table 6.6. Above all else, it was established that the community felt a distinct need for the product, whether for its social, economic, health, education, or other benefits.

Besides the obvious and oft-repeated barriers of financial and physical access, there were other barriers on the micro- and macro-levels that were successfully identified through this research project. Product reliability and the risk of market spoilage, for example, were placed in much higher prominence than may have been previously realized. Increasing efforts made by solar lantern companies to establish stronger on-the-ground distribution and maintenance centers or offer warranties, as well as industry initiatives by organizations such as Lighting Africa to create a quality control and rating system [281], may help overcome this challenge.

For foreign companies that want to enter a particular market, conditions that create an enabling environment are also vital. For example, a sliding exchange rate was demonstrated to be an

important element in product pricing. Similarly, the products' perceived value can be strongly influenced by the local price and availability of kerosene, and the stability or volatility of that fuel source could play a significant role in the products' diffusion. While significant challenges persist, the relative maturity of the overall solar industry in Kenya should not be underappreciated. The government has recently implemented measures that make it easier to import solar equipment and operate businesses in the country than in many other energy poor countries, and growing government backing will help companies operate with increasing agility and efficacy.

As the section on creating a long term model explains, the unresolved goal of scaling up lantern distribution at Mpala was the least successful of all project components. Nonetheless, there were many ideas that emerged and conclusions that could be drawn from the study in order to build a successful business model in the future. For example, it was demonstrated that a focus on financing and product reliability is key to implementing a successful distribution campaign. This is because community members are willing to invest in a new technology as long as it can demonstrate economic savings in a reasonable amount of time, and does not impart financial stress on the customer. Even if the products are built to last, the availability of spare parts and/or trained repairmen is also crucial to ensuring a sustainable industry. This fact was demonstrated by the time and effort that was required to train workers in the January 2011 visit, as well as the numerous requests for spare parts from the community members who were all too familiar of the consequences of a lack thereof, before agreeing to purchase the lanterns.

Marketing and consumer awareness are important, but because the intrinsic value of the products can often be communicated very quickly, a greater emphasis must be placed on physical access. This last-mile distribution can be achieved through proprietary or piggy-backed channels.

Discussions with community members and other industry participants suggest that actors such as medical workers, schools, or religious communities should also be engaged with, as potentially promising partners for distribution. This is due to factors such as community influence, strength of networks, and physical mobility. Targeting locally-organized women's groups may also be an effective way to position the technology, as women tend to shoulder a disproportionate share of the fuel burden through activities such as the procurement of firewood, supervision of studying children, and cooking in the home.

As an alternative to providing direct financing access, it may also be useful to explore community-level solutions such as centralized charging stations or collective rental agreements. Variations of these models have been implemented by organizations such as UNIDO (UNIDO, Vienna, Austria), SELCO (SELCO, Bangalore, India), and EGG-Energy (EGG-Energy, Dar es Salaam, Tanzania). There is a significant advantage in that each individual's or household's financial burden is reduced. There are trade-offs, however, because no individual or household ends up directly owning the product, and there is a strong reliance on communal ties. Depending on the specific community, this last point could be seen as a positive or negative attribute. Finally, while an import-driven model run by a large company can use economies of scale to cast a large distribution net, this model also creates reliance by customers on external actors. It is therefore worth exploring the feasibility of home-made or locally-produced and distributed lanterns. This idea will be discussed more in depth under policy recommendations.

6.9.3 Policy Recommendations

The outcomes of this study lead to several personal recommendations for policymakers. While these recommendations are geared specifically towards the solar lighting industry, many are relevant to other technologies – solar or otherwise – as well.

Government need to prioritize energy access as an agenda item: The first step towards providing energy access to the 1.3 billion people around the world who still cannot meet their fundamental energy needs with modern fuel sources is to ensure that the concept of energy access becomes – and remains – a key priority area for governments. This is a personal issue for those countries whose electrification rates are below average. But this can be significantly aided by electrified countries as well, who can make meaningful contributions through a transfer of technology and knowledge, commitment of financial assistance, and reinforcement of political resolve as part of their broader efforts to provide development assistance.

Global conferences, such as the June 2012 Conference on Sustainable Development ("Rio+20") are, therefore, important because they convene the world's leaders to discuss pressing issues such as energy access. The fact that this topic may become a focal point should help galvanize the international community to prioritize energy access in their programming. Just as the Millennium Development Goals (MDGs) helped issues such as clean water and maternal health care receive prominence in global agendas, inclusion of energy access in the post-2015 context or still-under-discussion Sustainable Development Goals (SDGs) would also help provide mandates for monetary and time expenditures towards the issue. Government buy-in and

prioritization is therefore the first crucial step towards achieving successful energy access initiatives.

The public and private sector should form strategic partnerships to address this urgent concern: While government assistance is crucial, efforts towards electrification should not focus exclusively on top-down or donor-driven models. Rather, a private sector and entrepreneurial approach should be taken to achieve scale, efficiency, and sustainability in the diffusion of energy technology, particularly solar lanterns. This is because, as has been shown before, value can and will be associated with this technology, which can be shown to be cost effective against conventional fuel sources. There is therefore a need for a coordinated effort between the public and private sectors in order to operate effectively. This will require an evidence-based approach to ensure that the best policies and technologies are supported and enabled. Case studies such as this will therefore help strengthen the case for promoting and investing in solar lantern technology in particular.

The government can help do this by creating a favorable environment that will attract private sector investments and business operations. According to the Doing Business index, Kenya ranked 106th out of 183 economies in terms of ease of doing business in 2011, when this study took place, with rankings of 128th and 111th in terms of starting a business and getting access to electricity, respectively [288]. This shows that there is a lot of room for improvement in countries such as Kenya, where it takes on average 11 procedures and 33 days to register a new business. Making the process simpler and more transparent will do a lot towards ensuring that companies feel welcome in starting a business there. Political stability, combined with consistent and predictable policies, is also essential in order to mitigate risk and secure long-term investments by companies seeking to enter into new markets.

In addition to implementing systemic reforms, governments should implement regulatory measures that promote the solar lantern industry. This could perhaps come in the form of subsidies, as have been popular in many countries around the world, although the common feed-in tariff for SHSs [289] would not be directly applicable to an off-grid community. Or, for example, import taxes for solar lanterns could be reduced or eliminated so that the technologies are even more price competitive with conventional fuel sources. Care should be taken, however, not to over-subsidize these products to the point of creating a dependency on this financial assistance for the industry. Finally, governments should be willing to consider measures that reflect a more broad-based embrace of renewable technologies and other energy alternatives to the national grid. This could include reducing financial assistance (e.g. tax benefits, subsidies, etc.) that excessively-favor non-renewable utilities, promoting and educating the general public on the benefits of renewable energy, and setting targets for renewable energy production or consumption in their energy portfolios.

Access to a broader range of financial instruments should be provided for energy service: Due to the key role that financing plays in accessing new technology, such as solar lanterns, it is important that innovative financial tools are properly utilized to make the technology affordable at prices that still allow for solar lantern companies to operate without a reliance on donations or subsidies. This will likely require considerable involvement from micro-finance institutions and other community-based lending programs. The creation and strengthening of such institutions should, therefore, be supported by the government and its policies, as they will provide the necessary link between supplier and consumer. Since micro-finance institutions rely so much on

credibility, governments should be careful that the industry is properly monitored to ensure that these lending agencies are trustworthy and reliable.

Many micro-finance institutions were initially created to directly fund income-generating activities and ,therefore, may be more inclined to finance, say, a group of women hoping to sew textiles for profit rather than fund the purchase of technology or personal electronics. However, micro-finance institutions should realize the role that solar lanterns and other energy technologies play in wealth creation. For example, solar lanterns can directly increase the number of productive hours, power communications electronics (mobile phones, radios, etc.), and enhance people's literacy in modern technology. These considerations should, therefore, be taken into account as micro-finance institutions evaluate peoples' lending requests and portfolios.

Solar lantern companies wishing to expand their financing offerings should explore existing solutions and partnering with micro-finance organizations. It is far easier for financing organizations to add a technology to their product offerings than for a technology company to try to directly enter into the financing field. Micro-finance organizations that already specialize in the financing of technologies for rural and off-grid areas such, as water filters or high-yield grain [290] are particularly appealing because they have already proven their track record, earned their trust, and helped establish a credit history and chain of accountability with the community members. A strategic partnership would allow each organization to specialize and exploit their competitive advantage. The value of each organization's role should, therefore, be effectively communicated, in order to create a strong partnership.

Regulations should be put into place to ensure product quality and prevent market spoilage: It has been shown that maintaining high standards for product quality is essential in building a strong and sustainable industry. Given that consumers will be asked to spend the equivalent of multiple days' worth of wages to purchase these technologies, they will have certain expectations for the products' performance. Granted, sometimes a lack of proper consumer awareness can create unreasonably high expectations that simply cannot be met [291], [292]. However, there are certainly minimum thresholds for product lifetimes that should be met in order to create a strong reputation. The most obvious benchmark is the duration that is equivalent to the breakeven point that would make the lanterns cost effective compared to conventional fuel costs. This could take days, weeks, or months. Yet another factor is the remoteness of the community and the effort required to maintain or replace a broken or worn-down device.

Governments should, therefore, regulate the industry through consumer protection measures such as quality assurance or reliability programs. Such measures would include the strenuous testing of products for mechanical and electrical failure. Lighting Africa has already created its own quality assurance testing and rating program but successful implementation of this mechanism will require the full support of local governments in adopting and adhering to these certifications. For example, governments could agree to ban products that do not meet these standards or reduce import tariffs for those products that have been approved to make them more cost competitive. Failure to take action can easily up-end the industry, if unreliable or imitation products start flooding the market, as solar home systems nearly did in Kenya [278].

Product reliability is not just a matter of trustworthy versus fraudulent companies, however. Given the rugged conditions that these products are operating in, it is almost impossible to ensure that a product will be able to survive months and years without problems. Hence, even the best-

constructed products will have individual components with varying lifetimes. For example, a solar panel may last 25 years, but a battery only 2 years. Solar lantern companies should, therefore, be encouraged to offer warranty programs and/ or, depending on the circumstances, consider the training and hiring of licensed local repairmen/ women in the field. Such measures would reassure consumers in mitigating risk, enhance feedback mechanisms between suppliers and consumers, and even result in job creation. Solar lantern companies could also greatly improve the versatility and lifetimes of their products if they design lanterns with easily-replaceable spare parts, rather than sticking to proprietary or special-order components.

Governments should work towards promoting local production capacity in the long term: As discussed earlier, there is a strong potential for locally-produced lanterns. Governments should, therefore, encourage and support the local production and innovation of this technology. Kenyan-made prototypes for solar lanterns have already emerged from this study. These are based on converted hurricane lanterns. For these lanterns, the only component that was specially-ordered was the solar panel itself. While the quality of each lantern may not be as high as factory-produced plastic designs, the theory is that the local artisans and workers who assemble these lanterns from locally-available parts will also be better positioned to repair the lanterns if or when they do break.

Overall, this may be a less efficient approach without the aid of local large-scale manufacturing capacity. Entrepreneurship also, cannot happen overnight, or without the support of the required policies. Renny Mutai [293], for example, cites government support, limited business skills, and

a shortage of technology experts as some of the factors constraining micro and small enterprises (MSEs) from boosting technological capabilities in Kenya.

Yet, there is a real opportunity for grassroots innovation that could "trickle up" from emerging to developed markets, much as have many mobile phone-based technologies; studies of mobile platform technologies have shown numerous examples where users in emerging markets are not only leap-frogging landline technologies, but are also innovating new banking or health-based services in order to satisfy unmet needs [294]–[298].

The constrained circumstances of off-grid communities could certainly push innovation and the functional boundaries of technology. Our survey already showed that these communities routinely use car batteries to power many things besides cars. It is, therefore, entirely conceivable that an "app"-based design approach, incorporating open-source or modular add-ons to, say, scale lighting or battery capacity, or connect new types of devices, could result. The telecom industry itself could continue to evolve, given that solar lanterns could open new markets for mobile phones in even more remote areas, through their provision of mobile charging capabilities.

Prospective local entrepreneurs should, therefore, have access to the financial and training tools that they may need to find energy-related business opportunities at any stage of the supply chain, rather than wait on promises for transmission grids that may never come. This bottom-up approach would, therefore, result in job creation and knowledge transfer that would ensure stronger long-term investment and sustainability by the communities themselves. Such approaches would secure a vested interest from local stakeholders who may open up new market opportunities that were not previously considered by or accessible to foreign companies.

Governments should be very mindful of this balance. Given the sheer number of people living in energy poverty and suffering its real effects, governments should continue to create an enabling environment in order to open up their markets and allow foreign companies who have the strength of scale and efficiency to enter and distribute the technology and its concept to as many people as possible. These businesses should also be able to operate without fear of their intellectual property being misappropriated, or for a resurgence of local imitation products. The governments should also simultaneously support and invest in local research and development that would help create local production facilities, train local entrepreneurs, and ensure that these locally-produced models are of good quality and financially competitive in their own markets.

6.10 Concluding Remarks

Solar energy has the potential to play a remarkable role in providing energy access to the 1.3 billion people around the world who still lack access to modern fuel sources for their energy needs. Solar lanterns, in particular, present a viable opportunity to provide cost-effective and self-sufficient lighting at the reach of BOP consumers who live on less than $2/day. In this study, a year-long survey assessment was conducted on a rural off-grid community in Central Kenya to determine the different factors that affected the adoption of solar lanterns in the community and assess their impact on people's socio-economic, health, and education levels.

The lanterns were shown to have a 96% adoption rate in the sample community, and resulted in a 14.7% drop in annual lighting-related expenditures. Kerosene usage was virtually eliminated and community members reported a positive impact on their health levels and education habits as well. It was also shown that the availability of a financing option was crucial

to making these lanterns affordable to the community members, with monthly installments on par with average kerosene expenditures being chosen over an up-front payment scheme in all but two cases. The lanterns were not perfect products, however, and many underwent wear and tear throughout the course of the year. Proper training was provided to community members in order to maintain and extend the lifetime of the lanterns, thus increasing their effective value.

The results of this study can be used to formulate evidence-based policy and business strategies that promote solar lanterns and other related technologies as viable tools for energy access and economic development. Policymakers should recognize the need for such solutions and their potential impact on communities with a sense of urgency. They should therefore work with the private sector in order to create favorable environments to attract investments and entrepreneurship. These companies, in turn, should develop innovative financing mechanisms that work well with consumers' financial portfolios, while also finding creative approaches to their distribution chains to reach markets in both urban and remote areas. Finally, it is crucial that these ventures work to ensure that they deliver high quality products that retain consumer confidence in this and other increasingly sophisticated technologies.

CHAPTER SEVEN

CONCLUSIONS AND FUTURE WORK

7.1 CONCLUSION

The following subcategories contain the concluding remarks on each of the chapters in this dissertation.

7.1.1 Failure Mechanisms of Flexible Organic Solar Cell Structures under Bending

This Chapter examines the effects of cyclic bending on the deformation and failure of layers that are relevant to flexible organic solar cells (with Polyethylene Terephthalate (PET) substrates and Poly-3-hexylthiophene: [6,6]-phenyl-C61-butyric acid methyl ester (P3HT:PCBM) active layers). The deformation and cracking mechanisms are elucidated along with the stresses and crack driving forces associated with the bending of flexible organic solar cells. The changes in the optical properties (transmittance) of the individual layers and multilayers are then explored for layers/multilayers deformed to flexural strains and stresses that are computed using finite element models. The implications of the results are then discussed for the design of flexible organic solar cells.

7.1.2 Effects of pre-buckling on the bending of organic electronic structures

This Chapter explores the extent to which pre-buckling of layers (in thin film multilayered structures) can be used to increase the flexibility of organic electronic devices. The deformation of wavy/buckle profiles, with a range of nano- and micro-scale wavelengths, is modeled using finite element simulations. The predictions from the models are then validated using experiments that involve the bending of layered structures that are relevant to flexible organic electronics.

The introduction of pre-buckled profiles is shown to increase the range of deformation that is applied to model structures, prior to onset of significant stresses and strains. The implications of the work are discussed for the design of robust flexible organic solar cells.

7.1.3 Cold Welding of Organic Light Emitting Diode: Interfacial and Contact Models

This section presents the results of on analytical and computational study of the contacts and interfacial fracture associated with the cold welding of Organic Light Emitting diodes (OLEDs). The effects of impurities (within the possible interfaces) are explored for contacts and interfacial fracture between layers that are relevant to model OLEDs. The models are used to study the effects of adhesion, pressure, thin film layer thickness and dust particle modulus (between the contacting surfaces) on contact profiles around impurities between cold-welded thin films. The lift-off stage of thin films (during cold welding) is then modeled as an interfacial fracture process. A combination of adhesion and interfacial fracture theories is used to provide new insights for the design of improved contact and interfacial separation during cold welding. The implications of the results are discussed for the design and fabrication of cold welded OLED structures.

7.1.4 Study of Solar Powered LED: Implications for Policy

The problem of access to electricity is still a major challenge to about 2 billion people that still live in rural and urban off-grid areas on incomes of $1-2/day. Since the cost of linking these people to the grid is high, there is a need to explore the development of alternative energy solutions for the provision of electricity in such contexts. There is also a need to develop new insights for the formulation of evidence-based policy that could enable the development of strategies to provide electricity to people that live in off-grid areas. This chapter presents the results of a survey that provides insights for the formulation of evidence-based policy for the

adoption of solar lanterns into rural/urban off-grid areas. The two year questionnaire study was carried out in Mpala Village in the Laikipia district of Kenya. The study identifies the factors that resulted in the adoption rate of 96% and a decrease of 14.7% in annual family expenditures. The social and health impacts are also elucidated before discussing the implications of the results for the formulation of evidence-based solar energy policy in developing countries.

"Without policy incentives to overcome socioeconomic inertia these could take more than 50 years to penetrate to their market potential. [286] These results underscore the pitfalls of 'wait-and-see'. This past century, accelerated technology development from wartime and postwar research produced commercial aviation, radar, computer chips, lasers and the Internet, among other things. Researching, developing and commercializing carbon-free primary power technologies capable of 10–30TW by the mid-twenty-first century could require efforts, perhaps international, pursued with the urgency of the Manhattan Project or the Apollo Space Programme. The roles of governments and market entrepreneurs in the eventual deployment of such technologies need to be considered more comprehensively than we can do here. But the potentially adverse effect of humanity on the Earth's climate could well stimulate new industries in the twenty-first century, as did the Second World War and the 'cold war' in this century."[2]

7.2 FUTURE WORKS

7.2.1 Failure Mechanisms of Flexible Organic Solar Cell Structures under Bending

This chapter focused primarily on the mechanical characterization of bendable organic photovoltaic cells with little investigation in the optoelectronic aspect. Further work could be done on the flexible manufactured OPV to analyze the systems efficiency effect on bending. This

could be a novel work for adaptation in the electronic industry in the quest to go in the direction of foldable electronics and electronic textiles including an architect's design of drape-able solar panel structures.

7.2.2 Effects of Pre-buckling on the Bending of Organic Electronic Structures

Since this section looks in details as to the effect of pre-buckled structures on the bending of organic electronic structures, it would be worthwhile to apply such finding in the flexible electron industry to serve as a guideline on the production of foldable and wearable electronics.

7.2.3 Cold Welding of Organic Light Emitting Diode: Interfacial and Contact Models

Further analyses where done on previous work from literature to address the effects of dust particles on organic light emitting diodes fabrication. A holistic comparison with literature on the pull-off technique in cold welding would be very essential for the experimentalist who would want to harness all the excellent privileges of a clean room system. The study shows that the surface contacts improve with increased pressure, reduced film thickness and reduced interfacial nanoparticle stiffness. However, improved contacts result in higher lift-off forces for interfacial separation during the pattern transfer stage of cold welding. Increased pressure may also lead to sink-in of dust particles, which may lead to device damage. An intermediate pressure range is, therefore, needed for the effective cold welding of Au-Au and Au-Ag layers. Also, the analytical model shows that the void length is dependent on the effective modulus and height of the dust particle.

7.2.4 Study of Solar Powered LED: Implications for Policy

A replication of this study to other deprived comminutes would be a very admirable future work to undertake. 'The United Nations Framework Convention on Climate Change calls for

‘‘stabilization of greenhouse-gas concentrations in the atmosphere at a level that would prevent dangerous anthropogenic interference with the climate system . . .’’. A standard base- line scenario that assumes no policy intervention to limit greenhouse-gas emissions has 10 TW of carbon-emission-free power being produced by the year 2050, equivalent to the power provided by all today’s energy sources combined.’[2], [299]–[303]

To achieve this by 2050, then similar studies and implementation policies need to be made throughout the world whereby communities would be required to use carbon emission free power.

APPENDIX A: ANALYTICAL CALCULATION OF CONTACT LENGTH AS A FUNCTION OF APPLIED PRESSURE FOR COLD WELDING

The surface energy between the film and the substrate is the product of pressure (P), surface contact area $(L_c \times a)$ and effective height of the particle (h_{eff}).[22] This is written as:

$$U_e = -P \times (L_c \times a) \times h = -PahL_c \qquad \text{A1}$$

Since $L_c = L - s$, the total energy in Equation 1 can now be written as:

$$U_s = \frac{6E_{eff} Ih^2}{s^3} - Pah(L - s) \qquad \text{A2}$$

Differentiating Equation (A2) with respect to s gives:

$$\frac{dU_s}{ds} = -\frac{18E_{eff} Ih^2}{s^4} + Pah \qquad \text{A3}$$

The length of the void can be calculated from Equation (A3) at the equilibrium, $dU_s/ds = 0$. This is given by

$$s^4 = \frac{18E_{eff} Ih^2}{Pah} = \frac{18E_{eff} Ih}{Pa}. \qquad \text{A4}$$

Defining the second moment of area as $I = at^3/12$, equation (A4) can be written as:

$$s = \left(\frac{3E_{eff} t_f^3 h}{2P}\right)^{\frac{1}{4}} = L - L_c \cdot \qquad \text{A5}$$

Hence,

$$\frac{L_c}{L} = 1 - \left(\frac{3E_{eff} t_f^3 h}{2PL^4}\right)^{\frac{1}{4}} \qquad \text{A6}$$

Introducing the effective modulus and changing h to h_{eff} gives:

$$\frac{L_c}{L} = 1 - \left(\frac{3\left(\frac{E_d E_f}{E_f\left(1-(\upsilon_d)^2\right) + E_d\left(1-(\upsilon_f)^2\right)} \right) t^3 h_{eff}}{2PL^4} \right)^{\frac{1}{4}} \quad . \qquad \text{A7}$$

REFERENCE

[1] A. Shakouri, “Overview of Renewable Energy Sources,” 2009.

[2] M. I. Hoffert *et al.*, “Energy implications of future stabilization of atmospheric CO2 content,” *Lett. to Nat.*, vol. 394, no. October, pp. 287–291, 1998.

[3] D. Meissner and J. Perlin, “‘Regional Workshop on Materials Science for Solar Energy Conversion,’” 2013.

[4] O. E. Akogwu, “Deformation and failure mechanisms in flexible and organic electronic structures,” *Proquest*, vol. 20111003, 2010.

[5] W. D. J. Callister and D. G. Rethwisch, *Materials Science and Engineering: An Introduction*, 7th ed. New York, NY: John Wiley & Sons, Inc., 1940.

[6] X. Zhao, B. Mi, Z. Gao, and W. Huang, “Recent progress in the numerical modeling for organic thin film solar cells,” *Sci. China Physics, Mech. Astron.*, vol. 54, no. 3, pp. 375–387, Mar. 2011.

[7] S. J. Fonash, “Introduction,” in *Solar Cell Device Physics*, 2nd Ed., Elsevier Inc., 2010, pp. 1–5.

[8] Plumbot, “Thin-film-solar-cell,” *plumbot.com*, 2011. .

[9] S. Logothetidis and A. Laskarakis, “Organic against inorganic electrodes grown onto polymer substrates for flexible organic electronics applications,” *Thin Solid Films*, vol. 518, no. 4, pp. 1245–1249, Dec. 2009.

[10] J. A. S. Williams, “A review of electronics demanufacturing processes,” *Resour. Conserv. Recycl.*, vol. 47, no. 3, pp. 195–208, Jun. 2006.

[11] A. Laskarakis, D. Georgiou, S. Logothetidis, S. Amberg-Scwhab, and U. Weber, "Study of the optical response of hybrid polymers with embedded inorganic nanoparticles for encapsulation of flexible organic electronics," *Mater. Chem. Phys.*, vol. 115, no. 1, pp. 269–274, May 2009.

[12] H. Ma, H.-L. Yip, F. Huang, and A. K.-Y. Jen, "Interface engineering for organic electronics," *Adv. Funct. Mater.*, vol. 20, no. 9, pp. 1371–1388, 2010.

[13] H. Kallmann and M. Pope, "Photovoltaic effect in organic crystals," *J Chem Phys*, vol. 30, pp. 585–586, 1959.

[14] C. W. Tang, "2-layer organic photovoltaic cell," *Appl Phys Lett*, vol. 48, pp. 183–185, 1986.

[15] Heliatek GmbH, "Heliatek consolidates its technology leadership by establishing a new world record for organic solar technology with a cell efficiency of 12%," Dresden, 2013.

[16] T. Tong *et al.*, "Adhesion in organic electronic structures," *J. Appl. PHYSICS, Am. Inst. Phys.*, vol. 106, no. 83708, pp. 1–7, 2009.

[17] G. Harsányi, "Polymer films in sensor applications: a review of present uses and future possibilities," *Sens. Rev.*, vol. 20, no. 2, pp. 98–105, 2000.

[18] P. A. . Lane and Z. H. . Kafafi, "Solid-State Organic Photovoltaics: A Review of Molecular and Polymeric Devices," in *Organic Photovoltaics Mechanisms, Materials, and Devices*, N. S. Sariciftci and S.-S. Sun, Eds. CRC press 2005, 2010.

[19] *DOE Fundamentals Handbook- Electrical Science*, 1 of 4. Washington, D.C.: U.S. Department of Energy, 1992, pp. 1–92.

[20] T. Markvart and L. CastaÑer, “Semiconductor Materials and Modelling,” in *Practical Handbook of Photovoltaics: Fundamentals and Applications*, Elsevier B.V, 2003, pp. 95–121.

[21] Y. Zhang *et al.*, “Mechanics of Ultra-Stretchable Self-Similar Serpentine Interconnects,” *Acta Mater.*, vol. 61, no. 20, pp. 7816–7827, Dec. 2013.

[22] Y. Duan, Y. Huang, and Z. Yin, “Transfer printing and patterning of stretchable electrospun film,” *Elsevier J. Thin Solid Film.*, vol. 544, pp. 152–156, 2013.

[23] Y. Song *et al.*, “Digital cameras with designs inspired by the arthropod eye,” *Nature*, vol. 497, pp. 95–99, 2013.

[24] S. P. Lacour, J. Jones, S. Wagner, T. Li, and Z. Suo, “Stretchable Interconnects for Elastic Electronic Surfaces,” *Proc. IEEE*, vol. 93, no. 8, pp. 1459–1466, 2005.

[25] D. Kim *et al.*, “Epidermal electronics,” *Science (80-.).*, vol. 333, pp. 838–843, 2011.

[26] M.-C. Choi, Y. Kim, and C.-S. Ha, “Polymers for flexible displays: From material selection to device applications,” *Prog. Polym. Sci.*, vol. 33, no. 6, pp. 581–630, Jun. 2008.

[27] T. Sekitani *et al.*, “Stretchable active- matrix organic light-emitting diode display using printable elastic conductors,” *Nat. Mater.*, vol. 8, no. 6, pp. 494–499, 2009.

[28] S. P. Lacour, S. Wagner, Z. Huang, and Z. Suo, “Stretchable gold conductors on elastomeric substrates,” *Appl. Phys. Lett.*, vol. 82, no. 15, pp. 2404–2406, 2003.

[29] T. Sekitani, Y. Noguchi, K. Hata, T. Fukushima, T. Aida, and T. Someya, “A rubberlike stretchable active matrix using elastic conductors,” *Science (80-.).*, vol. 321, no. 5895, pp.

1468–72, 2008.

[30] S. P. Lacour, S. Wagner, R. J. Narayan, T. Li, and Z. Suo, “Stiff subcircuit islands of diamondlike carbon for stretchable electronics,” *J. Appl. Phys.*, vol. 100, no. 1, p. 14913, 2006.

[31] D.-Y. Khang, H. Jiang, Y. Huang, and J. A. Rogers, “A Stretchable Form of Single-Crystal Silicon for High-Performance Electronics on Rubber Substrates,” *Science (80-.).*, vol. 311, no. 5758, pp. 208–212, 2006.

[32] H. Ko *et al.*, “A hemispherical electronic eye camera based on compressible silicon optoelectronics,” *Nature*, vol. 454, no. 27, pp. 748–753, 2008.

[33] S. Wagner *et al.*, “Low-dimensional Systems and Nanostructures,” *Phys. E*, vol. 25, no. 2, pp. 326–334, 2004.

[34] T. Someya, T. Sekitani, S. Iba, Y. Kato, H. Kawaguchi, and T. Sakurai, “A large-area, flexible pressure sensor matrix with organic field-effect transistors for artificial skin applications,” *Proc. Natl. Acad. Sci. U. S. A.*, vol. 101, no. 27, pp. 9966–9970, 2004.

[35] S. C. B. Mannsfeld *et al.*, “Highly sensitive flexible pressure sensors with microstructured rubber dielectric layers,” *Nat. Mater.*, vol. 9, no. 10, pp. 859–864, 2010.

[36] K. Demirkan, “Interfaces of electrical contacts in organic semiconductor devices,” ProQuest, Delaware, 2008.

[37] O. Akogwu, D. Kwabi, S. Midturi, M. Eleruja, B. Babatope, and W. O. Soboyejoa, “Large strain deformation and cracking of nano-scale gold films on PDMS substrate,” *Elsevier J. Mater. Sci. Eng.*, vol. B, no. 170, pp. 32–40, 2010.

[38] O. E. Akogwu, “DEFORMATION AND FAILURE MECHANISMS IN FLEXIBLE AND ORGANIC ELECTRONIC STRUCTURES,” Princeton University, 2010.

[39] O. Akogwu, D. Kwabi, S. Midturi, M. Eleruja, B. Babatope, and W. O. Soboyejo, “Large strain deformation and cracking of nano-scale gold films on PDMS substrate,” *Mater. Sci. Eng. B*, vol. 170, no. 1–3, pp. 32–40, Jun. 2010.

[40] A. Blau *et al.*, “Flexible, all-polymer microelectrode arrays for the capture of cardiac and neuronal signals.,” *Biomaterials*, vol. 32, no. 7, pp. 1778–86, Mar. 2011.

[41] C. T. Pan, Z. H. Liu, Y. C. Chen, and C. F. Liu, “Design and fabrication of flexible piezo-microgenerator by depositing ZnO thin films on PET substrates,” *Sensors Actuators A Phys.*, vol. 159, no. 1, pp. 96–104, Apr. 2010.

[42] C. Koidis, S. Logothetidis, a Laskarakis, I. Tsiaoussis, and N. Frangis, “Thin film and interface properties during ZnO deposition onto high-barrier hybrid/PET flexible substrates.,” *Micron*, vol. 40, no. 1, pp. 130–4, Jan. 2009.

[43] C.-J. Chiang, C. Winscom, S. Bull, and A. Monkman, “Mechanical modeling of flexible OLED devices,” *Org. Electron.*, vol. 10, no. 7, pp. 1268–1274, Nov. 2009.

[44] S. R. Dupont, E. Voroshazi, P. Heremans, and R. H. Dauskardt, “Adhesion properties of inverted polymer solarcells: Processing and film structure parameters,” *Org. Electron. physics, Mater. Appl.*, vol. 14, no. 5, pp. 1262–1270, 2013.

[45] N. Lu and S. Yang, “Mechanics of stretchable sensors,” *Elsevier Curr. Opin. Solid State Mater. Sci.*, p. 8, 2015.

[46] M. Kanari, M. Kunimoto, T. Wakamatsu, and I. Ihara, “Critical bending radius and

electrical behaviors of organic field effect transistors under elastoplastic bending strain," *Thin Solid Films*, vol. 518, no. 10, pp. 2764–2768, Mar. 2010.

[47] M. R. McGurk, H. W. Chandler, P. C. Twigg, and T. F. Page, "Modelling the hardness response of coated systems: the plate bending approach," *Surf. Coatings Technol.*, vol. 68–69, pp. 576–581, 1994.

[48] M. R. McGurk and T. F. Page, "Exploration of the plate bending model for predicting the hardness response of coated systems," *Surf. Coatings Technol.*, vol. 92, no. 1–2, pp. 87–95, 1997.

[49] W. Cao, Y. Zheng, Z. Li, E. Wrzesniewski, W. T. Hammond, and J. Xue, "Flexible organic solar cells using an oxide/metal/oxide trilayer as transparent electrode," *Org. Electron.*, vol. 13, no. 11, pp. 2221–2228, Nov. 2012.

[50] S. Logothetidis, "Flexible organic electronic devices: Materials, process and applications," *Mater. Sci. Eng. B*, vol. 152, no. 1–3, pp. 96–104, Aug. 2008.

[51] P. H. Townsend, D. M. Barnett, and T. A. Brunner, "Elastic relationships in layered composite media with approximation for the case of thin films on a thick substrate," *J. Appl. Phys.*, vol. 62, no. 11, pp. 4438–4444, 1987.

[52] F. Zhu, "Transparent Electrode for OLEDs," in *Organic Light-Emitting Materials and Devices*, 2007, pp. 483–525.

[53] B. Kim, H. Shin, I. Choi, and Y. Joo, "Electrical failure and damage analysis of multi-layer metal films on flexible substrate during cyclic bending deformation," *18th IEEE Int. Symp. Phys. Fail. Anal. Integr. Circuits*, pp. 1–4, Jul. 2011.

[54] D. Briand, F. Molina-Lopez, A. V. Quintero, C. Ataman, J. Courbat, and N. F. de Rooij, "Why Going Towards Plastic and Flexible Sensors?," *Procedia Eng.*, vol. 25, pp. 8–15, Jan. 2011.

[55] K. L. Lerner and B. W. Lerner, "Photovoltaic Cell," *The gale encyclopedia of science (Vol 5)*. The Gale Group, Inc., Canada, pp. 3072–3073, 2004.

[56] GBI Research, "Thin Film Photovoltaic (PV) Cells Market Analysis to 2020 CIGS Copper Indium Gallium Diselenide to Emerge as the Major Technology by 2020," 2011.

[57] A. Bernanose, "Electroluminescence of organic compounds," *Br. J. Appl. Phys.*, vol. 6, no. S4, p. S54, 1955.

[58] G. A. Chamberlain, "Organic solar cells: A review," *Sol. cells*, vol. 8, no. 1, pp. 47–83, 1983.

[59] M. Pope, H. P. Kallmann, and P. Magnante, "Electroluminescence in organic crystals," *J. Chem. Phys.*, vol. 38, no. 8, pp. 2042–2043, 1963.

[60] W. Helfrich and W. G. Schneider, "Recombination radiation in anthracene crystals," *Phys. Rev. Lett.*, vol. 14, no. 7, p. 229, 1965.

[61] R. M. Swart and G. G. Roberts, "Langmuir-Blodgett Films." Plenum Press: New York, 1990.

[62] N. Tessler, G. J. Denton, and R. H. Friend, "Lasing from conjugated-polymer microcavities," *Nature*, vol. 382, no. 6593, pp. 695–697, 1996.

[63] C. H. Peters, A. R. Guichard, A. C. Hryciw, M. L. Brongersma, and M. D. McGehee, "Energy transfer in nanowire solar cells with photon-harvesting shells," *J. Appl. Phys.*,

vol. 105, no. 12, p. 124509, 2009.

[64] P. A. LANE, “Solid State Organic Solar Cells,” in *ACS symposium series*, 2010, vol. 1039, pp. 185–198.

[65] S. Aazou *et al.*, “Organic Bulk Heterojunction Solar Cells Based on P3HT and Anthracene-Containing PPE-PPV: Fabrication, Characterization and Modeling,” *J. Optoelectron. Adv. Mater.*, vol. 13, no. 5–6, pp. 395–404, 2013.

[66] M. Kaltenbrunner *et al.*, “Ultrathin and lightweight organic solar cells with high flexibility.,” *Nat. Commun.*, vol. 3, no. 770, pp. 1–7, Jan. 2012.

[67] J. Escarre, K. Söderström, C. Battaglia, F.-J. Haug, and C. Ballif, “High fidelity transfer of nanometric random textures by UV embossing for thin film solar cells applications,” *Sol. Energy Mater. Sol. Cells*, vol. 95, no. 3, pp. 881–886, 2011.

[68] T. Udomphol, “Lecture 3: Elements of the theory of plasticity,” in *Suranaree University of Technology*, 2007.

[69] L. Grande, V. T. Chundi, D. Wei, C. Bower, P. Andrew, and T. Ryhänen, “Graphene for energy harvesting/storage devices and printed electronics,” *Particuology*, vol. 10, no. 1, pp. 1–8, Feb. 2012.

[70] P. Docampo, J. M. Ball, M. Darwich, G. E. Eperon, and H. J. Snaith, “Efficient organometal trihalide perovskite planar-heterojunction solar cells on flexible polymer substrates,” *Nat. Commun.*, vol. 4, no. 2761, p. 4, 2013.

[71] Robert H Olley, “You’re Not Sustainable, PET,” *Science 2.0, Join the revolution*. [Online]. Available: www.sciencecodex.com. [Accessed: 12-Oct-2010].

[72] T. Lenau, "PET (polyethylene terephthalate)," *Design inSite*. [Online]. Available: http://www.designinsite.dk/htmsider/m0011.htm. [Accessed: 01-Jan-2015].

[73] A. Das, C. H. Lei, M. Elliott, J. E. Macdonald, and M. L. Turner, "Non-lithographic fabrication of PEDOT nano-wires between fixed Au electrodes," *Elsevier Org. Electron.*, vol. 7, no. 4, pp. 181–187, 2006.

[74] R. H. Friend and K. Pichler, "Color filters for organic light-emissive devices." Google Patents, 2005.

[75] D. Troadec, G. Veriot, R. Antony, and A. Moliton, "Organic light-emitting diodes based on multilayer structures," *Synth. Met.*, vol. 124, no. 1, pp. 49–51, 2001.

[76] Z. Zhong, Y. Dai, D. Ma, and Z. Y. Wang, "Facile synthesis of organo-soluble surface-grafted all-single-layer graphene oxide as hole-injecting buffer material in organic light-emitting diodes," *J. Mater. Chem.*, vol. 21, no. 16, pp. 6040–6045, 2011.

[77] M. S. White *et al.*, "Ultrathin , highly flexible and stretchable PLEDs," *Nat. Photonics*, no. July, pp. 1–6, 2013.

[78] K. A. Sierros, N. J. Morris, K. Ramji, and D. R. Cairns, "Stress-corrosion cracking of indium tin oxide coated polyethylene terephthalate for flexible optoelectronic devices," *Thin Solid Films*, vol. 517, pp. 2590–2595, 2009.

[79] D. S. Ginley and C. Bright, "Transparent conducting oxides," *MRS Bull*, vol. 25, pp. 15–18, 2000.

[80] M. P. de Jong, L. J. van IJzendoorn, and M. J. A. de Voigt, "Stability of the interface between indium-tin-oxide and poly(3,4-ethylenedioxythiophene)/poly(styrenesulfonate) in

polymer light emitting diodes," *Appl Phys Lett*, vol. 77, p. 2255, 2000.

[81] E. Gautier, A. Lorin, J. M. Nunzi, A. Schalchli, J. J. Benattar, and D. Vital, "Electrode interface effects on indium-tin-oxide polymer/ metal light emitting diodes," *Appl Phys Lett*, vol. 69, p. 1071, 1996.

[82] E. Perzon *et al.*, "Design, synthesis and properties of low band gap polyfluorenes for photovoltaic devices," *Synth. Met.*, vol. 154, no. 1–3, pp. 53–56, 2005.

[83] Y. S. Kim *et al.*, "Effect of solvents on the performance and morphology of polymer photovoltaic devices," *Curr. Appl. Phys.*, vol. 10, no. 4, pp. 985–989, 2010.

[84] M. Al-lbrahim, O. Ambacher, S. Sensfuss, and G. Gobsch, "Effects of solvent and annealing on the improved performance of solar cells based on poly(3-hexylthiophene): Fullerene," *Appl. Phys. Lett*, vol. 86, p. 201120, 2005.

[85] H. S. Nalwa, *Handbook of Organic Conductive Molecules and Polymers, Conductive Polymers Vol. 3: Spectroscopy and Physical Properties,*. J. Wiley & Sons, 1997.

[86] T. L. Alford, L. C. Feldman, and J. W. Mayer, *Fundamentals of Nanoscale Film Analysis*. New York: Springer Science+Business Media, Inc., 2007.

[87] S.-S. Sun and L. R. Dalton, *Introduction to organic electronic and optoelectronic materials and devices*. CRC Press, 2011.

[88] S. A. Odom, S. R. Parkin, and J. E. Anthony, "Tetracene derivatives as potential red emitters for organic LEDs," *Org. Lett.*, vol. 5, no. 23, pp. 4245–4248, 2003.

[89] B. Geffroy, P. Le Roy, and C. Prat, "Organic light-emitting diode (OLED) technology: materials, devices and display technologies," *Polym. Int.*, vol. 55, no. 6, pp. 572–582,

2006.

[90] W. Brütting, S. Berleb, and A. G. Mückl, “Device physics of organic light-emitting diodes based on molecular materials,” *Org. Electron.*, vol. 2, no. 1, pp. 1–36, 2001.

[91] G. Hughes and M. R. Bryce, “Electron-transporting materials for organic electroluminescent and electrophosphorescent devices,” *J. Mater. Chem.*, vol. 15, no. 1, pp. 94–107, 2005.

[92] H. Aziz, Z. D. Popovic, N.-X. Hu, A.-M. Hor, and G. Xu, “Degradation mechanism of small molecule-based organic light-emitting devices,” *Science (80-.).*, vol. 283, no. 5409, pp. 1900–1902, 1999.

[93] R. H. Friend *et al.*, “Electroluminescence in conjugated polymers,” *Nature*, vol. 397, no. 6715, pp. 121–128, 1999.

[94] P. K. H. Ho *et al.*, “Molecular-scale interface engineering for polymer light-emitting diodes,” *Nature*, vol. 404, no. 6777, pp. 481–484, 2000.

[95] T. M. Tong, “Adhesion and Interfacial Fracture : From Organic Light Emitting Devices and Photovoltaic Cells to Solar Lanterns for Developing Regions,” PRINCETON UNIVERSITY, 2012.

[96] J. J. Duga *et al.*, “The economic effects of fracture in the united states,” *Batelle Columbus Lab.*, 1983.

[97] P. Bouten, P. Slikkerveer, and Y. Leterrier, “Mechanics of ITO on plastic substrates for flexible displays.,” in *Flexible Flat Panel Displays*, Grawford., England: Wiley, 2005, p. 117.

[98] D. Cairns *et al.*, "Strain-dependent electrical resistance of tin-doped indium oxide on polymer substrates.," *Appl Phys Lett*, vol. 76, pp. 1425–1427, 2000.

[99] M. A. Biot, "Surface instability of rubber in compression," *Appl. Sci. Res. Sect. A*, vol. 12, no. 2, pp. 168–182, 1963.

[100] A. N. Gent and I. S. Cho, "Surface instabilities in compressed or bent rubber blocks," *Rubber Chem. Technol.*, vol. 72, no. 2, pp. 253–262, 1999.

[101] E. Hohlfeld and L. Mahadevan, "Unfolding the sulcus," *Phys. Rev. Lett.*, vol. 106, no. 10, p. 105702, 2011.

[102] W. Hong, X. Zhao, and Z. Suo, "Formation of creases on the surfaces of elastomers and gels," *Appl. Phys. Lett.*, vol. 95, no. 11, p. 111901, 2009.

[103] Z. Suo, "Finite Deformation: Special Cases," 2013.

[104] N. S. Lu, X. Wang, Z. G. Suo, and J. J. Vlassak, "Metal films on polymer substrates stretched beyond 50%," *Appl. Phys. Lett.*, vol. 91, p. 221909, 2007.

[105] W. Soboyejo, *Mechanical Properties of Engineered Materials*. New York, NY: Marcel Dekker, Inc., 2003.

[106] H. M. Ma, X.-L. Gao, and J. N. Reddy, "A microstructure-dependent Timoshenko beam model based on a modified couple stress theory," *Elsevier J. Mech. Phys. Solids*, vol. 56, pp. 3379–3391, 2008.

[107] N. M. Whirter, "Sports Architecture," in *Guinness Book of World Records*, 2015th ed., G. Glenday, Ed. Jim Pattison Group, 1955, p. 200.

[108] Y. Wang, W. Wei, X. Liu, and Y. Gu, "Research progress on polymer heterojunction solar

cells," *Sol. Energy Mater. Sol. Cells*, vol. 98, pp. 129–145, Mar. 2012.

[109] Konarka, "Konarka Website," *Konarka Website*, 2010. [Online]. Available: http://www.konarka.com/. [Accessed: 10-Dec-2010].

[110] E. D. GŁOWACKI, N. S. SARICIFTCI, and C. W. TANG, *Organic Solar Cells*. New York, NY: Springer New York, 2013.

[111] M. Jørgensen, K. Norrman, and F. C. Krebs, "Stability/degradation of polymer solar cells," *Sol. Energy Mater. Sol. Cells*, vol. 92, no. 7, pp. 686–714, 2008.

[112] Y. Lu, J. Y. Huang, C. Wang, S. Sun, and J. Lou, "Cold welding of ultrathin gold nanowires," *Nat. Nanotechnol.*, vol. 5, no. 3, pp. 218–224, 2010.

[113] R. W. J. Messler, *Principles of welding: processes, physics, chemistry, and metallurgy*. John Wiley & Sons, 2008.

[114] A. Lozier, O. O. Popoola, J. J. Mason, and M. Forstein, "Bone fracture fixation system." Google Patents, 2008.

[115] A. Barcellona, G. Buffa, L. Fratini, and D. Palmeri, "On microstructural phenomena occurring in friction stir welding of aluminium alloys," *J. Mater. Process. Technol.*, vol. 177, no. 1, pp. 340–343, 2006.

[116] W. F. Savage, E. F. Nippes, and E. S. Szekeres, "A Study of weld interface phenomena in a low alloy steel," *Weld. J.*, vol. 55, no. 9, p. 260, 1976.

[117] H. Haga, K. Aoki, and T. Sato, "The mechanisms of formation of weld defects in high-frequency electric resistance welding," *Weld. J.*, vol. 60, no. 6, p. 104s--109s, 1981.

[118] D. V Wagle and G. A. Baker, "Cold welding: a phenomenon for spontaneous self-healing

and shape genesis at the nanoscale," *Mater. Horizons*, 2015.

[119] W. O. Akande, "Interfacial Reliability and Failure Mechanisms in Organic Light Emitting Diodes," Princeton University, 2010.

[120] R. Toniolo and I. A. Hümmelgen, "Simple and fast organic device encapsulation using polyisobutene," *Macromol. Mater. Eng.*, vol. 289, no. 4, pp. 311–314, 2004.

[121] Y. Zhang, M. Andreasson, H. Zhou, J. Liu, T. Andersson, and J. Fan, "Encapsulation of OLED device by Using Anisotropic Conductive Adhesive," in *High Density packaging and Microsystem Integration, 2007. HDP'07. International Symposium on*, 2007, pp. 1–4.

[122] A. P. Ghosh, L. J. Gerenser, C. M. Jarman, and J. E. Fornalik, "Thin-film encapsulation of organic light-emitting devices," *Appl. Phys. Lett.*, vol. 86, no. 22, p. 223503, 2005.

[123] J. Song and D. J. Srolovitz, "Molecular dynamics investigation of patterning via cold welding," *J. Mech. Phys. Solids*, vol. 57, no. 4, pp. 776–787, 2009.

[124] J. K. Kim *et al.*, "Layer-by-Layer All-Transfer-Based Organic Solar Cells," *Langmuir*, vol. 29, no. 17, pp. 5377–5382, 2013.

[125] M. B. Tucker, D. R. Hines, and T. Li, "A quality map of transfer printing," *J. Appl. Mech.*, vol. 106, p. 103504, 2009.

[126] T.-N. Chen *et al.*, "Deposition and characterization of ultra-high barrier coatings for flexible electronic applications," *Vacuum*, vol. 84, no. 12, pp. 1444–1447, Jun. 2010.

[127] C. Ababei, S. Yuvarajan, and D. L. Schulz, "Toward integrated PV panels and power electronics using printing technologies," *Sol. Energy*, vol. 84, no. 7, pp. 1111–1123, Jul. 2010.

[128] C. J. Brabec and J. R. Durrant, “S olution-Processed Organic Solar Cells,” vol. 33, no. July, 2008.

[129] E.-H. Kil *et al.*, “Imprintable, bendable, and shape-conformable polymer electrolytes for versatile-shaped lithium-ion batteries.,” *Adv. Mater.*, vol. 25, no. 10, pp. 1395–400, Mar. 2013.

[130] D. Yu *et al.*, “Adhesion in flexible organic and hybrid organic/inorganic light emitting device and solar cells,” *J. Appl. Phys.*, vol. 116, no. 7, p. 74506, Aug. 2014.

[131] P. A. Troshin *et al.*, “Material structure-composite morphology-photovoltaic performance relationship for organic bulk heterojunction solar cells.,” *Chem. Commun. (Camb).*, vol. 48, no. 76, pp. 9477–9, Oct. 2012.

[132] Y. Kim, H. Kim, S. Graham, A. Dyer, and J. R. Reynolds, “Durable polyisobutylene edge sealants for organic electronics and electrochemical devices,” *Sol. Energy Mater. Sol. Cells*, vol. 100, pp. 120–125, May 2012.

[133] P. D. and V. B. Mukesh Kumar, “Enhanced Open Circuit Voltage in Aluminum Confined Post-Annealing of poly(3-hexylthiophene)/fullerene Bulk Heterojunction Solar Cells under Electric Field,” no. 4 V, 2012.

[134] J. Guo, H. Ohkita, H. Benten, and S. Ito, “Charge Generation and Recombination Dynamics in Poly (3-hexylthiophene)/ Fullerene Blend Films with Different Regioregularities and Morphologies,” no. 6, pp. 6154–6164, 2010.

[135] J.-F. Salinas *et al.*, “On the use of Woods metal for fabricating and testing polymeric organic solar cells: An easy and fast method,” *Sol. Energy Mater. Sol. Cells*, vol. 95, no. 2, pp. 595–601, Feb. 2011.

[136] D. Yokoyama, Z. Qiang Wang, Y.-J. Pu, K. Kobayashi, J. Kido, and Z. Hong, "High-efficiency simple planar heterojunction organic thin-film photovoltaics with horizontally oriented amorphous donors," *Sol. Energy Mater. Sol. Cells*, vol. 98, pp. 472–475, Mar. 2012.

[137] H. Hoppe and N. S. Sariciftci, "Organic solar cells: An overview," *J. Mater. Res.*, vol. 19, no. 7, pp. 1924–1945, Mar. 2011.

[138] B. Watts, W. J. Belcher, L. Thomsen, H. Ade, and P. C. Dastoor, "A Quantitative Study of PCBM Diffusion during Annealing of P3HT:PCBM Blend Films," *Macromolecules*, vol. 42, no. 21, pp. 8392–8397, Nov. 2009.

[139] R. A. J. Janssen, J. C. Hummelen, and N. S. Sariciftci, "P olymer – Fullerene Solar Cells," vol. 30, no. January, pp. 33–36, 2005.

[140] G. Li *et al.*, "High-efficiency solution processable polymer photovoltaic cells by self-organization of polymer blends," vol. 4, no. November, pp. 2–6, 2005.

[141] M. Li *et al.*, "Mechanics analysis of two-dimensionally prestrained elastomeric thin film for stretchable electronics," *Acta Mech. Solida Sin.*, vol. 23, no. 6, pp. 592–599, Dec. 2010.

[142] N.-H. Zhang and J.-J. Xing, "An alternative model for elastic bending deformation of multilayered beams," *J. Appl. Phys.*, vol. 100, no. 10, p. 103519, 2006.

[143] C. M. Stafford *et al.*, "A buckling-based metrology for measuring the elastic moduli of polymeric thin films," *Nat. Mater.*, vol. 3, no. August, pp. 545–550, 2004.

[144] C. M. Stafford *et al.*, "A buckling-based metrology for measuring the elastic moduli of

polymeric thin films," *Nat. Mater.*, vol. 3, no. 8, pp. 545–550, 2004.

[145] Z. Jia, M. B. Tucker, and T. Li, "Failure mechanics of organic–inorganic multilayer permeation barriers in flexible electronics," *Compos. Sci. Technol.*, vol. 71, no. 3, pp. 365–372, Feb. 2011.

[146] D. J. Lipomi, B. C.-K. Tee, M. Vosgueritchian, and Z. Bao, "Stretchable organic solar cells," *Adv. Mater.*, vol. 23, no. 15, pp. 1771–1775, 2011.

[147] Y. Su *et al.*, "Postbuckling analysis and its application to stretchable electronics," *J. Mech. Phys. Solids*, vol. 60, no. 3, pp. 487–508, Mar. 2012.

[148] B. Y. Sun and J. A. Rogers, "Inorganic Semiconductors for Flexible Electronics **," *Adv. Mater.*, vol. 19, pp. 1897–1916, 2007.

[149] J. Du, T. Tong, W. Akande, A. Tsakiridou, and W. Soboyejo, "Pressure Effects on the Lamination of Organic Light-Emitting Diodes," *Disp. Technol. J.*, vol. 9, no. 8, pp. 601–606, 2013.

[150] A. Aref-Azar, F. Biddlestone, J. N. Hay, and R. N. Haward, "The effect of physical ageing on the properties of poly (ethylene terephthalate)," *Polymer (Guildf).*, vol. 24, no. 10, pp. 1245–1251, 1983.

[151] D. J. Lipomi, H. Chong, M. Vosgueritchian, J. Mei, and Z. Bao, "Toward mechanically robust and intrinsically stretchable organic solar cells : Evolution of photovoltaic properties with tensile strain," *Sol. Energy Mater. Sol. Cells*, vol. 107, pp. 355–365, 2012.

[152] D. Tahk, H. H. Lee, and D.-Y. Khang, "Elastic moduli of organic electronic materials by the buckling method," *Macromolecules*, vol. 42, no. 18, pp. 7079–7083, 2009.

[153] D. G. Neerinck and T. J. Vink, “Depth profiling of thin ITO films by grazing incidence X-ray diffraction,” *Thin Solid Films*, vol. 278, no. 1, pp. 12–17, 1996.

[154] E. F. Schubert, “Refractive index and extinction coefficient of materials.” pp. 100–167, 2004.

[155] K. Sivaramakrishnan and T. L. Alford, “Conduction and transmission analysis in gold nanolayers embedded in zinc oxide for flexible electronics,” *Appl. Phys. Let.*, vol. 96, no. 109, p. 201, 2010.

[156] B. Lewis and D. Paine, “Applications and processing of transparent conducting oxides,” *MRS Bull*, vol. 25, pp. 22–27, 2000.

[157] D. Paine, H. Yeom, and B. Yaglioglu, “Transparent conducting oxide materials and technology,” in *Flexible Flat Panel Displays*, Grawford G., England: Wiley, 2005, pp. 80–98.

[158] K. Baedeker, “U ber die elektrische Leitfahigkeit und die thermoelektrische Krafteiniger Schwermetallverbindungen,” *Ann Phys*, vol. 22, pp. 749–766, 1907.

[159] L. Bert Groenendaal, “Conductive polymers,” in *Flexible Flat Panel Displays*, Crawford G., England: Wiley, 2005, p. 157.

[160] K. A. Arpin *et al.*, “Multidimensional architectures for functional optical devices,” *Adv. Mater.*, vol. 22, no. 10, pp. 1084–1101, 2010.

[161] C. Battaglia *et al.*, “Nanoimprint lithography for high-efficiency thin-film silicon solar cells,” *Nano Lett.*, vol. 11, no. 2, pp. 661–665, 2010.

[162] C. H. Hsueh and A. A. Wereszczak, “Multiple cracking of brittle coatings on strained

substrates," *J. Appl. Phys.*, vol. 96, no. 6, pp. 3501–6, 2004.

[163] M. Kaltenbrunner *et al.*, "Ultrathin and lightweight organic solar cells with high flexibility," *Nat. Commun.*, vol. 3, no. 770, pp. 1–7, 2012.

[164] Y. Zhang, Y. Huang, and J. A. Rogers, "Mechanics of stretchable batteries and supercapacitors," *Curr. Opin. SOLID STATE Mater. Sci. ELSEVIER LTD.*, p. 10, 2015.

[165] H. Y. Low and S. J. Chua, "Mechanical properties of organic light-emitting thin films deposited on polymer-based barrier substrate: potential for flexible organic light-emitting displays," *Mater. Lett.*, vol. 53, no. 4–5, pp. 227–232, 2002.

[166] J. Asare, B. Agyei-Tuffour, O. K. Oyewole, V. C. Anye, D. Y. Momodu, and W. O. Soboyejo, "Effects of Deformation on Failure Mechanisms and Optical Properties of Flexible Organic Solar Cell Structures," *Adv. Mater. Res.*, vol. 1132, pp. 125–143, 2016.

[167] J. Asare, B. Agyei-Tuffour, O. K. Oyewole, G. M. Zebaze-Kana, and W. O. Soboyejo, "DEFORMATION AND FAILURE OF BENDABLE ORGANIC SOLAR CELLS," *Adv. Mater. Res.*, vol. 1132, pp. 116–124, 2016.

[168] I. Bernardeschi *et al.*, "A soft, stretchable and conductive biointerface for cell mechanobiology," *Biomed. Microdevices*, 2015.

[169] O. K. Oyewole, J. Asare, D. O. Oyewole, V. C. Anye, M. G. Z. Kana, and W. O. Soboyejo, "EFFECTS OF ADHESION AND STRETCHING ON FAILURE MECHANISMS AND OPTICAL PROPERTIES OF ORGANIC SOLAR CELLS," *Adv. Mater. Res.*, vol. 1132, pp. 89–105, 2016.

[170] O. K. Oyewole *et al.*, "Micro-wrinkling and delamination-induced buckling of stretchable

electronic structures," *J. Appl. Phys.*, vol. 117, no. 23, p. 235501, 2015.

[171] P. Zioupos and J. D. Currey, "Pre-failure toughening mechanisms in the dentine of the narwhal tusk: microscopic examination of stress/strain induced microcracking," *J. Mater. Sci. Lett.*, vol. 15, no. 11, pp. 991–994, 1996.

[172] A. L. Volynskii, S. Bazhenov, O. V. Lebedeva, and N. F. Bakeev, "Mechanical buckling instability of thin coatings deposited on soft polymer substrates," *J. Mater. Sci.*, vol. 35, pp. 547–554, 2000.

[173] J. Groenewold, "Wrinkling of plates coupled with soft elastic media," *Physica A*, vol. 298, pp. 32–45, 2001.

[174] M. Huang, P. Rugheimer, M. G. Lagally, and F. Liu, "Bending of nanoscale ultrathin substrates by growth of strained thin films and islands," *Phys. Rev. B*, vol. 72, no. 8, p. 85450, 2005.

[175] R. Huang, "UT-MSSM Report No. 04/01," Univ. Texas, Austin, 2004.

[176] J. Lee *et al.*, "Stretchable GaAs Photovoltaics with Designs That Enable High Areal Coverage," *Adv. Mater.*, vol. 23, no. 8, 2011.

[177] A. I. Mardare, M. Kaltenbrunner, N. S. Sariciftci, S. Bauer, and A. W. Hassel, "Ultra-thin anodic alumina capacitor films for plastic electronics," *Phys. Status Solidi*, vol. 209, no. 5, pp. 813–818, May 2012.

[178] Y. Zhang *et al.*, "Buckling in serpentine microstructures and applications in elastomer-supported ultra-stretchable electronics with high areal coverage," *Soft Matter*, vol. 9, no. 33, p. 8062, 2013.

[179] S. Hwang *et al.*, "Biodegradable Elastomers and Silicon Nanomembranes/Nanoribbons for Stretchable, Transient Electronics and Biosensors," *Nano Lett.*, 2015.

[180] C. J. Brabec, F. Padinger, J. C. Hummelen, R. A. J. Janssen, and N. S. Sariciftci, "Realization of large area flexible fullerene-conjugated polymer photocells: a route to plastic solar cells," *Synth. Met.*, vol. 102, no. 1, pp. 861–864, 1999.

[181] S. Tarasovs and J. Andersons, "Buckling of a coating strip of finite width bonded to elastic half-space," *Int. J. Solids Struct.*, vol. 45, no. 2, pp. 593–600, 2008.

[182] N. E. Dowling, *Mechanical behavior of materials: engineering methods for deformation, fracture, and fatigue*. Prentice hall, 1993.

[183] M. S. White *et al.*, "Ultrathin, highly flexible and stretchable PLEDs," *Nat. Photonics*, vol. 7, no. 10, pp. 811–816, 2013.

[184] A. Manekkathodi, M.-Y. Lu, C. W. Wang, and L.-J. Chen, "Direct Growth of Aligned Zinc Oxide Nanorods on Paper Substrates for Low-Cost Flexible Electronics," *Adv. Mater.*, vol. 22, no. 36, pp. 4059–4063, 2010.

[185] M. Drack, I. Graz, T. Sekitani, T. Someya, M. Kaltenbrunner, and S. Bauer, "An Imperceptible Plastic Electronic Wrap," *Adv. Mater.*, vol. 27, no. 1, pp. 34–40, 2015.

[186] D.-H. Kim, J. Xiao, J. Song, Y. Huang, and J. A. Rogers, "Stretchable, curvilinear electronics based on inorganic materials," *Adv. Mater.*, vol. 22, no. 19, pp. 2108–2124, 2010.

[187] W. M. Choi, J. Song, D.-Y. Khang, H. Jiang, Y. Y. Huang, and J. A. Rogers, "Biaxially Stretchable 'Wavy' Silicon Nanomembranes," *Nano Lett.*, vol. 7, no. 6, pp. 1655–1663,

2007.

[188] Y. Shang *et al.*, “Super-Stretchable Spring-Like Carbon Nanotube Ropes,” *Adv. Mater.*, vol. 24, no. 21, pp. 2896–2900, 2012.

[189] F. Xu, W. Lu, and Y. Zhu, “Controlled 3D buckling of silicon nanowires for stretchable electronics,” *ACS Nano*, vol. 5, no. 1, pp. 672–678, 2010.

[190] O. K. Oyewole *et al.*, “Micro-wrinkling and delamination-induced buckling of stretchable electronic structures,” *J. Appl. Phys.*, vol. 117, no. 23, p. 235501, 2015.

[191] J. Asare *et al.*, “Cold welding of organic light emitting diode: Interfacial and contact models,” *AIP Adv.*, vol. 6, no. 6, p. 65125, 2016.

[192] O. K. Oyewole *et al.*, “Lamination of organic solar cells and organic light emitting devices : Models and experiments,” *J. Appl. Phys.*, vol. 118, no. 75302, 2015.

[193] N. Bowden, S. Brittain, A. G. Evans, J. W. Hutchinson, and G. M. Whitesides, “Spontaneous formation of ordered structures in thin films of metals supported on an elastomeric polymer,” *Nature*, vol. 393, no. May, p. 146, 1998.

[194] C. Chen, J. Wang, and Z. Chen, “Surface restructuring behavior of various types of poly (dimethylsiloxane) in water detected by SFG,” *Langmuir*, vol. 20, no. 23, pp. 10186–10193, 2004.

[195] M. Morra, E. Occhiello, R. Marola, F. Garbassi, P. Humphrey, and D. Johnson, “On the aging of oxygen plasma-treated polydimethylsiloxane surfaces,” *J. Colloid Interface Sci.*, vol. 137, no. 1, pp. 11–24, 1990.

[196] P. H. Townsend, D. M. Barnett, and T. A. Brunner, “Elastic relationships in layered

composite media with approximation for the case of thin films on a thick substrate," *J. Appl. Phys.*, vol. 62, no. 11, pp. 4438–4444, 1987.

[197] S. Timoshenko and S. Woinowsky-Krieger, *Theory Of Plates And Shells*, 2nd ed. 1959.

[198] S. Timoshenko and J. N. Goodier, *Theory of Elasticity*, Second. New York: McGraw-Hill, 1951.

[199] S. Il Kim, K. W. Lee, B. B. Sahu, and J. G. Han, "Flexible OLED fabrication with ITO thin film on polymer substrate," *Jpn. J. Appl. Phys.*, vol. 54, pp. 90301–4, 2015.

[200] M. Sibiński, K. Znajdek, S. Walczak, M. Słoma, M. Górski, and A. Cenian, "Comparison of ZnO:Al, ITO and carbon nanotube transparent conductive layers in flexible solar cells applications," *Mater. Sci. Eng. B*, vol. 177, no. 15, pp. 1292–1298, Sep. 2012.

[201] Z. Wang *et al.*, "Flexible ITO-free Organic Solar Cells Based on MoO3/ Ag Anodes," *IEEE Photonics J.*, vol. 1943, no. 655, pp. 1–19, 2015.

[202] B. Ray and M. a. Alam, "Random vs regularized OPV: Limits of performance gain of organic bulk heterojunction solar cells by morphology engineering," *Sol. Energy Mater. Sol. Cells*, vol. 99, pp. 204–212, Apr. 2012.

[203] A. Bietsch and B. Michel, "Conformal contact and pattern stability of stamps used for soft lithography," *J. Appl. Phys.*, vol. 88, no. 7, pp. 4310–4318, 2000.

[204] D. Y. Momodu, T. Tong, M. G. Z. Kana, A. V Chioh, and W. O. Soboyejo, "Adhesion and degradation of organic and hybrid organic-inorganic light-emitting devices," *J. Appl. Phys.*, vol. 84504, pp. 1–10, 2014.

[205] O. van der Sluis, a. a. Abdallah, P. C. P. Bouten, P. H. M. Timmermans, J. M. J. den

Toonder, and G. de With, “Effect of a hard coat layer on buckle delamination of thin ITO layers on a compliant elasto-plastic substrate: An experimental–numerical approach,” *Eng. Fract. Mech.*, vol. 78, no. 6, pp. 877–889, Apr. 2011.

[206] J. A. Rogers, T. Someya, and Y. Huang, “Materials and mechanics for stretchable electronics,” *Science (80-.).*, vol. 327, no. 5973, pp. 1603–1607, 2010.

[207] K. Kim *et al.*, “Stretchable and transparent electrodes based on in-plane structures,” *Nanoscale © R. Soc. Chem. 2012*, vol. 0, no. 1–3, p. 20, 2015.

[208] M. Kaltenbrunner *et al.*, “An ultra-lightweight design for imperceptible plastic electronics,” *Nature*, vol. 499, no. 7459, pp. 458–463, 2013.

[209] J. Fahlteich, M. Fahland, W. Schönberger, and N. Schiller, “Permeation barrier properties of thin oxide films on flexible polymer substrates,” *Thin Solid Films*, vol. 517, no. 10, pp. 3075–3080, Mar. 2009.

[210] T. Sugiyama, K. Chonan, and M. Kambe, “Enhanced Light Trapping of Thin Film Si Solar Cell in Glass-Laminated Module,” in *Mater. Res. Soc. Symp. Proc.*, 2012, vol. 1426.

[211] H. Aguas *et al.*, “Silicon thin film solar cells on commercial tiles,” *Energy Environ. Sci.*, vol. 4, pp. 4620–4632, 2011.

[212] R. B. Katragadda and Y. Xu, “A novel intelligent textile technology based on silicon flexible skins,” *Sensors Actuators A Phys.*, vol. 143, no. 1, pp. 169–174, May 2008.

[213] J.-Y. Lee, S. T. Connor, Y. Cui, and P. Peumans, “Semitransparent organic photovoltaic cells with laminated top electrode,” *Nano Lett.*, vol. 10, no. 4, pp. 1276–1279, 2010.

[214] W. O. Akande, Y. Cao, N. Yao, and W. Soboyejo, “Adhesion and the cold welding of

gold-silver thin films," *J. Appl. Phys.*, vol. 107, no. 43519, pp. 1–8, 2010.

[215] Y. Cao, C. Kim, S. R. Forrest, and W. Soboyejo, "Effects of dust particles and layer properties on organic electronic devices fabricated by stamping," *J. Appl. Phys.*, vol. 98, no. 3, p. 33713, 2005.

[216] C. Kim, Y. Cao, W. O. Soboyejo, and S. R. Forrest, "Patterning of active organic materials by direct transfer for organic electronic devices," *J. Appl. Phys.*, vol. 97, no. 11, p. 113512, 2005.

[217] M. B. Tucker, D. R. Hines, and T. Li, "A quality map of transfer printing," *J. Appl. Phys.*, vol. 106, no. 10, p. 103504, 2009.

[218] T.-F. Guo, S. Pyo, S.-C. Chang, and Y. Yang, "High performance polymer light-emitting diodes fabricated by a low temperature lamination process," *Adv. Funct. Mater.*, vol. 11, no. 5, pp. 339–343, 2001.

[219] H. Czichos, "The mechanism of the metallic adhesion bond," *J. Phys. D. Appl. Phys.*, vol. 5, no. 10, p. 1890, 1972.

[220] J. J. Dumond and H. Y. Low, "Recent developments and design challenges in continuous roller micro-and nanoimprinting," *J. Vac. Sci. Technol. B*, vol. 30, no. 1, p. 10801, 2012.

[221] A. M. Kendale and D. L. Trumper, "Microcontact printing," US7665983 B2, 2010.

[222] M. Geissler *et al.*, "Fabrication of metal nanowires using microcontact printing," *Langmuir*, vol. 19, no. 15, pp. 6301–6311, 2003.

[223] L. M. Campos *et al.*, "Applications of Photocurable PMMS Thiol- Ene Stamps in Soft Lithography," *Chem. Mater.*, vol. 21, no. 21, pp. 5319–5326, 2009.

[224] C. Kim and S. R. Forrest, “Fabrication of Organic Light-Emitting Devices by Low-Pressure Cold Welding,” *Adv. Mater.*, vol. 15, no. 6, pp. 541–545, 2003.

[225] Z. Wang, R. Xing, X. Yu, and Y. Han, “Adhesive lithography for fabricating organic electronic and optoelectronics devices,” *Nanoscale*, vol. 3, no. 7, pp. 2663–2678, 2011.

[226] M. M. Ling and Z. Bao, “Thin film deposition, patterning, and printing in organic thin film transistors,” *Chem. Mater.*, vol. 16, no. 23, pp. 4824–4840, 2004.

[227] C. Kim, P. E. Burrows, and S. R. Forrest, “Micropatterning of organic electronic devices by cold-welding,” *Science (80-.).*, vol. 288, no. 5467, pp. 831–833, 2000.

[228] Z. S. Pereira and E. Z. Da Silva, “Cold welding of gold and silver nanowires: a molecular dynamics study,” *J. Phys. Chem. C*, vol. 115, no. 46, pp. 22870–22876, 2011.

[229] Y. Cao, S. Allameh, D. Nankivil, S. Sethiaraj, T. Otiti, and W. Soboyejo, “Nanoindentation measurements of the mechanical properties of polycrystalline Au and Ag thin films on silicon substrates: Effects of grain size and film thickness,” *Mater. Sci. Eng. A*, vol. 427, no. 1, pp. 232–240, 2006.

[230] E. E. Gdoutos and V. Balopoulos, “Growth of Interfacial Cracks in Sandwich Beams,” pp. 37–42, 2010.

[231] M. B. Modi and S. K. Sitaraman, “Interfacial fracture toughness measurement for thin film interfaces,” *Eng. Fract. Mech.*, vol. 71, no. 9–10, pp. 1219–1234, Jun. 2004.

[232] B. Lauke and T. Schu, “Essential work of interfacial fracture : a method to characterise adhesion at polymer } polymer interfaces,” vol. 21, pp. 55–58, 2001.

[233] B. Agyei-Tuffour *et al.*, “Influence of Pressure on Contacts Between Layers in Organic,”

Adv. Mater. Res., vol. 1132, pp. 204–216, 2016.

[234] C. H. Mastrangelo and C. H. Hsu, "A simple experimental technique for the measurement of the work of adhesion of microstructures," *Solid-State Sens. Actuator Work. 5th Tech. Dig. IEEE*, vol. 212, p. 208, 1992.

[235] J. H. Burroughes *et al.*, "Light-emitting diodes based on conjugated polymers," *Nature*, vol. 347, no. 6293, pp. 539–541, 1990.

[236] F.-T. Chiang and J.-P. Hung, "Investigation of the fracture characteristics of the interfacial bond between bone and cement: experimental and finite element approaches," *J. Mech. Sci. Technol.*, vol. 24, no. 6, pp. 1235–1244, Jun. 2010.

[237] I. N. Sneddon, "The relation between load and penetration in the axisymmetric Boussinesq problem for a punch of arbitrary profile," *Int. J. Eng. Sci.*, vol. 3, no. 1, pp. 47–57, 1965.

[238] G. Wei, B. Bhushan, and S. Joshua Jacobs, "Nanomechanical characterization of multilayered thin film structures for digital micromirror devices.," *Ultramicroscopy*, vol. 100, no. 3–4, pp. 375–389, Aug. 2004.

[239] L. J. Gibson, M. F. Ashby, G. N. Karam, U. Wegst, and H. R. Shercliff, "The Royal Society 450," *R. Soc.*, vol. 450, 1995.

[240] V. Raghavan, *Material Science and Engineering*, 4thEdition ed. Prentice Hall of India Ltd, 1994.

[241] PeriodicTable.com, "Technical data for Gold," *Mathematica's ElementData function from Wolfram Research, Inc.*, 2006. [Online]. Available:

http://periodictable.com/Elements/079/data.html. [Accessed: 01-Jan-2016].

[242] PeriodicTable.com, "Technical data for Silver," *Mathematica's ElementData function from Wolfram Research, Inc.*, 2016. [Online]. Available: http://periodictable.com/Elements/047/data.html. [Accessed: 01-Jan-2016].

[243] H. R. Brown, "Adhesion between polymers," *IBM J. Res. Dev.*, vol. 38, no. 4, pp. 379–389, Jul. 1994.

[244] F. Erdogan and G. C. Sih, "On the crack extension in plates under plane loading and transverse shear," *J. basic Eng.*, vol. 85, no. 4, pp. 519–525, 1963.

[245] K. B. Broberg, "On crack paths," *Eng. Fract. Mech.*, vol. 28, no. 5, pp. 663–679, 1987.

[246] J. F. Kalthoff, "On the propagation direction of bifurcated cracks," in *Proceedings of an international conference on Dynamic Crack Propagation*, 1973, pp. 449–458.

[247] H. Bergkvist and L. Guex, "Curved crack propagation," *Int. J. Fract.*, vol. 15, no. 5, pp. 429–441, 1979.

[248] J. Gunnars, P. Stahle, and T. C. Wang, "On crack path stability in a layered material," *Comput. Mech. Springer*, vol. 19, no. 6, pp. 545–552, 1997.

[249] P. Qiao and J. Wang, "Mechanics and fracture of crack tip deformable bi-material interface," *Int. J. Solids Struct.*, vol. 41, no. 26, pp. 7423–7444, Dec. 2004.

[250] J. W. Hutchinson and Z. Suo, "Mixed mode cracking in layered materials," *Adv. Appl. Mech.*, vol. 29, no. 63, p. 191, 1992.

[251] Z. Suo and J. W. Hutchinson, "Interface crack between two elastic layers," *Int. J. Fract.*, vol. 43, no. 1, pp. 1–18, 1990.

[252] J. Wang and P. Qiao, “Interface crack between two shear deformable elastic layers,” *J. Mech. Phys. Solids*, vol. 52, no. 4, pp. 891–905, Apr. 2004.

[253] R. C. Ostergaard, B. F. Sorensen, and P. Brondsted, “Measurement of Interface Fracture Toughness of Sandwich Structures under Mixed Mode Loadings,” *J. Sandw. Struct. Mater.*, vol. 9, no. 5, pp. 445–466, Sep. 2007.

[254] S. Liu, Y. Mei, and T. Y. Wu, “Bimaterial interfacial crack growth as a function of mode-mixity,” *Components, Packag. Manuf. Technol. Part A, IEEE Trans.*, vol. 18, no. 3, pp. 618–626, 1995.

[255] N. Rahbar, Y. Yang, and W. Soboyejo, “Mixed mode fracture of dental interfaces,” *Mater. Sci. Eng. A*, vol. 488, no. 1, pp. 381–388, 2008.

[256] J. Cui, Q. Huang, Q. Wang, and T. J. Marks, “Nanoscale covalent self-assembly approach to enhancing anode/hole-transport layer interfacial stability and charge injection efficiency in organic light-emitting diodes,” *Langmuir*, vol. 17, no. 7, pp. 2051–2054, 2001.

[257] D. Hegemann, H. Brunner, and C. Oehr, “Plasma treatment of polymers for surface and adhesion improvement,” *Nucl. instruments methods Phys. Res. Sect. B Beam Interact. with Mater. atoms*, vol. 208, pp. 281–286, 2003.

[258] C. M. Haanyika, “Rural electrification policy and institutional linkages,” *Energy Policy*, vol. 34, no. 17, pp. 2977–2993, 2006.

[259] J. Sheffield *et al.*, “Energy options for the future,” *J. fusion energy*, vol. 23, no. 2, pp. 63–109, 2004.

[260] J. K. Kaldellis and D. Zafirakis, “Present situation and future prospects of electricity

generation in Aegean Archipelago islands," *Energy Policy*, vol. 35, no. 9, pp. 4623–4639, 2007.

[261] G. TAMULAITIS, "LEDs IN DEVELOPING WORLD," *Int. J. High Speed Electron. Syst.*, vol. 20, no. 2, pp. 343–358, 2011.

[262] K. Alanne and A. Saari, "Distributed energy generation and sustainable development," *Renew. Sustain. Energy Rev.*, vol. 10, no. 6, pp. 539–558, 2006.

[263] W. Clark and W. Isherwood, "Distributed generation: remote power systems with advanced storage technologies," *Energy Policy*, vol. 32, no. 14, pp. 1573–1589, 2004.

[264] R. T. Kivaisi, "Installation and use of a 3 kW p PV plant at Umbuji village in Zanzibar," *Renew. energy*, vol. 19, no. 3, pp. 457–472, 2000.

[265] C. R. Henderson, J. F. Manwell, and J. G. McGowan, "A wind/diesel hybrid system with desalination for Star Island, NH: feasibility study results," *Desalination*, vol. 237, no. 1, pp. 318–329, 2009.

[266] R. M. Shrestha and G. B. Bhattarai, "Electricity planning with demand-side management in Nepal: Economics and environmental implications," *Energy Policy*, vol. 21, no. 7, pp. 757–767, 1993.

[267] D. Egré and J. C. Milewski, "The diversity of hydropower projects," *Energy Policy*, vol. 30, no. 14, pp. 1225–1230, 2002.

[268] Sirte, "Hydropower Resource Assessment of Africa. 15-17 December 2008," in *Ministerial Conference on Water for Agriculture and Energy in Africa: The Challenges of Climate Change*, 2008, pp. 1–34.

[269] M. O. Abdullah, V. C. Yung, M. Anyi, A. K. Othman, K. B. A. Hamid, and J. Tarawe, "Review and comparison study of hybrid diesel/solar/hydro/fuel cell energy schemes for a rural ICT Telecenter," *Energy*, vol. 35, no. 2, pp. 639–646, 2010.

[270] J. A. Alaii *et al.*, "Perceptions of bed nets and malaria prevention before and after a randomized controlled trial of permethrin-treated bed nets in western Kenya," *Am. J. Trop. Med. Hyg.*, vol. 68, no. 4 suppl, pp. 142–148, 2003.

[271] T. J. Lybbert and D. A. Sumner, "Agricultural technologies for climate change in developing countries: Policy options for innovation and technology diffusion," *Food Policy*, vol. 37, no. 1, pp. 114–123, 2012.

[272] E. M. Rogers, *Diffusion of innovations*. Simon and Schuster, 2010.

[273] S. K. Singh, "The diffusion of mobile phones in India," *Telecomm. Policy*, vol. 32, no. 9, pp. 642–651, 2008.

[274] B. K. Sovacool, A. L. D'Agostino, and M. J. Bambawale, "The socio-technical barriers to Solar Home Systems (SHS) in Papua New Guinea: 'Choosing pigs, prostitutes, and poker chips over panels,'" *Energy Policy*, vol. 39, no. 3, pp. 1532–1542, 2011.

[275] G. TARDE, "La Psychologie Économique," 1902.

[276] D. Collins, J. Morduch, S. Rutherford, and O. Ruthven, *Portfolios of the poor: how the world's poor live on $2 a day*. Princeton University Press, 2009.

[277] A. Karamchandani, M. Kubzansky, and P. Frandano, "Emerging markets, emerging models: Market-based solutions to the challenges of global poverty," *Online http//www. mim. Monit. com/downloads/emergingmarke ts_full. pdf (accessed August 16, 2011)*,

2009.

[278] D. Kammen, “Investing in Future Resources,” *Environ. Rev.*, vol. 7, no. 3, pp. 8–14, 2000.

[279] K. Bagwell and M. H. Riordan, “High and declining prices signal product quality,” *Am. Econ. Rev.*, vol. 81, no. 1, pp. 224–239, 1991.

[280] P. Polak, “Out of Poverty: What Works When Traditional Methods Fail.” San Francisco, CA: Berrett-Koehler Publishers, Inc, 2008.

[281] PSI, “What is Social Marketing,” *Accessed online April 2009 at: http://www.psi.org/resources/research-metrics/publications/social-marketing-research-series/ what-social-marketing.*, 2003. .

[282] R. Thaler, “Toward a positive theory of consumer choice,” *J. Econ. Behav. Organ.*, vol. 1, no. 1, pp. 39–60, 1980.

[283] WorldBank, “Lighting Africa, Solar Lighting for the Base of the Pyramid— Overview of an Emerging Market,” *World Bank*, vol. 347, no. 9012. p. 77, 2010.

[284] A. Jacobson, “Connective power: solar electrification and social change in Kenya,” *World Dev.*, vol. 35, no. 1, pp. 144–162, 2007.

[285] E. Mills and A. Jacobson, “The need for independent quality and performance testing for emerging off-grid white-LED illumination systems for developing countries,” *Light Eng.*, vol. 16, no. 2, pp. 5–24, 2008.

[286] R. Grüner, S. Lux, K. Reiche, and T. Schmitz-Günther, “Solar lanterns test: shades of light,” *Appropr. Technol.*, vol. 36, no. 2, p. 26, 2009.

[287] K. Radecsky, “Solid-State lighting on a shoestring budget: the economics of off-grid

lighting for small businesses in Kenya," *Lawrence Berkeley Natl. Lab.*, 2009.

[288] G. World Bank, "Ease of Doing Business in Kenya," *Accessed online February 25, 2015 at: http://www.doingbusiness.org/data/exploreeconomies/kenya/*, 2012. [Online]. Available: http://www.worldbank.org/.

[289] A. Pegels, "Renewable energy in South Africa: Potentials, barriers and options for support," *Energy Policy*, vol. 38, no. 9, pp. 4945–4954, 2010.

[290] J. Brown, S. Proum, and M. Sobsey, "Sustained use of a household-scale water filtration device in rural Cambodia," *J. Water Health*, vol. 7, no. 3, pp. 404–412, 2009.

[291] B. K. Sovacool, "The political economy of energy poverty: A review of key challenges," *Energy Sustain. Dev.*, vol. 16, no. 3, pp. 272–282, 2012.

[292] B. K. Sovacool and M. Dworkin, "Overcoming the global injustices of energy poverty," *Environ. Sci. Policy Sustain. Dev.*, vol. 54, no. 5, pp. 14–28, 2012.

[293] R. Mutai, "Micro and Small Enterprise Sector and Existing Support System with emphasis on High-Tech oriented Entrepreneurship in Kenya," *J. Lang. Technol. Entrep. Africa*, vol. 3, no. 1, pp. 99–108, 2011.

[294] DUMA, "duma," *Accessed March 20, 2012 at: http://www.myduma.org/.*, 2012.

[295] V. Govindarajan and R. Ramamurti, "Reverse innovation, emerging markets, and global strategy," *Glob. Strateg. J.*, vol. 1, no. 3–4, pp. 191–205, 2011.

[296] R. Jana, "Innovation Trickles in a New Direction," *Accessed online March 11, 2009 at: http://www.bloomberg.com/bw/magazine/content/09_12/b4124038287365.htm*, 2009.

[297] W. A. Kaplan, "Can the ubiquitous power of mobile phones be used to improve health

outcomes in developing countries," *Glob. Heal.*, vol. 2, no. 9, pp. 1–14, 2006.

[298] R. Wootton, "Telemedicine support for the developing world," *J. Telemed. Telecare*, vol. 14, no. 3, pp. 109–114, 2008.

[299] D. Bodansky, "The United Nations framework convention on climate change: a commentary," *Yale J. Int'l l.*, vol. 18, p. 451, 1993.

[300] J. T. Houghton and B. A. Callander, *Climate change 1992*. Cambridge University Press, 1992.

[301] J. Leggett *et al.*, "Emissions scenarios for the IPCC: an update," *Clim. Chang.*, pp. 69–95, 1992.

[302] J. H. Ausubel, H. D. Langford, and others, *Technological trajectories and the human environment*. National Academies Press, 1997.

[303] J. T. Houghton Filho and H. BA, "N., Kattenberg, A., and Maskell, K.(Eds.): Climate Change 1995, The Science of Climate Change: Intergovernmental Panel on Climate Change." Cambridge Univ. Press, New York, 1996.

LIST OF PUBLICATIONS

Publications from Thesis Work

1. **J. Asare**, E. Türköz, B. Agyei-Tuffour, O. K. Oyewole, A. A. Fashina, J. Du, M. G. Zebaze Kana, W. O. Soboyejo, "Effects of pre-buckling on the bending of organic electronic structures," AIP Adv., 2017
2. **J. Asare**, Adeniji, S. A., Oyewole, O. K., Agyei-Tuffour, B., Du, J., Arthur, E., Fashina, A. A., Zebaze Kana, M. G., Soboyejo, W. O., "Cold welding of organic light emitting diode: Interfacial and contact models," AIP Adv., vol. 6, no. 6, p. 65125, 2016.
3. **J. Asare**, O.K. Oyewole, V.C. Anye, D.Y. Momodu, W.O. Soboyejo, Effects of Deformation on Failure Mechanisms and Optical Properties of Flexible Organic Solar Cell Structures, Adv. Mater. Res. 1132 (2016) 125–143. doi:10.4028/www.scientific.net/AMR.1132.125
4. **J. Asare**, O.K. Oyewole, W.O. Soboyejo, DEFORMATION AND FAILURE OF BENDABLE ORGANIC SOLAR CELLS, Adv. Mater. Res. 1132 (2016) 116–124. doi:10.4028/www.scientific.net/AMR.1132.116**.**
5. T M Tong, **J Asare**, E R Rwenyagila, V Anye, O K Oyewole, A A Fashina, W O Soboyejo. "A Study of Factors that Influence the Adoption of Solar Powered Lanterns in a Rural Village in Kenya" *Perspectives on Global Development and Technology*, Vol. 14 (2015) 448-491. doi 10.1163/15691497-12341356

Award from Thesis Work

- **Best Contribution Prize at the ICTP Regional Workshop - smr 2515**

Themed: "Regional Workshop on Materials Science for Solar Energy Conversion"

Organizing Committee and Sponsors - ICTP, ANSOLE, NanoAfNet, NRF, ALC and TWAS

Venue**:** **iTHEMBA Labs (Laboratory for Accelerator Based Science), Cape Town, South Africa**

Selected Conference Proceedings and Abstract Publications

1. **J. Asare** et al., "Layer thickness determination in flexible organic solar cells made of metal organic frameworks", *1st Nigeria International Conference on Zeolite (Book of Extended Abstracts)*, pp. 73-77, December 2014.

2. **J. Asare** et al., "Determination of Layer Thickness in Flexible Organic Solar Cell by Optical Simulations and RBS Technique", *7th International Conference of the Africa Materials Research Society (Book of Abstracts)*, pg. 30, December 2013.

3. **J. Asare**, M. Z. Kana, B. Agyei-Tuffour, O. K. Oyewole, O. S. Oladipupo, K.O. Onogu, A. Oberafo, and W. Soboyejo, "Optical measurement and Flexural Characteristics of Bendable Organic Photovoltaic Cells", Proceedings of the Materials Science and Technology Society of Nigeria, Vol II, Nov 25-29, 2013, pp. 65-69.

Selected List of Conferences and Presentations

- **1st Nigeria International Conference on Zeolite:** New Trends in Zeolite Developments and Applications

  Extended abstract entitled **"Layer thickness determination in flexible organic solar cells made of metal organic frameworks"** was accepted for presentation and publication.

  Venue: **NICON Luxury Abuja, Nigeria**

- **IPF 2014: Capacity Building for Industrial Physics in Developing Economies**

  Organizers and Sponsors: The American Institute of Physics (AIP) , International Centre for Theoretical Physics (ICTP), Sao Paulo Research Foundation (FAPESP) and South American Institute for Fundamental Research (SAIFR)

  Venue: **The University of Campinas (UNICAMP), Campinas, Sao Paulo, Brazil**

- **7th International Conference of the Africa Materials Research Society**

  Africa Materials Research Society Conference

  Abstract entitled **"Determination of Layer Thickness in Flexible Organic Solar Cell by Optical Simulations and RBS Technique"** was accepted for presentation

  Venue: **African Union Conference Center, Addis Ababa, Ethiopia**

- **ICTP Workshop- smr 2515;** "Regional Workshop on Materials Science for Solar Energy Conversion". **Won the Best Poster Contribution Prize**

Organizing Committee and Sponsors - ICTP, ANSOLE, NanoAfNet, NRF,ALC and TWAS

Venue**: iTHEMBA Labs (Laboratory for Accelerator Based Science), Cape Town, South Africa**

- **11th ANNUAL NIGERIAN MATERIALS CONGRESS - NIMACON 2012"**

  ORAL presentation of paper titled; "OPTICAL MEASUREMENTS AND FLEXURAL CHARACTERISTICS OF BENDABLE ORGANIC PHOTOVOLTAIC CELLS" authored by me Joseph Asare et al.

  Venue: **Ile-Ife, Nigeria**

- **"The Second African School of Fundamental Physics and its Application - 2012" and "The GRID School".** Website: http://africanschoolofphysics.web.cern.ch/africanschoolofphysics/

  Venue: **KNUST, Kumasi, Ghana, West Africa**

- **"NIGERIAN MATERIALS CONGRESS 2011"**

  ORAL presentation of paper titled; "EFFECTS OF BENDING ON THE OPTOELECTRONIC PROPERTIES AND FAILURE MECHANISM IN ORGANIC PHOTOVOLTAICS" authored by me Joseph Asare with M.G. Zebaze Kana, W.O. Soboyejo.

  Venue: **Akure, Nigeria**

Other Publications

1. B. Agyei-Tuffour, E.R. Rwenyagila, J. Asare, O.K. Oyewole, M.G.Z. Kana, D.M. O'Carroll, and W.O. Soboyejo, "Influence of Pressure on Contacts Between Layers in Organic," Adv. Mater. Res., vol. 1132, pp. 204–216, 2016.

2. E. Annan, K. Kan-Dapaah, S.T. Azeko, K. Mustapha, J. Asare, M.G. Zebaze Kana, and W. Soboyejo, "Clay Mixtures and the Mechanical Properties of Microporous and Nanoporous Ceramic Water Filters," J. Mater. Civ. Eng., p. 4016105, 2016.

3. B. Agyei-Tuffour, E. R. Rwenyagila, J. Asare, M. G. Z. Kana, and W. O. Soboyejo, "Effects of pressure on nano- and micro-scale morphological changes in conjugated polymer photovoltaic cells," J. Mater. Res., pp. 1–9, 2016.

4. A.A. Fashina, K.K. Adama, O.K. Oyewole, V.C. Anye, J. Asare, M.G. Zebaze Kana, and W.O. Soboyejo, "Surface texture and optical properties of crystalline silicon substrates," J. Renew. Sustain. Energy, vol. 7, no. 6, p. 63119, 2015.

5. E. Nyankson, B. Agyei-Tuffour, J. Asare, E. Annan, E.R. Rwenyagila, D.S. Konadu, and A. Yaya, "NANOSTRUCTURED TiO2 AND THEIR ENERGY APPLICATIONS-A REVIEW," ARPN J. Eng. Appl. Sci., vol. 8, no. 10, pp. 871–886, 2013.

6. O. K. Oyewole, J. Asare, D. O. Oyewole, V. C. Anye, M. G. Z. Kana, and W. O. Soboyejo, "EFFECTS OF ADHESION AND STRETCHING ON FAILURE

MECHANISMS AND OPTICAL PROPERTIES OF ORGANIC SOLAR CELLS," Adv. Mater. Res., vol. 1132, pp. 89–105, 2016.

7. O. K. Oyewole, D. O. Oyewole, J. Asare, Z. K. M. G, and W. O. Soboyejo, "FAILURE MECHANISMS IN LAYERS RELEVANT TO STRETCHABLE ORGANIC SOLAR CELLS," Adv. Mater. Res., vol. 1132, pp. 106–115, 2016.

8. O.K. Oyewole, D. Yu, J. Du, J. Asare, V.C. Anye, A. Fashina, M.G.Z. Kana, and W.O. Soboyejo, "Lamination of organic solar cells and organic light emitting devices : Models and experiments," J. Appl. Phys., vol. 118, no. 75302, 2015.

9. O.K. Oyewole, D. Yu, J. Du, J. Asare, D.O. Oyewole, V.C. Anye, a. Fashina, M.G. Zebaze Kana, and W.O. Soboyejo, "Micro-wrinkling and delamination-induced buckling of stretchable electronic structures," J. Appl. Phys., vol. 117, no. 23, p. 235501, 2015.

10. D. Yu, O.K. Oyewole, D. Kwabi, T. Tong, V.C. Anye, J. Asare, E. Rwenyagila, A. Fashina, O. Akogwu, J. Du, and W.O. Soboyejo, "Adhesion in flexible organic and hybrid organic/inorganic light emitting device and solar cells," J. Appl. Phys., vol. 116, no. 7, p. 74506, Aug. 2014.